

FRACTAL AND EDGE-BASED TECHNIQUES FOR KIDNEY  
ENHANCEMENT AND SEGMENTATION ON MAGNETIC  
RESONANCE IMAGES (MRI)

ALAA RATEB MAHMOUD AL-SHAMASNEH

FACULTY OF COMPUTER SCIENCE AND  
INFORMATION TECHNOLOGY  
UNIVERSITY OF MALAYA  
KUALA LUMPUR

2020

**FRACTAL AND EDGE-BASED TECHNIQUES FOR KIDNEY  
ENHANCEMENT AND SEGMENTATION ON MAGNETIC  
RESONANCE IMAGES (MRI)**

**ALAA' RATEB MAHMOUD AL-SHAMASNEH**

**THESIS SUBMITTED IN FULFILMENT OF THE  
REQUIREMENTS FOR THE DEGREE OF DOCTOR OF  
PHILOSOPHY**

**FACULTY OF COMPUTER SCIENCE AND  
INFORMATION TECHNOLOGY  
UNIVERSITY OF MALAYA  
KUALA LUMPUR**

**2020**

UNIVERSITY OF MALAYA

ORIGINAL LITERARY WORK DECLARATION

Name of Candidate: ALAÁ RATEB

Matric No: 17042188/1

Name of Degree: Doctor of Philosophy

Title of Project Paper/Research Report/Dissertation/Thesis (“this Work”):

**FRACTAL AND EDGE-BASED TECHNIQUES FOR KIDNEY ENHANCEMENT  
AND SEGMENTATION ON MAGNETIC RESONANCE IMAGES (MRI)**

Field of Study: Artificial intelligent (Computer Science(

I do solemnly and sincerely declare that:

- (1) I am the sole author/writer of this Work;
- (2) This Work is original;
- (3) Any use of any work in which copyright exists was done by way of fair dealing and for permitted purposes and any excerpt or extract from, or reference to or reproduction of any copyright work has been disclosed expressly and sufficiently and the title of the Work and its authorship have been acknowledged in this Work;
- (4) I do not have any actual knowledge nor do I ought reasonably to know that the making of this work constitutes an infringement of any copyright work;
- (5) I hereby assign all and every rights in the copyright to this Work to the University of Malaya (“UM”), who henceforth shall be owner of the copyright in this Work and that any reproduction or use in any form or by any means whatsoever is prohibited without the written consent of UM having been first had and obtained;
- (6) I am fully aware that if in the course of making this work, I have infringed any copyright whether intentionally or otherwise, I may be subject to legal action or any other action as may be determined by UM.

Candidate’s Signature

Date:

Subscribed and solemnly declared before,

Witness’s Signature

Date:

Name:

Designation:

# **FRACTAL AND EDGE-BASED TECHNIQUES FOR KIDNEY ENHANCEMENT AND SEGMENTATION ON MAGNETIC RESONANCE IMAGES (MRI)**

## **ABSTRACT**

Recently, many rapid developments in digital medical imaging have made further contributions to healthcare systems. However, the segmentation of regions of interest in medical images plays a vital role in assisting doctors in their medical diagnoses and for the early detection of disease. Since health issues related to the kidneys are increasing exponentially, this thesis focused on developing methods for the segmentation of MRI images of the kidney. Kidney images frequently suffer from low contrast, low resolution and noise, and are blur. Hence, it is necessary to enhance the images in order to improve the segmentation. Therefore, the current thesis focused on enhancing the fine details of the kidney region and the segmentation of the kidney images. To solve the above issues, the proposed work introduced a new model for enhancing low-contrast MRI kidney images based on fractional entropy. It is true that fractional entropy is able to handle complex situations such as images that are affected by the above challenges, and as such, the proposed work explored the same in this thesis to find solutions. However, sometimes, due to the presence of neighbouring organs and other regions in the background, the enhancement model must be one that can sharpen those details, thereby making the segmentation problem a challenging one. Therefore, this thesis was aimed at proposing a new method for kidney segmentation based on an active contour model driven by fractional-based energy minimization. Since the special characteristic of fractional calculus is its ability to preserve high-frequency contours regardless of contrast variations and noise, the proposed work explored this characteristic for the segmentation of kidney images. However, it should be noted that this method is said to be computationally expensive.

Therefore, the thesis proposed a new method based on edge information for the segmentation of kidney images. It is true that the pixels representing the contours of the kidney share a unique spatial relationship. The proposed work used the same basis for the detection of the pixels in the edge domain, which represented the contours of the kidney in the enhanced images. Overall, this study made three contributions, namely, a fractional entropy-based method for the enhancement of kidney images, a fractional-based minimization function for kidney image segmentation, and an edge-based method for kidney image segmentation. The developed methods were tested on datasets using standard measures to evaluate the methods. The results of the proposed methods were compared with existing methods to show that the proposed methods are effective and useful.

Keywords: Fractal; Local Fractional Entropy; Active Contours; Kidney Enhancement; Kidney Segmentation.

# TEKNIK BERASASKAN FRAKTAL DAN *EDGE* UNTUK PENAMBAHBAIKAN DAN SEGMENTASI PADA IMEJ RESONANS MAGNETIK (MRI) BUAH PINGGANG

## ABSTRAK

Kebelakangan ini, perkembangan pesat dalam pengimejan perubatan digital telah memberi sumbangan tambahan kepada sistem penjagaan kesihatan. Secara tidak langsung, segmentasi dalam imej perubatan telah memainkan peranan penting bagi memudahkan urusan doktor. Doktor boleh menggunakan hasil segmentasi untuk perubatan diagnosis dan pengesanan awal penyakit. Oleh kerana isu kesihatan yang berkaitan dengan buah pinggang semakin meningkat, tumpuan tesis ini adalah bagi membangunkan kaedah segmentasi imej buah pinggang dari MRI data. Secara umum, imej buah pinggang didapati dalam kontras rendah, resolusi rendah, bising dan kabur. Untuk meningkatkan prestasi segmentasi, terdapat keperluan untuk penambahbaikan. Oleh itu, tesis yang dicadangkan memberi tumpuan kepada peningkatan butiran halus kawasan buah pinggang dan pembahagian imej buah pinggang dari imej data secara keseluruhan. Untuk mencari penyelesaian kepada isu-isu di atas, kerja yang dicadangkan memperkenalkan model baru untuk meningkatkan imej buah pinggang MRI kontras rendah berdasarkan entropi pecahan. Memang benar entropi fraksional mempunyai keupayaan untuk mengendalikan situasi kompleks seperti imej yang terjejas oleh cabaran di atas, maka, kerja yang dicadangkan mencari penyelesaian dalam tesis ini. Walaubagaimanapun, kadang-kadang, disebabkan oleh kehadiran organ-organ jiran dan kawasan-kawasan lain di latar belakang, model peningkatan mungkin dapat mempertajam butiran tersebut, yang membuat segmentasi lebih mencabar. Oleh itu, tesis ini bertujuan untuk mencadangkan satu kaedah baru untuk pemisahan buah pinggan berdasarkan model kontur aktif yang didorong oleh pengurangan tenaga berasaskan pecahan. Oleh kerana kalkulus pecahan mempunyai hak istimewa mengekalkan kontur frekuensi tinggi tanpa mengira kontras variasi dan bunyi, kerja yang dicadangkan ini juga dapat membahagikan imej buah pinggang. Walau bagaimanapun, diperhatikan bahawa kaedah ini dikatakan agak mahal. Oleh itu, tesis ini

mencadangkan kaedah baru berdasarkan maklumat terkini untuk membahagikan imej buah pinggang. Boleh dikatakan bahawa piksel itu mewakili kontur buah pinggang dan mempunyai hubungan perkongsian ruang yang unik. Kerja yang dicadangkan menggunakan asas yang sama untuk mengesan piksel di domain lain yang mewakili kontur buah pinggang dalam imej yang dipertingkatkan. Secara keseluruhan, terdapat tiga sumbangan, iaitu, kaedah berasaskan entropi pecahan untuk peningkatan imej buah pinggang, fungsi pemotongan berasaskan pecahan untuk segmentasi imej buah pinggang dan kaedah berasaskan pinggir untuk pemisahan imej buah pinggang. Kaedah yang dibangunkan diuji pada dataset menggunakan langkah-langkah standad. Keputusan kaedah yang dicadangkan dibandingkan dengan kaedah sediaada bagi menunjukkan bahawa kaedah yang dicadangkan adalah berkesan dan berguna.

Kata kunci: Fraktal; Entropi Pecahan Tempatan; Kontur Aktif; Peningkatan Buah Pinggang; Segmentasi Buah Pinggang.

## ACKNOWLEDGEMENTS

All praise to Allah, the Almighty, the Benevolent for His blessings and guidance to me and bestowing upon me wisdom, ideas and strength to successfully complete this PhD thesis.

I would like to express my very special thanks to my supervisors, Associate Professor Dr. Hamid Abdullah Jalab, Associate Professor Dr. Shivakumara Palaiahnakote, and Dr. Unaizah Hanum Binti Obaidellah for guidance and contribution of time, ideas and energy in making my PhD experience productive and stimulating. My supervisors gave me the opportunity to carry out my research with few obstacles.

I would like to thank the Faculty of Computer Science and Information Technology, University of Malaya for providing me with a great academic environment and also offering me a well-equipped laboratory.

Most prominently, I would like to extend my warmest gratitude to my beloved parents, my husband (Alaá Selawi), my children, and sisters for their precious support, patience and assurance throughout my education in University of Malaya (UM). They always being my stand all through the period of my education, and I will always be appreciative for their never-ending love, sacrifice and generosity. Special thanks to all my fellow friends, especially Dr. Nadia, and Dr. Amira and all of those who supported me in any respect during the completion of my research. This study was supported by Postgraduate Research Grant (PPP) of University of Malaya, Malaysia. Grant no: PG019-2015B.

## TABLE OF CONTENTS

Abstract .....	iii
Abstrak .....	v
Acknowledgements .....	vii
Table of Contents .....	viii
List of Figures .....	xii
List of Tables.....	xv
List of Symbols and Abbreviations.....	xvi
<b>CHAPTER 1: INTRODUCTION.....</b>	<b>1</b>
1.1 Background.....	1
1.2 Kidney Imaging Application .....	4
1.3 Types of Kidney Imaging .....	7
1.3.1 Ultrasound (US).....	7
1.3.2 Magnetic Resonance Imaging(MRI).....	8
1.3.3 Computed Tomography(CT).....	9
1.4 Research Motivation .....	10
1.4.1 Enhancement of kidney MRI Images.....	10
1.4.2 Segmentation of Kidney MR Images.....	11
1.4.3 An Efficient Kidney MR Segmentation.....	12
1.5 Research Challenges.....	13
1.5.1 Challenges of Kidney MR Enhancement.....	13
1.5.2 Challenges of Kidney MR Segmentation - Active Contour Model.....	14
1.5.3 Challenges of Kidney MRI Segmentation - Edge based Model.....	14
1.6 Problem Statement.....	15
1.7 Research Questions .....	15

1.8	Objectives.....	16
1.9	Scope of Research .....	16
1.10	Thesis Organization .....	17
1.11	Summary .....	18
<b>CHAPTER 2: LITERATURE REVIEW .....</b>		<b>19</b>
2.1	Background.....	19
2.2	Kidney Image Enhancement .....	19
2.2.1	Image Noising.....	22
2.2.2	Low-Contrast Enhancement.....	25
2.2.3	Fractional Differential Approach.....	28
2.2.4	Motivation of Kidney MR Enhancement.....	31
2.3	Kidney Image Segmentation .....	33
2.3.1	Active Contour Model.....	34
2.3.2	Level Set Method.....	40
2.3.3	Motivation of Kidney MR Segmentation-Active Contour Model.....	52
2.3.4	Edge-based Method.....	53
2.3.5	Motivation of Kidney MRI Segmentation-Edge based Model.....	56
2.4	Evaluation Metrics .....	58
2.4.1	Image Quality Assessment.....	60
2.4.2	Segmentation Assessment.....	61
2.5	Chapter Summary.....	63
<b>CHAPTER 3: RESEARCH METHODOLOGY .....</b>		<b>64</b>
3.1	Background.....	64
3.2	Research phases .....	64

3.2.1	Requirement Stages.....	69
3.3	Analysis stage .....	70
3.3.1	Datasets collection.....	70
3.3.1.1	Ground Truth Data .....	72
3.3.2	Hardware and software setup.....	75
3.4	Summary.....	75

**CHAPTER 4: FRACTIONAL ENTROPY BASED METHOD FOR KIDNEY IMAGE ENHANCEMENT .....76**

4.1	Background.....	76
4.2	The proposed method .....	76
4.2.1	Local Fractional Entropy.....	76
4.3	Experimental Results.....	82
4.3.1	Qualitative Result of Proposed and Existing Method.....	85
4.3.2	Quantitative Result.....	91
4.4	Discussion .....	92
4.5	Chapter Summary .....	94

**CHAPTER 5: FRACTIONAL BASED MINIMIZATION FUNTION FOR KIDNEY IMAGE SEGMENTATION.....95**

5.1	Background.....	95
5.2	The proposed Method .....	95
5.2.1	Overview of Chan–Vese (CV) algorithm .....	96
5.2.2	The LFMLF Energy Minimization Function for Kidney Segmentation ..	97
5.3	Experimental Results .....	100
5.3.1	Qualitative Result .....	103

5.3.2	Quantitative Result .....	108
5.4	Discussion .....	110
5.5	Chapter Summary .....	111
 <b>CHAPTER 6: Edge Based Method for Kidney Image Segmentation .....</b>		<b>112</b>
6.1	Background.....	112
6.2	The proposed Edge-Based Method for Kidney Segmentation.....	112
6.3	Experimental Results .....	117
6.3.1	Qualitative Result .....	118
6.3.2	Quantitative Result.....	120
6.4	Evaluating two proposed Segmentation methods.....	121
6.4.1	Qualitative Result .....	122
6.4.2	Quantitative Result.....	123
6.5	Discussion .....	124
6.6	Summary .....	125
 <b>CHAPTER 7: CONCLUSION AND FUTURE WORK .....</b>		<b>126</b>
7.1	Background.....	126
7.2	Summary of the Proposed Work .....	126
7.3	Contributios of the Proposed Work .....	127
7.4	Limitaitons of the Proposed Work .....	128
7.5	Recommendations for Future Work .....	129
References .....		130
List of Publications .....		141

## LIST OF FIGURES

Figure 1.1	: Four Basic Components Of The Computer-Aided Diagnosis System (CAD).....	2
Figure 1.2	: Sample of Low- And High-Contrast MRI Kidney Images.....	2
Figure 1.3	: Sample of Automatically Segmented MRI Kidney Images.....	4
Figure 1.4	: Pixelated Normal Kidney Anatomy.....	6
Figure 1.5	: Polycystic Kidney Disease.....	6
Figure 1.6	: Abdominal Ultrasound 1. Renal Cortex 2. Pelvicalyceal System 3. Renal Sinus 4. Liver.....	8
Figure 1.7	: Contrast-Enhanced MR Image; 1-Cortex 2- Medulla 3-Pelvis...	9
Figure 1.8	: CT Kidney Image.....	10
Figure 1.9	: MR Image; 1- Liver 2-Renal Column 3-Muscles.....	11
Figure 1.10	: Challenges of Kidney MRI Enhancement (different organs overlapped in medical image) .....	14
Figure 1.11	: Challenges of Kidney MRI Active Contour Model Segmentation (several neighboring tissues have similar intensities) .....	14
Figure 1.12	: Challenges of Kidney MRI Edge Based Model Segmentation (Non-uniform shape of the organs with missing lines, edges, boundaries)	15
Figure 2.1	: (A) Original Image (B) Histogram.....	19
Figure 2.2	: Different Modalities for Medical Imaging.....	20
Figure 2.3	: Major Issue Related to The Medical Images.....	21
Figure 2.4	: Kidney Image Enhancement Challenges.....	32
Figure 2.5	: Motivation for the Proposed Work on Kidney Segmentation.....	53

Figure 2.6	: Challenges of Kidney Boundary Detection.....	57
Figure 3.1	: 0General Flow Of The Proposed Methods.....	68
Figure 3.2	: Sample from Dataset-1 Which Consist 230 MRI Images Collected from A Hospital in Saudi Arabia.....	73
Figure 3.3	: Sample of Ground Truth for Dataset-1.....	73
Figure 3.4	: Sample from Dataset-2 Which Consists Of 20 Images Collected from Wikimedia Commons as Standard Dataset.....	74
Figure 3.5	: Sample of Ground Truth for Dataset-2.....	75
Figure 4.1	: Contrast is Increased after Enhancement .....	80
Figure 4.2	: The Result of Proposed Enhancement Model on Different Kidney Images.....	81
Figure 4.3	: Determining the Value for $\alpha$ with the average BRISQUE Measure	84
Figure 4.4	: Enhancement Results of The Proposed and Existing Methods.....	87
Figure 4.5	: Histogram for Enhancement Results of the Proposed and Existing. Methods Where X Line Refer to Gray Level and Y Line Refer to Pixel Count	89
Figure 5.1	: Low Contrast Input Image.....	100
Figure 5.2	: Segmented Image Using the Proposed Algorithm.....	100
Figure 5.3	: Determining the Optimal Value for The Alpha to Segment the Kidney Images By Varying Fractional Power A And Calculating Mean Accuracy.....	103
Figure 5.4	: Determining the Number Optimal Iterations for Kidney Segmentation for Dataset-1 And Dataset-2 By the Proposed Method.....	103
Figure 5.5	: Examples of Kidney Segmentation Using the Proposed Method for Dataset-1.....	105
Figure 5.6	: The experimental results of the proposed and existing models for kidney segmentation dataset1. (A) Input images, (B) Hasan et al. (C) Chan et al. (D) Li et al. (E) Ibrahim et al. (F) Proposed Method	106

Figure 5.7	: Example of Kidney Segmentation Using the Proposed Method for Dataset-2.....	107
Figure 5.8	: The experimental results of the proposed and existing models for kidney segmentation. (A) Input images, (B) Hasan et al, (C) Chan et al, (D) Li et al, (E) Ibrahim et al, (G) Proposed Method	108
Figure 6.1	: Samples of MRI Kidney Image.....	113
Figure 6.2	: Canny Edge Image.....	113
Figure 6.3	: Label Object Sample Example 1.....	114
Figure 6.4	: Label Object Sample Example 2.....	114
Figure 6.5	: Object Centroid Example 1.....	115
Figure 6.6	: Object Centroid Example 2.....	115
Figure 6.7	: The Result of Proposed Segmentation Model on Different Kidney Images.....	116
Figure 6.8	: Examples of Kidney Segmentation Using the Proposed Edge-based Method for Kidney segmentation.....	119
Figure 6.9	: Samples of Kidney Segmentation Using Proposed Edge-Based Method on Dataset-2	120
Figure 6.10	: The Comparison results between the two proposed segmentation methods using dataset1 (A) Input images, (B) Ground Truth, (C) Proposed segmentation1, (D) Proposed segmentation2	122

## LIST OF TABLES

Table 2.1	: Overview of Active Contour Segmentation Method.....	39
Table 2.2	: Overview of Level-Set Segmentation Method.....	49
Table 2.3	: Overview of Edge Based Model Segmentation.....	55
Table 4.1	: Histogram Flatness (HFM) and Histogram Spread (HS) Measures for Test Image of Figure 4.1 .....	82
Table 4.2	: The Enhancement Performance of the Proposed and Existing Methods	92
Table 5.1	: Performance of The Proposed and Existing Methods for Dataset- 1.....	109
Table 5.2	: Performance of The Proposed and Existing Methods for Dataset- 2.....	110
Table 6.1	: Perform of The Proposed and Existing Methods for Dataset-1...	121
Table 6.2	: Performance of the proposed edge-based method for kidney image segmentation on Dataset-2.....	121
Table 6.3	: The Comparison results between the two proposed segmentation methods using dataset-1 .....	124
Table 6.4	: The Comparison results between the two proposed segmentation methods using dataset-2 .....	124

## LIST OF SYMBOLS AND ABBREVIATIONS

ACM	:	Active Contour Methods
ADPKD	:	Autosomal Dominant Polycystic Kidney Diseases
AFDA	:	Adaptive Fractional Differential Algorithm
AIV	:	Adjust Intensity Values
AKI	:	Acute Kidney Injury
BEAS	:	B-Spline Explicit Active Surfaces
BRISQUE	:	Blind/Reference Less Image Spatial Quality Evaluator
BT	:	Binary Tomography
CADs	:	Computer Aided Diagnosis Systems
CCA	:	Connected Component Analysis
CCA	:	Connected Component Analysis
CEUS	:	Contrast-Enhanced Ultrasound
CKD	:	Chronic Kidney Disease
CLAHE	:	Contrast Limited Adaptive Histogram Equalization
CNGGVF	:	Component-Normalized Generalized GVF
CS	:	Compress Sensing
CT	:	Computed Tomography
CV	:	Chan-Vese
DCE-MR	:	Dynamic Contrast Enhanced MR
DRLSE	:	Distance Regularized Level Set Evolution
DSC	:	Dice's Similarity Coefficient
DW-MRI	:	Diffusion Weighted Resonance Imaging
DWT	:	Discrete Wavelet Transform
EM	:	Expectation Maximization

ET	:	Electron Tomography
FCM	:	Fuzzy C Mean
FN	:	False Negative
FR	:	Full Reference
G&DVF	:	Gradient And Direction Vector Flow
GFR	:	Glomerular Filtration Rte
GMM	:	Gaussian Mixture Model
GVC	:	Gradient Vector Convolution
HISTEQ	:	Histogram Equalization
IQA	:	Image Quality Assessment
JSC	:	Jaccard's Similarity Coefficient
LFE	:	Local Fractional Entropy
LFML	:	Local Fractional Mittag-Leffler
LFMLF	:	Local Fractional Mittag-Leffler' Function
MGRF	:	Markov Gibbs Random Field
MRI	:	Magnetic Resonance Imaging
MSTV	:	Maximally Stable Temporal Volume
NIQE	:	Natural Image Quality Evaluator
NLTV	:	Non-Local Total Variation
NR	:	Non-Reference
NSS	:	Natural Scene Statistics
PCs	:	Principle Component
PKD	:	Polycystic Kidney Disease
ROI	:	Region Of Interest
RR	:	Reduced Reference
SGVF	:	Sigmoid Gradient Vector Flow

SRAD	:	Speckle-Reducing Anisotropic Diffusion
SSM	:	Statistical Shape Model
SVD	:	Singular-Value Decomposition
SVM	:	Support Vector Machines
TE	:	Echo Time
TKV	:	Total Kidney Volume
TN	:	True Negative
TP	:	True Positive
TR	:	Repetition Time
UI	:	User Interaction
US	:	Ultrasound

Universiti Malaya

# CHAPTER 1: INTRODUCTION

## 1.1 Background

This chapter presents the motivation for this work. In particular, it discusses the background, importance of medical imaging, need of kidney imaging, the statement of research problem with questions, and objectives, following by scope of the research.

The kidneys are vital body organs that filter and remove waste products from the blood. They are retroperitoneal organs situated close to the centre of the back and below the rib cage. One kidney is located on each side of the spine. Every year, many people in developing countries are diagnosed with kidney diseases because of hypertension, diabetes mellitus, and glomerulonephritis.

The early diagnosis of diseases and disorders is crucial because the impedance of kidney function can be life-threatening. Various types of abnormalities such as renal cysts, renal calculi, and renal infections are related to the renal system.

The two most common kidney diseases are acute kidney injury (AKI) and chronic kidney disease (CKD), with a worldwide increase of 0.5%–0.7% and 8%–16%, respectively (Bellomo, Kellum, & Ronco, 2012; Jha, Garcia-Garcia, & Iseki, 2013; Remuzzi, Benigni, Finkelstein, & Grunfeld, 2013). These diseases leading to kidney failure, mortality, and several other complications.

The use of the total kidney volume (TKV) for disease diagnosis can help to determine treatment and intrusive diagnostics. The kidney volume is calculated from the outer dimensions of the kidney using the ellipsoid method.

A typical computer-aided diagnosis (CAD) system has four basic components, as shown in Figure 1.1, namely, the image pre-processing, image segmentation of the region of interest (ROI), image feature extraction, and classification of the segmented ROI. Image enhancement is the first component of a CAD system. The enhancement part

directly affects the output of the second part, that is, the segmentation. The output of a CAD system is related to the previously mentioned components and their adaptations. Therefore, the image enhancement component must be accurately determined for a specific problem (such as noising, low-contrast image).

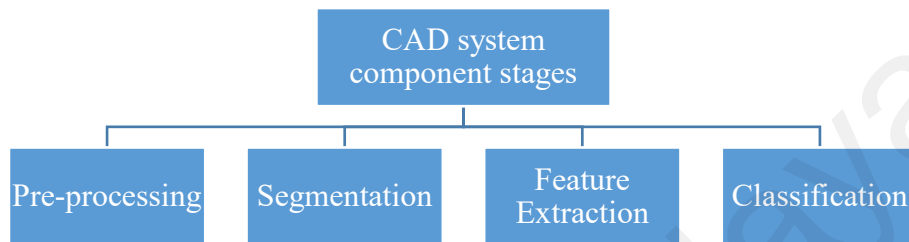
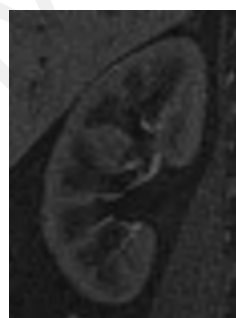


**Figure 1.1: Four Basic Components of the Computer-Aided Diagnosis System (CAD)**

Image enhancement or enhancing the quality of original images is a fundamental step in improving the edge details of kidney images acquired from low-contrast MRI. Figure 1.2 displays an example of low- and high-contrast MRI kidney images. A good selection of enhancement techniques can extensively improve the accuracy of a CAD system.



Low contrast MRI kidney image  
(brisque =40.46)



High contrast MRI kidney image  
(brisque =15.730)

**Figure 1.2: Sample of Low- and High-Contrast MRI Kidney Images**

Blind/Referenceless Image Spatial Quality Evaluator (BRISQUE) (Mittal et al., 2012). A lower BRISQUE value means that a given image has a better perceptual quality. This work considers poor-quality (low contrast) images affected by geometrical transformation, distortion, noise, and different modalities in capturing images for enhancement and segmentation. Therefore, to confirm poor-quality images, the proposed work uses two quality measures: (i) BRISQUE, and (ii) the naturalness image quality evaluator (NIQE). Deciding the threshold value to verify the degree of poor-quality images, these two measures are used to estimate good- and poor-quality MRI images chosen randomly from different datasets. Based on an experimental rationale, the proposed work determines the optimal cut-off threshold(s) for the measures to judge poor-quality images.

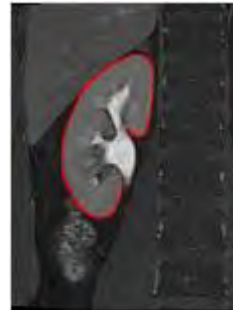
The precise segmentation of medical images is significant but considered as a challenge because of pathological changes and large variations in renal shapes. As such, developing an automatic method to extract the ROI of a kidney is difficult because of image noise, inhomogeneity, discontinuous boundaries as well as the similar visual appearance of neighbouring parts of various structures.

During kidney segmentation, as shown in Figure 1.3, the precise and effective segmentation of kidney edges in medical images is important for many applications associated with surgical planning and diagnosis. Effective methods, including the use of a low-contrast agent for neighbouring parts, have been applied to overcome kidney MRI challenges such as the issue of partial volume, high artefacts and leakage gradient response, high signal-to-noise ratio, and intensity inhomogeneity (Chehab & Bratslavsky, 2016; A. J. Huang, Lee, & Rusinek, 2004; Nikken & Krestin, 2007).

Automated segmentation systems for different imaging technologies, like ultrasound (US) images, computed tomography (CT) images, and MRI, are essential for detecting abnormalities through different medical imaging modalities.



MRI kidney image



MRI segmented kidney image

**Figure 1.3: Sample of Automatically Segmented MRI Kidney Images**

Many popular existing models for the enhancement and segmentation of kidney images are mentioned in this section, and the limitations associated with each model are given in detail to address the issue of kidney enhancement and segmentation methods.

## 1.2 Kidney Imaging Applications

Medical imaging plays an important role in the visual representations process of the human tissue and organ functions for the purposes of clinical analysis, diagnosis, and treatment. Medical imaging techniques such as magnetic resonance, ultrasound, and computed tomography, are important for outlining the human anatomy and its physiology, and for identifying potential abnormalities. Furthermore, medical imaging is important for follow-ups on diseases that have been already diagnosed and treated.

Renal imaging is a vital process in clinical assessments of the kidney. Ultrasound (US) images, CT images, and MRI are examples of conventional renal imaging procedures with explicit attributes that are helpful for extracting data about the anatomy of the kidney and its status. Several clinical investigations demand numerous imaging acquisition systems to enhance the treatment and diagnosis process (Lima, Rodrigues, & Mota, 2017; Pedro L Rodrigues, Rodrigues, Fonseca, & Lima, 2013; Pedro L. Rodrigues, Vilaça, Oliveira, & Cicione, 2013).

The kidney participates in the homeostasis of the entire body and controls the acid-base balance, electrolyte concentration, and extracellular liquid volume. According to the National Institute of Health in 2014, 4.4 million (1.9%) of adults were diagnosed with kidney disease in the USA (Blackwell & Lucas, 2014), while 50,476 individuals died of nephritis, nephrotic disorder, and nephrosis (Xu, Kochanek, & Murphy, 2016).

The kidney is comprised of four distinct structures with various functions, namely, the renal cortex, the renal column, the renal medulla, and renal pelvis (Clapp, 2009) (Figure 1.4). Different kidney diseases affect various parts of the kidney. For instance, a kidney tumour (Siemer, Lahme, Altziebler, & Machtens, 2007) typically occurs in the renal cortex and the renal column; hypertrophy (Jun, Xiaodong, & Erping, 2006) may occur in the renal column; medullary cysts and kidney diseases (Hart, Gorry, & Hart, 2002) generally affect the renal medulla; and the malignant growth of transitional cells, and cancer of the ureter and renal pelvis (Lucké & Schlumberger, 1958) may form in the region of the renal pelvis. Changes in the volume of various segments may alter different renal functions (Gloger, Tönnies, Laqua, & Völzke, 2015). The renal cortical has been verified to be powerful biomarkers of renal function in numerous clinical situations (Beland, Walle, & Machan, 2010); (Stevens, Coresh, Greene, & Levey, 2006). The volume of the renal medulla and the renal cortex is highly interesting for epidemiological studies (Gloger, Tönnies, Laqua, et al., 2015); (Mounier-Vehier, Lions, Devos, & Jaboureck, 2002). The volume of the renal pelvis should be determined to diagnose renal pelvis disease in children (Koff, Binkovitz, & Coley, 2005). In community medicine and epidemiological investigations, image information is necessary. Hence, the automatic, exact, and productive kidney segmentation has extraordinary clinical benefits, and for the evaluation of renal function and morphology (Will, Martirosian, & Würslin, 2014).

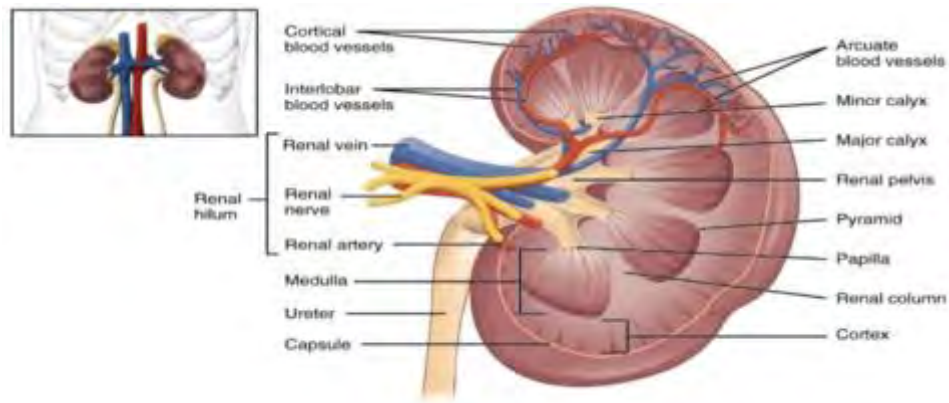


**Figure 1.4: Pixelated Normal Kidney Anatomy<sup>1</sup>**

Various renal abnormalities, such as renal cysts, renal calculi, and end stage kidney failure, are related to the renal system. The polycystic kidney disease (PKD), the chronic kidney disease (CKD), and the acute kidney injury (AKI) which are the most widely recognized ailments that affect the kidney. This disease causes both kidneys to be enlarged.

The seriousness of the renal function disability is related to the shape of the kidneys. Typically, the larger the kidney, the more disjointed will be the renal failure (Figure 1.5). CKD is a general medical issue with a developing rate in the aging population (Couser, Remuzzi, Mendis, & Tonelli, 2011).



**Figure 1.5: Polycystic Kidney Disease<sup>2</sup>**

<sup>1</sup> (Image courtesy: [cnx.org/content/col11496/1.6/](http://cnx.org/content/col11496/1.6/))

<sup>2</sup> [http://phil.cdc.gov/PHIL/Images/02071999/00002/20G0027\\_lores.jpg](http://phil.cdc.gov/PHIL/Images/02071999/00002/20G0027_lores.jpg)

### **1.3 Types of Kidney Imaging**

The kidney is comprised of five distinct structures, namely, the renal cortex, renal sinus, renal medulla, renal pelvis, and renal parenchyma, and they can be seen and assessed through imaging. The US, MRI and CT, are used to produce renal images to assess the condition of the kidney. These imaging modalities have unique imaging abilities and are utilized for clinical purposes, and therefore, can ideally be used for investigations based on their quality of enhancement, segmentation, and non-kidney removal components.

#### **1.3.1 Ultrasound (US)**

The US diagnostic radiology technique, also called medical ultrasonography or sonography, works at a frequency above the hearing range of humans to produce images from inside the body. An ultrasound machine transmits sound waves, which are extremely high for hearing, to the human body, and the sound echoes are converted into an image called a sonogram. The US images enabling medical experts to utilize each sound and visual to evaluate a patient's health (Bavu, Gennisson, & Couade, 2011). A kidney ultrasound is clinically utilized to survey the morphology and size of the kidney (Figure 1.6). The parenchyma shows up as a hypoechogenic (dark), while the medulla has a lower echogenicity than the surrounding parenchyma. The renal sinus and renal pelvis show up as large areas in the centre of the kidney. The US modality can recognize stones, tumours, and cysts. Kidney diseases, including cystic, hydronephrosis, and nephrolithiasis kidney infections, are traditionally assessed through the US method (Noble & Brown, 2004);(Brown, Rosen, & Wolfe, 1997) instead of other imaging modalities. The US has several advantages because it displays great detail without any type of radiation, costs less, and provides an examination in real time (Noble & Brown, 2004); (Brown et al., 1997) . US images, for the most part, have speckle noise, low image quality, artefacts,

and low contrast, thereby hampering segmentation. An MR system gives complete and useful functional information and an anatomical view of the kidney.

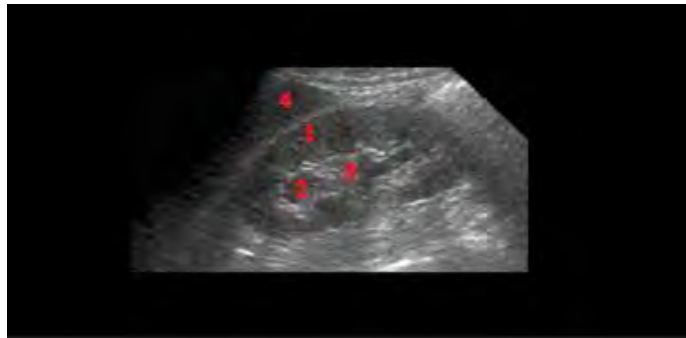


**Figure 1.6: Abdominal Ultrasound 1. Renal cortex 2. Pelvicalyceal system 3. Renal sinus 4. Liver<sup>3</sup>**

### 1.3.2 Magnetic Resonance Imaging (MRI)

Magnetic resonance is a medical imaging model that utilizes radio waves plus a magnetic field to produce precise images of parts and structures inside the body. MRI features remarkably in diagnoses by yielding different kinds of information about body structures, and may show problems that cannot be observed through other imaging methods (Bottrill, Nicholas, & Long, 2006). MRI can often be utilized to assess the chest and abdomen (heart, liver, kidneys, and spleen), blood vessels, bones and joints, breasts, abnormal tissues, and organs in the pelvis (Y. Chen, Chen, & Shi, 2013).

In MRI images, the renal structure and status, such as of the renal medulla, pelvis, and renal cortex, can be correctly visualized (Figure 1.7). Renal injuries and tumours can likewise be identified in MRI images, and even some renal masses can be recognized. Unlike the US, the MRI is unable to sufficiently identify calcifications such as renal stones (Chehab & Bratslavsky, 2016) (Nikken & Krestin, 2007). Renal function also be assessed by a dynamic MRI with a contrast enhanced features (DCE-MRI), where images are progressively produced after a contrast agent, such as gadolinium, has been injected into the patient. For investigations into kidney vasculature, the renal tissues are enhanced

<sup>3</sup> <http://w-radiology.com/abdominal-ultrasound.php>

by a contrast specialist to enable them be viewed so that their functions can be evaluated according to changes in the signal intensity after some time (Nikken & Krestin, 2007); (Bokacheva, Rusinek, Zhang, & Lee, 2008) (A. J. Huang et al., 2004). Generally, MRI gives the highest spatial resolution with an insignificant risk to patients because radiation is not required. In MRI images, a higher delicate tissue contrast is obtained in an examination compared to the other imaging modalities. Its drawbacks include costly equipment and a low temporal resolution (Chehab & Bratslavsky, 2016); (Nikken & Krestin, 2007); (A. J. Huang et al., 2004).

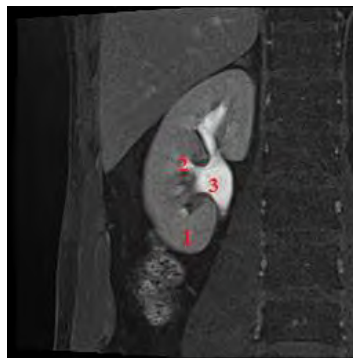


**Figure 1.7: Contrast-Enhanced MR image;  
1-Cortex 2- Medulla 3-Pelvis**

### 1.3.3 Computed Tomography (CT)

CT, which is also known as CAT scanning, is a medical imaging technique of multiple X-ray projections obtained from various sides to create precise cross-sectional images associated with regions of the human body. CT images allow medical doctors to obtain highly accurate 3-D images of specific areas of the body, such as soft tissues. CT is usually the preferred approach for diagnosing numerous cancers types (G.-H. Chen, Tang, & Leng, 2008). For the renal anatomy, the data obtained by CT, as shown in Figure 1.8, are similar to the data obtained from a renal ultrasound. The renal sinus can be viewed as water-dense structures, which show up in CT images with dark regions enclosed by the parenchyma. This methodology has a high sensitivity and resolution that enable it to

identify small lesions and cysts that cannot be typically detected by other imaging modalities.



**Figure 1.8: CT Kidney Image<sup>4</sup>**

## **1.4 Research Motivation**

It was noted in the previous section that there are several methods for kidney image enhancement and accurate segmentation. This section discusses the motivation for kidney image enhancement and segmentation. In other words, the challenges posed by images of different structures in the kidney.

### **1.4.1 Enhancement of Kidney MRI Images**

Kidney image enhancement becomes challenging because of the issues of low contrast, partial volume, high artefacts, leakage gradient response, low signal-to-noise ratio, intensity inhomogeneity, and non-uniform image background. Most methods focus on the removal of noise to enhance kidney images, and these involve different filtering approaches to decrease the noise impact. These techniques are useful for improving the whole image but not the local data. Similarly, other techniques address the issue of low contrast by using a fractional-based model (Raghunandan, Shivakumara, Jalab, & Ibrahim, 2017). However, these techniques are restricted to precise applications, like text detection and recognition. Consequently, none of these strategies have addressed the issue

---

<sup>4</sup> [https://w-radiology.com/abdominal\\_ct/](https://w-radiology.com/abdominal_ct/)

of low-contrast kidney images and investigated a generalized model for enhancing low-contrast images. Most techniques also utilize global data, not local data, to enhance the images. Consequently, a general model should be developed to enhance low-contrast MRI kidney images influenced by various factors, such as the MRI system, noise, and diseases.

Nevertheless, the enhancement process may magnify the details in the background because of the presence of neighbouring organs and other fine details, thereby making an accurate segmentation of the kidney region a challenging task. Therefore, it is essential for developing an approach that can accurately segment kidney images.

#### 1.4.2 Segmentation of Kidney MRI Images

The internal structure of the kidney is complex and difficult to recognize. Several neighbouring tissues or organs, including the renal column, muscles, and liver, have the same intensities, as shown in Figure 1.9. The variety of kidney shapes (in terms of length and volume) complicates the mechanized recognition and segmentation of the kidney.

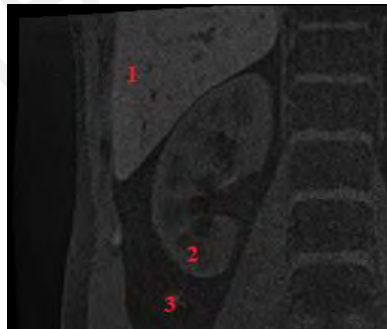


**Figure 1.9: MR image; 1- Liver 2-Renal Column 3- Muscles**

These limitations pose challenges to segmentation. Different methods of kidney segmentation have been observed, and most of these methods explore low-level features, such as colour, gradient and edge information, to formulate an energy minimization function or cost function to decrease errors between dominant pixels and other pixels in the images. None of the methods have been able to adequately address the issues of low contrast and degraded images for kidney segmentation. Generally, the methods (Hasan,

Meziane, Aspin, & Jalab, 2016; Chunming Li, Chenyang Xu, Changfeng Gui, & Martin D Fox, 2010) use the gradient descent-based energy minimization function in different ways. However, this energy minimization function suffers from inherent limitations, such as sensitivity to inhomogeneous intensity values. Hence, these methods are inadequate to address issues associated with kidney segmentation.

Furthermore, it has been observed that there are methods for segmenting kidney images (Abdulahi & Tapamo, 2015; Qiao, Lu, Su, & Chen, 2016). However, these methods use computationally expensive models to achieve results. Therefore, there is a demand for the development of an efficient method for segmenting the kidney region in enhanced images.

### **1.4.3 An Efficient Kidney MRI Segmentation**

The precise and proficient detection of the kidney boundary in low-contrast images is considered as the main difficulty in the detection of kidney MRI image edges. The exact identification of a kidney shape in medical images with decreased non-kidney components to acquire insignificant false edge detection is adequately vital for several applications in surgical planning and diagnosis.

Kidney image edge detection is a significant step in the segmentation procedure because the final appearance and nature of the segmented image depend greatly on the edge detection technique utilized. Most strategies utilize the Canny edge detection algorithm with various filters. However, these strategies suffer from inherent limitations such as sensitivity to noise and inhomogeneous intensity values (Les, Markiewicz, Dziekiewicz, & Lorent, 2018); (Nikolic, Tuba, & Tuba, 2016). In this proposed study, an effective strategy was applied to the kidney MRI segmentation model based on the use of kidney edge components, while preserving the kidney-segmented edge information from low-contrast MRI images. Canny used as pre-processing step for our second proposed segmentation method.

## **1.5 Research Challenges**

From the above discussion, it can be noted that the following are the main issues for kidney MRI segmentation. Moreover, the kidney image enhancement is challenging with respect to contrast, resolution variations and poor quality (low contrast). In addition, inhomogeneous pixel values make the enhancement more complex and challenging. In the same way, the accurate kidney region segmentation using enhanced images is another challenge due to the presence of other organs and the structure of the kidney. Therefore, the proposed work in this thesis is focused on the above two issues as its main challenges. The specific challenges based on the existing methods in the literature are listed in the subsequent sections on the respective topics (Chapter 2).

### **1.5.1 Challenges of Kidney MRI Enhancement**

The challenges in previous works (Figure 1.10)

- 1- There is no generalized model for kidney image enhancement. Most of the developed methods focus on a specific cause and application of kidney image enhancement.
- 2- Most of the developed methods consider noise to be the main cause of poor kidney image enhancement. However, this is not necessarily true for all situations because the image can be affected by low contrast, low resolution, blurring and poor quality.
- 3- A few methods take into account local information for image enhancement. In other words, most of the methods that have been developed are aimed at enhancing the whole image. This idea does not work for the process of kidney images enhancement because the kidney is only a small region of the image.



**Figure 1.10: Challenge of Kidney MRI Enhancement (Different Organs Overlapped in Medical Image)**

### **1.5.2 Challenges of Kidney MRI Segmentation - Active Contour Model**

The challenges in previous works (Figure 1.11)

- 1- Most of the developed methods has been developed for high-quality images, not for poor-quality images.
- 2- The methods are meant to address a particular cause, but there is no generalized segmentation of kidney model.
- 3- The methods do not consider efficiency as the main criterion, but rather are aimed at achieving accurate and better results.

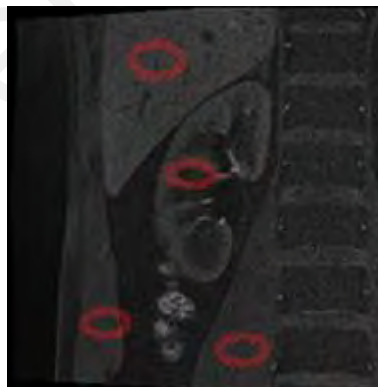


**Figure 1.11: Challenges of Kidney MRI Active Contour Model Segmentation (Several Neighboring Tissues Have Similar Intensities)**

### **1.5.3 Challenges of Kidney MRI Segmentation – Edge-based Model**

The challenges in previous works (Figure 1.12)

- 1- The methods were developed using edge information. However, some work well for highly contrast images.

- 2- The methods that use edge information are sensitive to background complexities, which are not work well for complex background images.
- 3- When the shape of the kidney changes, the efficiency of the edge-based methods degrades.



**Figure 1.12: Challenges of Kidney MRI Edge based Model Segmentation (Non-Uniform Shape of the Organs with Missing Lines, Edges, Boundaries)**

## 1.6 Problem Statement

It can be seen from the list of challenges in the preceding section that, there is a need to enhance kidney MRI images to improve the contrast images in preparation for the image segmentation step. Also, the segmentation and accurate detection of the kidney boundary are necessary to eliminate the unwanted structures of other regions (e.g., renal column, muscles, and liver) that share the same properties as the kidney, such as the intensity. These problems are regarded as open research issues in image processing. Thus, these were the two key issues that were addressed in this thesis.

## 1.7 Research Questions

The research questions are:

- 1- How to develop a new model for enhancing the fine details of the kidney from poor quality Magnetic Resonance Image?

- 2- How to segment the kidney region from the enhanced MRI images which contains information of other neighbouring organs and other background information?
- 3- How to develop an efficient method to segment the kidney region in MRI scans?

### **1.8 Objectives**

- 1- To develop a new method based on local fractional entropy for enhancing the quality of images, particularly in the kidney region.
- 2- To propose a new method using local fractional calculus for the accurate segmentation of the kidney region from enhanced images.
- 3- To explore an edge-based kidney segmentation for the enhanced images with minimum computational cost.

### **1.9 Scope of the Research**

It can be noted from the above discussion that there are several issues regarding kidney image enhancement, segmentation, classification, and identification of diseases, depending on the application. However, the scope of the proposed work was limited to the enhancement of kidney images and the segmentation of the kidney region. This was because these two issues are the main factors for achieving better results for the classification and identification of diseases. The successful classification and identification of diseases depend on the successful enhancement and segmentation of kidney images. Therefore, the scope of the proposed work was confined to the two issues mentioned above in this thesis.

## 1.10 Thesis Organization

This thesis organization is as follows:

Chapter 1 provides an introduction to the proposed methods and the motivation for this work. Next, it presents the research background, importance of medical imaging, types of kidney imaging, research challenges, problem statement with research followed by the objectives and scope of the research.

Chapter 2 presents a brief literature review of various kidney enhancement and segmentation methods for different medical imaging modalities, which are affected by major issues related to those medical images. A simple explanation is presented for problems in relation to quality, such as de-noising and low contrast, that are encountered in most of the images. The fractional differential approach is also described for kidney image segmentation, and an overview is given of state-of-the-art segmentation strategies, namely the active contour model, level set method, and edge-based method.

Chapter 3 presents the research methodology, which consists of four phases. Phase 1 involves the analysis, while the other three phases have to do with the design and implementation of the three proposed algorithms for kidney image enhancement and segmentation. The structure of each phase, experiment and evaluation is also described.

Chapter 4 presents a fractional entropy-based method for the enhancement of kidney images. The structural description for kidney image enhancement and the experimental results (quantitative and qualitative) are introduced in this chapter. Different low-contrast kidney MRI images are tested to determine accuracy of the proposed method. Several experimental results are described. To evaluate the accuracy of the methods, evaluation metrics based on (BRISQUE) (Mittal et al. 2012) and (NIQE) (Mittal et al. 2013) are used.

Chapter 5 presents a fractional-based minimization function for kidney image segmentation. The structural design for kidney image segmentation is introduced in this

chapter. The proposed segmentation scheme is examined against different datasets to evaluate the detection accuracy of the proposed method. Numerous experimental results (quantitative and qualitative) are described in this chapter. To evaluate the accuracy of the method, evaluation metrics based on the TPR, FPR, Jacquard index, and Dice coefficient are used. The proposed method is evaluated on two datasets of images.

Chapter 6 gives a detailed description of an edge-based method for kidney image segmentation. The proposed method is examined against a collected dataset to evaluate the detection accuracy of the proposed method. Several experimental results (quantitative and qualitative) are described. To evaluate the accuracy of the method, evaluation metrics based on sensitivity and accuracy are used.

Chapter 7 presents a summary of the three novel approaches for enhancing and segmenting kidney components by means of an active contour model and edge-based method for kidney image segmentation from low-contrast kidney MRI images, together with the contributions and limitations of the proposed methods, and recommendations for future work.

## **1.11 Summary**

This chapter presented the importance of the enhancement and segmentation of kidney images and motivation for the proposed research. The challenges faced regarding each topic were listed and discussed. Based on the challenges, the proposed work defined the problems as the research issues. To find a solution to the problems, the respective objectives were defined, and the scope and organization of the thesis were presented.

## CHAPTER 2: LITERATURE REVIEW

### 2.1 Background

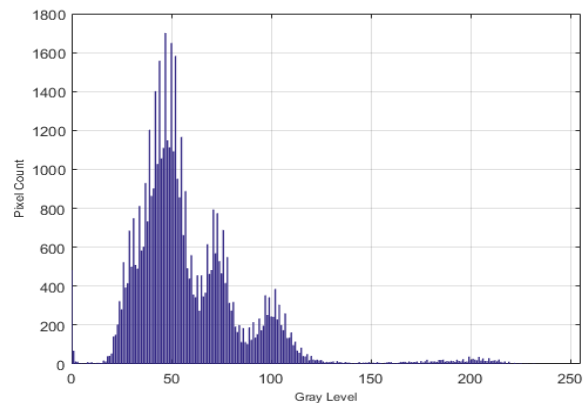
The previous chapter highlighted the importance of kidney image enhancement and segmentation. In addition, it listed the challenges of image enhancement and segmentation. However, the listed challenges should be justified through a review of state-of-the-art methods. Therefore, this chapter reviews the existing methods for the respective challenges to justify why they remain unsolved.

### 2.2 Kidney Image Enhancement

The aim of this section is to describe the detail of kidney images enhancement. Contrast enhancement are used to make images more legible to the human eye. Contrast manipulation involves changing the range of values in an image in order to increase the contrast. The motivation behind the image enhancement stage is by improving the contrast and removing noise. A contrast enhancement method maps the values of the intensities of an image to a new range. Figure 2.1 shows a low contrast original image with its histogram. In the histogram of the image (Figure 2.1(b)) all the values are unevenly distributed throughout the range.



(a)



(b)

**Figure 2.1: (a) Original Image (b) Histogram**

Various image enhancement techniques have been applied in medical imaging. The intensity adjustment technique is one of several image-enhancement approaches for enhancing the range of intensities in the output image. The low contrast of an image is increased by remapping the pixel's intensity to cover the entire intensity range [0, 255].

Histogram equalization is a computer image processing method that is used to enhance the contrast in an image. It spreads out the most frequent intensity values over the image. This strategy, for the most part, expands the global contrast of an image, where its usable information is characterised by a lower local contrast to gain a higher contrast.

Image enhancement is a fundamental step for enhancing the quality of original images. Many automated enhancement methods have been applied to different imaging technologies to enhance the quality of medical images, and these methods have been categorised in this chapter according to the different medical imaging modalities, as shown in Figure 2.2.

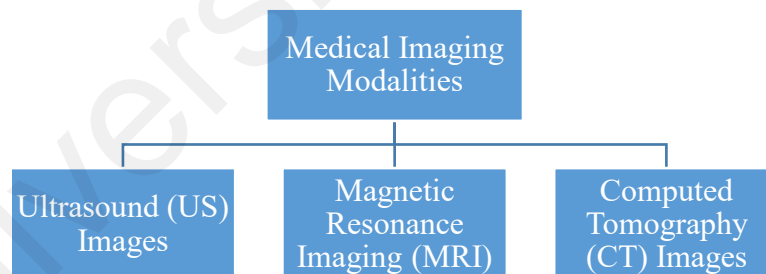


**Figure 2.2: Different Modalities for Medical Imaging**

Medical imaging is a powerful tool for visual illustrations of the internal organs of the human body (James & Dasarathy, 2014). kidney and its internal components can be visualized and evaluated through image modalities.

Images frequently suffer from low contrast, low resolution, noise, and blur, all of which affect image quality. For that reason, it is necessary to enhance the images to improve the process of segmenting the different components of an image. The proposed work reported

in this thesis is expected to enhance and segment poor-quality images associated with the abovementioned issues.

Three systems are used for imaging the kidneys and evaluating their functioning; namely, US, MRI, and CT. Each of these approaches has its own imaging capabilities and is used according to the purpose of the clinical evaluation at hand. These three imaging techniques are especially important in terms of their use in segmentation methods. Image acquisition methods affect image quality. Each imaging technique is subject to a specific issue; for example, ultrasound images tend to produce low-quality, low-contrast images, and are affected by speckle noise; MRI images suffer from low temporal resolution as do CT (ionizing radiation) images. Besides these issues, affected areas in such images are subject to poor quality due to geometric transformations, resulting in the poor-quality images that are considered in this work. To overcome these issues, the image enhancement model proposed in this thesis can adapt to properly enhance poor-quality images irrespective of the above-mentioned challenges.

One of the most important concerns is that most of the images suffer from different quality-related problems, as shown in Figure 2.3.

The existing image enhancement approaches have been categorised in this chapter according to the main goal of image enhancement, as shown in Figure 2.3.

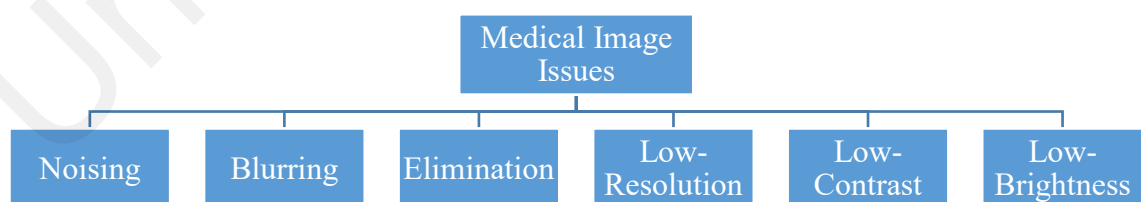


**Figure 2.3: Major Issues Related to Medical Images**

Most of the images suffer from different quality-related problems, the most important of which, according to the literature review, are noising, and low contrast. A simple explanation for each is presented below.

### 2.2.1 Image Noising

Image noise is unwanted signals in images and is usually an aspect of electronic noise. It can be produced by a camera or sensor and scanner.

#### a) Magnetic Resonance Imaging (MRI)

Issues related to noise are also common in MRI. Therefore, suitable methods to remove such noise – referred to as ‘de-noising’ – are necessary to enhance the quality of these MRI images, as described in the following literature.

Trinh, et al. (2011) proposed a novel learning method to eliminate Gaussian noise from MRI images based on Kernel Ridge Regression. However, this method does not work well for different noising degrees.

Yu & Li et al. (2012) implemented a new pre-processing method utilizing a total variation image de-noising model. A new watershed technique for MR renography image segmentation was proposed. To achieve smoothing and to improve the contrast in the image pre-processing procedure, a total variation model is used as a nonlinear filter. The pre-processing step is permitted to enhance and smooth the image, thereby enhancing the accuracy of the resulting watershed strategy.

A. Roy & Maity et al. (2014) suggested that the medical images are caught at low-measurement spaces in a compressed sensing (CS) paradigm for a different reasons. The reconstructed medical images after CS activity have been found to have an uneven force intensity of the organs. Some pre-processing task is fundamental for edge enhancement before the segmentation process is applied. Morphological tasks, namely erosion and dilation, might be utilized to catch the missing edges, shapes, boundary data and so on. Morphological tasks were then applied to the recreated MR images to acquire the detailed images, which were then added to the previous space. The segmentation was then done utilizing fuzzy c-means (FCM) clustering.

Kang, Lee, & Yoo et al. (2016) presented a semi-automated approach for kidney compartment segmentation of dynamic contrast-enhanced MRI images (DEC-MRI). An automatic and effective method for the segmentation of internal renal structures from MRI images is still lacking due to the low resolution of MRI images, contrast changes and intensity inhomogeneity in each kidney compartment. All of this makes segmenting the internal kidney structure a challenge. The presented method involved the following steps: 1) pre-processing of image to enhance the renal region; 2) use of connected component trees and maximally stable temporal volume (MSTV) for segmenting the whole kidney; 3) describing the segmented kidney voxels in an automated way by principle component (PC), application of the K-means clustering to the PCs, and labelling of the clusters; 4) application of the Otsu thresholding to remove noise and restore the kidney voxels that escaped detection. This method requires manual delineation and parameter settings and was designed to segment the kidney shape from a 2D ultrasound. It is not easy to segment the kidney shape from 3D ultrasound images by applying this approach.

#### **b) Computed Tomography (CT)**

Bhandari, et al. (2011) applied CT-image de-noising using a comparative analysis of curvelet- based techniques. Although this method performs well in decreasing the noise in an image, it is not effective enough for use with low-contrast-affected images.

Koyuncu, et al. (2017) proposed three algorithms for the denoising and enhancement of abdominal CT images. First, block-matching and a 3D filtering algorithm to achieve denoising to eliminate Gaussian noise in CT images. Second, the fast-linking spiking cortical model to eliminate fat tissues. Third, the Otsu algorithm to remove the redundant parts of an image (however, this method considers enhancement as a denoising process).

### **c) Ultrasound (US)**

US images that suffer from the problem of noise were described in the literature review Supriyanto, Tahir, & Nooh et al. (2011). Ultrasound images are usually filled with noise, and this can sometimes be a challenge to clinicians when it comes to measuring the kidney parameters. A segmentation instrument with a programmed recognition system is expected to facilitate clinicians or sonographers in completing their task in a shorter time. Supriyanto et al. (2011) developed a model that is able to automatically identify the centroid of a human kidney. An appropriate algorithm was constructed to handle fuzzy and noisy US images and also to recognize the centroid of the kidney. To reduce noise in an image, a Gaussian filter was utilized to eliminate small or unwanted objects. Next, a texture filter and morphological operator were used for the image segmentation. The algorithm failed to distinguish the centroid in some images because of noise in the kidney US images. The test outcome demonstrated that the product accomplished an accuracy of up to 96.43% in detecting the centroid.

F. Yang, Qin, & Xie et al. (2012) presented a new method for the segmentation of ultrasound (US) images of the kidney by a combination of non-local total variation (NLTV) image de-noising, with the distance regularized level set evolution (DRLSE). Initially, a de-noised US image is obtained by NLTV image de-noising. Next, DRLSE is applied in the kidney division to obtain a binary image. In this case, a black region and white region represents the kidney and background, respectively. In the last stage, the shape prior is applied to obtain a shape with smooth edges from the kidney shape space, which is then utilized to optimize the segmentation outcome of the second step.

Gungor & Karagoz et al. (2015) proposed a homogeneity map technique to decrease speckles in ultrasound images. The technique investigates the gradient data for improving the image quality. Also, the technique works as a de-noising filter for the removal of noise.

B. Li & Xie et al. (2015) proposed an adaptive fractional differential algorithm (AFDA) for enhancing medical images. Most medical images have a low resolution, low contrast, and significant noise, thereby making diagnosis difficult. The AFDA method, which segments edges, utilizes the improved Otsu algorithm and local information to process each pixel on the image. However, the method was developed to extract edges and enhance them in high-quality images, but not to improve poor-quality images.

Nikolic et al. (2016) presented an algorithm that is dependent on Canny edge detection for the recognition of inner organs in medical ultrasound images instead of using a Gaussian filter and median filter for removal noise. However, there is corruption of the edges.

Baselice, Ferraioli, Ambrosanio, Pascazio, & Schirinzi et al. (2018) used an enhanced wiener filter algorithm for ultrasound data restoration. The principal focus of the strategy is to decrease the impact of speckle noise by investigating the local Gaussian Marko random field. Moreover, the strategy adapts the wiener filter to such an extent that it tunes its portion to join the edges and preserves with an effective decrease in noise. The technique was produced for noise removal, but it does not enhance low-quality images of the kidney.

Most of methods mentioned focused on de-noising and noise removal for the enhancement of kidney images.

### **2.2.2 Low-Contrast Enhancement**

Contrast refers to the difference in intensity between the maximum and minimum pixels of an image. Contrast is determined by the difference between colors so that an object within an image can be distinguished from another object (Campbell, 1968).

### **a) Magnetic Resonance Imaging (MRI)**

The following literature review describes MRI images that suffer from the problem of low contrast. MRI systems use radio waves and magnetic waves to produce images of the body's internal organs. However, the combination of these waves does not guarantee that good-quality images will be produced. For this reason, the developed methods also take low-quality images into consideration.

Lausch, Ebrahimi, & Martel et al. (2011) presented a registration algorithm that is applied to abdominal dynamic contrast enhanced (DCE) MRI images. This algorithm is used to correct the intensity with a conjunction reference image scheme to minimize the effects of contrast during a registration performance related to intensity changes. However, this method only reduces the non-rigid motion and does not enhance poor-quality kidney images.

Min Zhang, Wu, Beeman, & Bennett et al. (2015) proposed efficient small blob identification based on local convexity, shape and intensity information. For detecting the blob, the technique improves the low-contrast data in the kidney images. It investigates the local convexity to enhance information in the kidney MRI images. The use of the technique is restricted to specific datasets and applications to enhance the contrast and noise removal application, but it does not enhance poor-quality kidney images.

### **b) Computed Tomography (CT)**

The following literature review describes CT images that suffer from the problem of low contrast.

Hassanpour et al. (2015), proposed a new method for enhancing contrast in poor-quality CT images. In this method, morphological Top-Hat transforms were used. This method can enhance the degree of contrast for different organs that overlap in medical

images. However, there is no evaluation metric available to determine the efficiency of this method.

Kallel & Hamida et al. (2017) stated that the performance of medical image processing methods, specifically in CT scans, is generally affected by low-contrast quality presented by medical imaging instruments. In this research, an advanced adaptive and basic method for the improvement of dark images was presented. This methodology is mainly based on adaptive gamma correction utilizing changes in discrete wavelet transform (DW) with single value decomposition (DWT-SVD). The limitation of this method is that the threshold utilized for the contrast must be set manually.

The article by Les et al. (2018) presented an inventive strategy for distinguishing the kidney region in computed tomography images. The method utilizes the examination of geometric coefficients and the investigation of brightness in the region conceivably involving the kidney. The kidney is physically marked (independently left and right kidney). Next, binary masks are made based on the shape of the kidney. Subsequent to the overlapping of the binary masks, the focuses that are frequently contained in the covered regions are checked. In this manner, the focuses are the beginning stages of the kidney acknowledgment calculations. To improve the representation of the kidney, a brightness correction is created, followed by geometric coefficients are calculated, after that image segmented using canny edge algorithm. However, this method needs user interaction to mark the left and right kidney.

### **c)      **Ultrasound (US)****

The following literature review describes US images that suffer from the problem of low contrast.

According to Rahman et al. (2013), the presence of noise and low contrast in ultrasound images makes the detection of the kidney a troublesome and challenging task. In this paper, Rahman developed and executed a system that can segment the human

kidney from ultrasound images. First, the input image is taken, and restoration is performed on that image. By lessening the noise and improving the quality of the image, a smooth resultant image is obtained utilizing a Gabor filter. Histogram equalization is utilized to improve the image quality. The entire procedure is divided into two stages: candidate extraction and pre-processing. The noise in low-contrast images is handled by a pre-processing step. After the removal of the noise, a proper segmentation algorithm is used to extract the kidney area. For a better outcome, a region-based segmentation is used to extract the kidney areas. Finally, refinement is performed to yield the fragmented kidney region from the original image. The eliminations for this examination require client interaction to decide on the seed point to initialize the segmentation process, and the kidney detection based on the intensities may not be reliable due to variations in the size and shape of the renal pelvis.

### **2.2.3 Fractional Differential Approach**

Fractional calculus is considered one of the numerous models of scientific formalism (Butzer & Westphal, 2000). Local fractional calculus is a generalized approach to integration and differentiation for functions defined on fractal sets (a fractal is defined as becoming a rough or fragmented form that can be broken down into smaller components, which can be observed as a smaller backup of the original form). During the last century, the notion of applying local fractional calculus from physics and engineering has attracted research in other domains. This has strengthened the relationships between the domains of fractal geometry and fractional calculus. Local fractional entropy is defined by calculating the local probability for each input pixel and multiplying for each pixel to enhance it. Fractal and fractional both refer to fundamental problems that arise in all fields of science and technology; fractals are geometrical objects with a non-integer dimension while fractional are the non-integer order of differential operators, as a result, the fractal falls within the realm of fractional calculus.

L'Hopital in 1695 pondered the importance of  $\frac{d^m f(x)}{d_x^m}$  for  $m = 1/2$  and, until the half of the nineteenth century (Butzer & Westphal, 2000). More recently, fractional calculus has been incorporated into the fields of anomalous diffusion, turmoil, polymer science, biophysics, and field hypothesis (Agrawal, 2002; Frederico & Torres, 2007; Herrmann, 2008). The idea behind the definition of a fractional derivative is to find an operator that generalizes the equation. Entropy measures the pixel intensity levels randomness, which reflects the complexity of image texture distribution in image.

The perception that the Shannon entropy can be characterized from the equation,

$$S = \lim_{t \rightarrow -1} \frac{d}{dt} \sum_i \bar{p}_i^t \quad 2.1$$

where  $p_i$  is the probability opened the likelihood of characterizing a new entropy function. Specifically, (Frederico & Torres, 2007) called attention to the fact that the Tsallis entropy can be communicated in an identical manner as the condition

$$S = \lim_{t \rightarrow -1} D_q^t \sum_i \rho_i^{-t} \quad 2.2$$

where the operator  $D_q^t$  is known as the Jackson derivative,  $q$  derivative defined as:

$$D_q^t = t^{-1} \frac{1 - q^{td/dt}}{1 - q} \quad 2.3$$

Jackson derivative plays important role in quantum groups (Jackson, Fukuda, Dunn, & Majors, 1910). Since the Jackson derivative assumes the significant role of detailing the non-commutative analytics, therefore, it is normal that quantum gatherings (Ubrico, 2001) may likewise play a significant role in the Tsallis formalism. Another types of entropy have been characterized with the utilization of variations of the Jackson  $q$ -subsidiary. (Borges & Roditi, 1998; Johal, 1998) proposed another thermos statistics that is dependent on the  $q$ -examination (Lavagno, Scarfone, & Swamy, 2007) and speculations of the Tsallis entropy.

G. Huang, Xu, Chen, & Men et al. (2015) proposed a new image enhancement algorithm that uses a fractional differential to enhance the edge information of an image. A type of filter that is dependent on the non-integer fractional differential is applied. The main idea of this method is to adjust two parameters of the filter, namely, the step and order, within a certain range. This method improves the noise-free state of the image and, at the same time, retains the contour data of the colour image. However, the data between neighbouring pixels are ignored during the image sampling

Ghatwary, Ahmed, & Jalab et al. (2015) presented an approach for tumours liver detection by classifying them through the fractional differential enhancement of CT images. The fractional differential is applied to improve the CT images of the liver by enhancing the texture and edge features. The detection process relies on the differentiation of normal tissues from abnormal tissues.

Al-abayechi, Jalab, Ibrahim, & Hasan et al. (2017) presented an image enhancement method based on a fractional Poisson for the segmentation of skin lesions using the watershed transform. The identification of abnormalities is done by the newly proposed segmentation method, which depends on a new filter to smooth the input images based on the fractional Poisson. The noise is eliminated, and a smooth image is obtained in the pre-processing step. Watershed and morphological operations are used to segment the skin tissue area.

Guan, Ou, Lai, & Lai et al. (2018) presented a novel image enhancement for medical images based on a fractional derivative and directional derivative. The method enhances the texture information for both high-frequency and low-frequency information by considering the surrounding data (such image edge, texture and clarity) and the structural features of various pixels, and takes into account the directional derivative framework when constructing the masks. In the first step, a mathematical system is proposed.

Secondly, the gradient of the image is calculated, and the mask is constructed with various values. Thirdly, to evaluate the image quality is selected.

Cao et al. (2018) presented an image enhancement using on fractional calculus. A fractional differential is used to enhance the texture information and remove noise, and a guided filter is used to estimate the illumination component to ensure the occurrence of fewer phenomena. A contrast limited adaptive histogram equalization is used to improve the contrast of the image.

The limitation of most of the methods mentioned is the use of global enhancements to enhance the images but not local enhancements, which are more effective due their ability to improve the regional contrast. The MRI kidney images usually contain different pixels quality in different regions; so that no need to consider local information, namely, the pixels in kidney edges, for enhancing the edge details in kidney images.

#### **2.2.4 Motivation of Kidney MR Enhancement**

With lifestyle changes come several health problems in equal proportion. New devices and frameworks have been developed to provide solutions to such problems. In some instances, despite the support of new systems in providing solutions for diseases, new problems are also being introduced because of complex situations (i.e., kidney diseases) and inherent limitations of the system function (Helena R Torres, Queirós, & Morais, 2018). For example, in kidney segmentation an MRI system generates a low-contrast image initially while scanning the body. Although the system generates a good-quality image after a few scans, it is difficult to predict the exact time and image number needed to obtain the desired quality. Accordingly, finding quality images involves laborious and time-consuming processes. Common diseases, including AKI and CKD, influence the shape of the kidney (Helena R Torres, Sandro Queiros, et al., 2018) because of swelling

of the neighbouring tissues of the kidney. Consequently, kidney enhancement has become a more complex and challenging task.

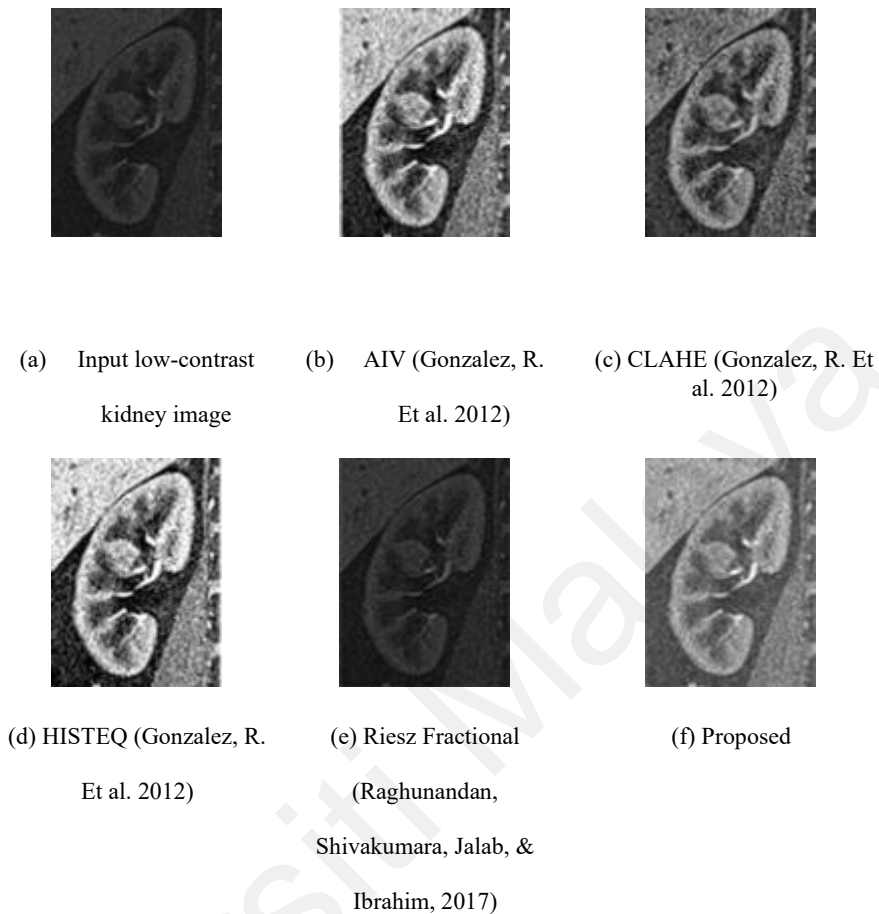


**Figure 2.4: Kidney Image Enhancement Challenges**

Figure 2.4(a) shows a low-contrast image created by the MRI system in which the kidney pixels and other tissues appear to be similar. Figure 2.4(b) presents the results of a method to adjust the intensity values to a specified range (AIV) (Gonzalez, Woods, & Eddins, 2012b). Figure 2.4(c) illustrates the results of a contrast limited adaptive histogram equalization (CLAHE) (Gonzalez, Woods, & Eddins, 2012a); Figure 2.4(d) shows the results of the histogram equalization (HISTEQ) (Gonzalez et al., 2012a). Figure 2.4(e) reveals the result of the Riesz fractional method (Raghunandan et al., 2018). Figure 2.4(f) displays the results of the proposed model.

In the strategies in Figure 2.4, the AIV, CLAHE, and Riesz fractional techniques did not enhance the edge details of the kidneys in comparison to the input image, whereas HISTEQ improved the details of the kidney edges and other areas in the image. However, the proposed model increased the contrast between the background and kidney edges. Thus, the edge details of the kidney boundary were sharpened. HISTEQ, AIV, and CLAHE are classical strategies that are used as a basis for developing new methods (Hart et al., 2002). However, such strategies are great when a full image is to be enhanced. The Riesz fractional technique (Raghunandan, Shivakumara, Jalab, & Ibrahim, 2018) is useful for improving low-contrast text images but not kidney images. As a result, the existing strategies used global enhancing which is not applied for kidney images which contain different levels of pixel intensity. Accordingly, there is a necessity to develop a new method that uses the local information for improving edge details in MR images of the kidney.

### **2.3 Kidney Image Segmentation**

In poor-quality images, the values of pixels of the kidney appear as highly similar to those of other bodily tissues; this means that the differences between such pixel values become difficult to determine. For this reason, image segmentation may not provide acceptable results due to the poor-quality images produced. This motivated us to propose an enhancement method to increase the contrast between the tissues of the kidney boundaries and other bodily tissues. This allows us to produce detailed images with sharpened edges, and this occurs when there are small changes in the intensity values that indicate the edges of the kidney in the image differences. On this basis, this image enhancement approach will be used in our proposed segmentation method.

One of the most significant topics in image processing and analysis is image segmentation. The objective is to slice an image into various segments and discrete areas, which is a significant initial step towards the analysis of the contents of an image. Image

segmentation is normally used to find boundaries (curves, lines, etc.) and to locate objects in images. It is used to label each pixel in an image (Petitjean & Dacher, 2011; H. R. Torres, Queiros, & Morais, 2018). Using different applications and modalities helped to show the challenges for kidney segmentation and the limitation also to show our motivation to proposing a new model for kidney segmentation from low-contrast MR images.

### 2.3.1 Active Contour Model

Active contour models can provide smooth contours and close shapes or surfaces to targeted objects with sub-pixel precision and have been applied to 2D and 3D image segmentations on different models (i.e. MRI, CT, US). These models can be formulated under an energy minimization system that is dependent on the hypothesis of surface development and geometric streams. A principal active contour model proposed by Kichenassamy et al. (1996) is known as the snake model because of the presence of contours. It can be effectively applied to manage a wide variety of computer vision applications. The snake model is described under the influence of image forces. Internal forces control the bending attributes, while image forces, for example, the gradient, serve to push the snake toward the image features.

The interior bending energy of the spline is defined as follows:

$$E_{int} = \alpha(s)|v_s(s)|^2 + \beta(s)|v_{ss}(s)|^2 \quad 2.4$$

Where  $v$ , vertices and the coefficients,  $\alpha$  and  $\beta$  are weighting parameters control the active contours, can be utilized to control the coherence attributes of the snake by changing its versatility and unbending nature. The application of this essential model is limited because of contour initialization. Berger (1990) was the first to essentially employ parametric models in the analysis of medical images to segment objects in 2D images. Be that as it may, this classic snake gives the precise area of the edges only if the initial

contour form is given adequately close to the edges, since they utilize only local data along the shape. This limitation demonstrates that essentially the snake alone is unable to serve the motivation behind a precise segmentation, and further adjustments and extensions are needed. (Cohen, 1991) merged an expansion force in the original snake model to stay away from local minima solutions, i.e., the bend ignores edges, and stops only if the edge is strong. However, this method does not work effectively for images with weak edges. Cohen & Cohen et al. (1993) utilized an interior expansion power to extend the spurious edges of the snake model. However, the snake method has a poor range of capture (less sensitive movement towards the real edges). Poon, Braun, & Fahrig et al. (1994) proposed an algorithm to limit the energy of the active contour model by utilizing simulated annealing. This technique improves the range of capture; however, noise and other image artefacts can cause incorrect districts or boundary discontinuities in items recovered by this strategy.

Erdt & Sakas et al. (2010) proposed a novel method for segmenting kidney images obtained. The global and local deformations of the kidney shape used to obtain the image segmentation. The shape of the model is adjusted in the global deformation, while protecting the global shape of the kidney. Moreover, the shape is deformed in the local deformation, while constrained utilizing local features. Both the global and local deformations are calculated so that the shape that is displayed fits the kidney boundaries.

Zhu, Zhang, Zeng, & Wang et al. (2010) proposed the gradient and vector flow (G&DVF) of the external force, which incorporates the GVF field and prior directional data manually given by the client. In (Qin, Zhu, Zhao, Bai, & Tian, 2013), a new external force called a component normalized-generalized GVF (CN-GGVF) was proposed, which enhanced the location of the concave regions, and the long and thin spaces.

(Prevost, Mory, & Correias et al. (2012) presented a modified system to segment the 3D contrast enhanced kidney images. The strategy is focused on two stages: first, the

kidney is automatically localized then, the segmentation achieved by maximizing the motion of the image gradient through the segmentation boundary. This task is mainly challenging because of the partial occultation of the organ.

Yao, Liu, & Liao et al. (2012) derived an external force sigmoid gradient vector flow (SGVF), which has a sigmoid limit before the GVF field is computed from the original image. The external force reduces the noise sensitivity and fits to minimize snake leakages. The fundamental solution of action is to improve the convergence of the snake for therapeutic image segmentation was jointly the work of (Wu, Wang, & Jia, 2013; Mengmeng Zhang, Li, Li, & Bai, 2013).

J. Huang, Yang, Chen, & Tang et al. (2013) proposed an active contour model to section kidney images by combining the local data with global shape prior. The local force, formed by the MLE of a Fisher-Tippett distribution, is utilized to describe the grey dimension, while the dark dimension insights are consolidated with the global characteristic of a kidney shape. The shape requirement is acquired by converting the segmented contour to a parameterized super-oval. The proposed model, which has two sub-problems, is comprehended by an exchanging minimization algorithm. One sub-problem is obtaining segmented contours for the fixed prior shape, and another sub-problem is discovering the deformation parameters of the super-ellipse for a given segmented shape. The two subproblems can be iteratively settled. A traditional gradient descent strategy is used for the parameters of the super-ellipse, while for the contour development issue, a fixed super-oval is adopted. Hung et al. (2013) made a convex relaxation of the functional and employed the split Bregman strategy to limit it because of the L1/L2 character of the convex relaxation. By doing this, the sectioned shape can be obtained quickly for a fixed super-ellipse, thereby improving the speed of the entire algorithm by the Fisher-Tippett distribution. Huang et al. proposed another active contour model to segment ultrasound kidney images. The drawback of this method is that it

requires manual interaction to prevent the model from fitting a non-kidney shape. This method is designed to segment 2D kidney images, so it cannot be easily extended into 3D kidney segmentation image.

In M. Zhang et al. (2013), a gradient vector convolution (GVC) field was proposed as the external force. This force is calculated by convoluting the gradient map of the image with a defined kernel. In any case, this method is limited to the segmentation of specific anatomical regions, for instance, the cardiovascular region in the left ventricle in MRI. M. Zhang et al. (2013) improved the GVF by utilizing a combination of a balloon and tangential power. This method is sensitive to a number of parameters.

Ling Li, Gu, & Wen et al. (2014) presented a segmentation method for kidney MRI images utilizing a multiscale geometric active contour model. The active contour methods (ACM) by (Caselles, Kimmel, & Sapiro, 1997) be separated into two classes: a parametric active shape model and a geometric active shape model. The geometric technique is a characteristics model. As a result of its arithmetical completeness, the geometric active contour is able to overcome many of the challenges of the parametric active contour. In any case, in medical images with heavy structural noise, the progression of the geometric active multiscale model will be seriously affected when dealing with this problem as the technique results in dimensional observational mode decomposition.

The main part of external forces was presented by Qin et al. (2013); Wu et al. (2013); Yao et al. (2012); M. Zhang et al. (2013); Zhu et al. (2010). The initial snake is set close to the targeted boundary to improve the segmentation accuracy, especially in the case where the proportion of image clutter and noise is high, for instance, in medical images. This inevitably incorporates the manual selection of several initial snake elements. Furthermore, they may fail to exactly drive the snake to the wanted boundary around weak edges (Y. Wang, Wu, & Jia, 2014).

In the paper by Abdulahi & Tapamo et al. (2015), a fast Chan-Vese (CV) with a simple shape display and connected component analysis (CCA) was proposed to segment the kidney in magnetic resonance imaging (MRI). A connected component analysis is performed on the mask acquired from a connected component set to reserve the conceivable applicant kidney by applying the associated segment investigation and shape prior after the fast CV. This demonstrated that the kidney can be productively outlined from the background. The study also compared Otsu's thresholding algorithm and the fast CV strategy. Further, the paper demonstrated that Otsu's adaptive thresholding model is better than the quick CV model as far as speed is concerned.

Evangelin & Suresh et al. (2015) presented a 2D model for the segmentation of the full kidney. To demonstrate the model in numerical experiments, a standardized gradient and Mahalanobis distance were utilized from the time courses of the segmented districts to a training set for image segmentation. The potential of the new methodology was exhibited in real MRI information from ten healthy volunteers. This segmentation term promotes the time course closeness of the voxels all through the kidney along these lines, thereby inferring that this segmentation has a high potential as a DCEMRI model for Kidney segmentation.

Qiao et al. (2016) proposed a new active contour method based on a diffusion stream strategy. The gradient vector flow (GVF) is used as an external force within the active contour. An adaptive diffusion stream is used, where the external GVF force is redefined according to the characteristics of the image. Hence, the active contour model can adaptively converge to specific concavities, while preserving the weak edges. Additionally, the procedure revolves around a tangent direction diffusion, which considers the convex shape of the kidney. An overview of the state-of-the-art segmentation strategies is shown in Table 2.1

A summary of image segmentation strategies is shown in Tables 2.1, 2.2 and 2.3. A few parameters are displayed in the tables, for example, the particular technique utilized in every class. The initialization strategy for each technique is also presented. The user interaction (UI) required by every strategy is additionally introduced. A segmentation method can be classified based on the amount of (UI) user interaction required, where (I0) refers to no user interaction required, (I1) initialization of segmentation methodology, (I2) region interest for the segmentation process, and (I3) modification contours during or after the segmentation method. Finally, the validation and limitations are also shown.

**Table 2.1: Overview of Active Contour Segmentation Method. (ND = not defined)**

Reference	Method of segmentation	Method of initialization	UI	Validation	Limitation
(Erdt & Sakas, 2010)	Surface deformation	To place shape model in kidney	I1, I3	30 Image	Does not work effectively for images with weak edges
(Prevost et al., 2012)	Active contours	Robust ellipsoid estimation	I3	21 images/ 64 images	Noise and other image artefacts cause incorrect districts or boundary discontinuities in items recovered by this strategy
(J. Huang, Yang, Chen, Tang, & Representation, 2013)	Active contours	ND	ND	-	Required manual interact to prevent the model from fitting non-kidney shape
(Ling Li et al., 2014)	Active contours	ND	ND	-	Discover the deformation parameters of the super-ellipse for given segmented shape
(Abdulahi & Tapamo, 2015)	Active contour	Initial-contour	I1	10 Images	Is to get the segmented

					contour for fixed prior shape,
(Qiao et al., 2016)	Active contours and adaptive diffusion flow	Threshold	I2	-	Unable to identify the kidney shape in low quality ct images

The active contour method for kidney segmentation has many limitations. Based on the above discussion and review, the active contour method does not work effectively for images with weak edges, while the snake method suffers from a poor capture range. Noise and other image artefacts can cause incorrect districts or boundary discontinuities in items recovered by this strategy. The proposed kidney detection methods will most likely be unable to identify the kidney shape in low-quality images.

### 2.3.2 Level Set Method

The level set technique presented by (Osher & Sethian, 1988) is a method for indicating active contours, and it is widely available in image segmentation. The level set method relies on the time, position, some energy functions, and geometry of the interface (Osher & Paragios, 2003). The level set function,  $\Phi(x, y)$  can be created for any input image to design the contour.

The outside and inside regions of the curve are given by the Lipschitz continuous function,  $\Phi$ , with the following characteristics:

$$\left. \begin{array}{l} \Phi(x, y) > 0 \text{ inside the contour} \\ \Phi(x, y) = 0 \text{ at the contour} \\ \Phi(x, y) < 0 \text{ outside the contour} \end{array} \right\} \quad 2.5$$

If the value of  $\Phi$  changes, some regions which are positive in the original will turn to negative, and some regions which are negative in the original will turn to positive. The contours will change position according to the level set function value.

Equation 2.4 for the level set function,  $\Phi$  can be written in general form as a non-linear partial differential equation :

$$\frac{\partial \phi}{\partial t} + v|\nabla \phi| = 0 \quad 2.6$$

In this equation,  $V$  is the velocity field, which is known as the speed function for the image segmentation part. The value of  $V$  depends on the level set function,  $\Phi$  and the image data.

C. Li, C. Xu, C. Gui, & M. D. Fox et al. (2010) presented a distance regularized level set evolution (DRLSE) as a new level set definition for image segmentation. The DRLSE was applied to the edge-based active contour method and gave a basic narrowband usage to drastically decrease the computational cost. The manual initialization used in this strategy is refined towards the kidney edges in an automated way.

The paper by Khalifa, El-Baz, & Gimel'farb et al. (2010) introduced a new work that combined a Markov Gibbs random field (MGRF) with a spatial variety of images with a mean curvature of the developing contours and its object background map to control the map direction and magnitude at every progression.

Hufnagel, Ehrhardt, Pennec, Schmidt-Richberg, & Handels et al. (2010) presented an automated segmentation method for multiple structure data by combining an implicit representation of segmentation with a statistical shape model (SSM). The model by Hufnagle et al. (2010) is explicitly represented via a shape prior knowledge point-based GGM-SSM. Then, the implicit level framework is incorporated with an explicit SSM, where the shape of the segmentation is represented by a zero dimension of a higher dimensional function.

Khalifa, Elnakib, Beache, & Gimel'farb et al. (2011) presented a 3D extension of a previous 2D stochastic controlling force introduced by (Khalifa et al., 2010) to deal with

the 3D geometric model for kidney region extraction from kidney images. The paper by (Khalifa, Elnakib, et al., 2011) described another novel and automated 3D segmentation method for the kidney from images of the stomach. The proposed 3D stochastic controlling force represented the previous 3D shapes, first a demand-intensity model, and second, a demand spatial interaction model between the kidney voxels and its background. The kidney border is removed from the surrounding stomach tissues using the geometric deformable model. The initial shape and appearance features are coordinated into a two-level joint Markov-Gibbs random field (MGRF) model of the kidney and its background.

Khalifa, Gimel'farb, El-Ghar, & Sokhadze et al. (2011) presented a new deformable model-based segmentation technique to exact the extraction of the kidney from images of the stomach. Khalifa et al. (2011) presented a 3D extension of a previous 2D stochastic controlling force introduced by (Khalifa, Elnakib, et al., 2011) to deal with an improved 3D approach for kidney segmentation using a level set-based deformable model. Its progression was constrained by a specially organized stochastic speed that represented the shape prior and features of the image intensity and spatial cooperation. The shape prior is learned from co-aligned 3D kidney data. The current visual appearances are described with marginal grey level distributions obtained by dismantling their mixture over the kidney data. The spatial interaction efforts between the kidney voxels are modelled by a 3D organized translation and rotation variation of the Markov-Gibbs random field (MGRF) for "object background" labels with a logically estimated potential. In (Khalifa, Soliman, Takieldean, & Shehata, 2016), the same team enhanced the strategy control by utilizing a non-negative matrix factorization technique to consolidate those features and also to derive the contour. (Khalifa, Soliman, Dwyer, & Gimel'farb, 2016) replaced the deformable model and random forest model, which were joined to the previous proposed features.

Noll, Li, & Wesarg et al. (2013) presented a programmed kidney detection and segmentation algorithm. The methodology uses essential kidney shape data to identify the kidney position. Following that, the level set calculation is applied to section the identification result. This combined technique may encourage doctors and unpractised learners to accomplish kidney identification and segmentation for symptomatic purposes. In this technique, the kidney is first identified utilizing an inquiry diagram approach. Then, a 3D ellipsoid model and an appropriate binary form are applied. As the last step, a level-set refinement and matching algorithm are used to segment the kidney. A consistent propagation speed with a defined limitation using a fast matching algorithm is used to the increase computational speed. However, this method has a low specificity and may wrongly detect other structures.

According to Lin Li, Ross, & Kruusmaa et al. (2013) because of noise in kidney images, these images, as a rule, have a low contrast, with shadows and blurry boundaries. Therefore, exact segmentation is challenging. Li et al. (2013) proposed another region-based level set strategy active contour calculation of images for kidney segmentation. The energy function of the calculation depends on the Chan-Vese energy function and distance. The image is divided into two sections. The calculation limits the contrast between each part and maximizes the distance of the density function between each part of the images of a phantom kidney and the real ultrasound medical images utilized for that.

Song, Wang, Liu, & Li, 2015a; H. Wang, Pulido, & Song et al. (2014) presented a segmentation of the renal area based on a two-level set technique. Wang and Song et al. (2015) utilized a distance regularized level set evolution procedure to portion the kidney boundary, followed by a region-scalable fitting force minimization method to segment the kidney. The parenchyma is chosen by subtracting the region from the gross kidney

area. This disadvantage of this framework is that the level set re-initialization results in numerical errors.

Hodneland, Hanson, Lundervold, Modersitzki, & Eikefjord et al. (2014) presented a combined dynamic contrast improved magnetic resonance imaging 4D DCE-MR model for the simultaneous registration and segmentation of the entire kidney. To use the model in numerical experiments, a normalized gradient is used as the information term in the registration together with a Mahalanobis distance from the time courses of the segmentation location to a training set for the supervised segmentation. The segmentation term influences the registration by enforcing a time course similitude of voxels inside and outside the kidney. Utilizing the time series information from ten diverse DCE-MRI examinations, conceivable and promising outcomes can be obtained, which are specifically identified by the smoothness of the voxel time courses and the small deviance in the lohexol-measured glomerular filtration rate (GFR). Energy minimization is achieved by evolving the contour and moving grid of the deformation.

Gloger, Liebscher, Tönnies, & Völzke et al. (2014) presented an automated kidney MR information segmentation utilizing the shape prior in a specific probability. In this research, a variation edge alignment force was proposed to guide the shape prior level set segmentation of the boundaries of the outer organs. The edge alignment force was developed and tested for an existing 3D level set method to segment the kidney parenchyma in MR datasets for an epidemiological study. Furthermore, the existing approach was extended to additional parenchyma features of all MR contrasts for segmentation. Information on the MR intensities of all the MR contrasts is incorporated into probability maps, which are generated through the use of discriminant. Reduction techniques combined with a probabilistic Bayesian approach. A method to calculate probability maps in proband-specific kidney regions was presented. The most accessible MR contrasts were used to create a singular probability map (Gloger et al., 2012),

Moreover, a variation plan was used to enhance the boundary force alignment. Another improvement was made (Gloger, Tönnies, Laqua, et al., 2015) through the computation of a subject explicit probability map. In a comparative work, the procedure was additionally connected to allow the segmentation of the kidney parts (medulla, and cortex). Tissues expressed in probability maps were joined with fuzzy clustering to separate the previous parenchyma into the relevant compartments. In (Gloger, Tönnies, Mensel, Völzke, & Biology, 2015), a support vector machine algorithm was joined to a Fourier descriptor for the shape features to generate the probability maps

Shehata, Khalifa, Soliman, & Alrefai et al. (2015b) proposed 3D kidney segmentation based on a geometric level-set deformable model from diffusion weighted magnetic resonance imaging (DW-MRI). This method combines different image features and has the potential to deal with a level set deformable model. The proposed deformable method is based on an adaptive prior guided by visual appearance. The level set is obtained by integrating the joint Markov-Gibbs random field (MGRF) of the kidney with the background. Experimental results showed that better segmentation occurred than in the level set. This can be explained by the additional adaptive shape model and the spatial features, which enabled the model to perform robust kidney segmentation despite the image noise, anatomical differences, and equivalent intensities of the kidney and surrounding tissues. In order to validate the performance, a comparison of various types of level set systems was made by (Shehata, Khalifa, Soliman, & Alrefai, 2015a). (Liu, Soliman, Gimel'farb, & El-Baz, 2015) proposed a similar method where parameter estimation was done through the MGRF, integration appearance and shape prior of the level set energy function.

In Song et al. (2015a), a distance regularized level set evolution (DRLSE) method was presented to segment the kidney area from 2D ultrasound images. This strategy was followed by an area-scalable energy minimization. The favorable position for this strategy

kept up the consistency for the level set function throughout the evolution. Although this strategy has great validity, it requires the interaction of the client to initialize the section strategy.

Marsousi, Plataniotis, & Stergiopoulos et al. (2017) proposed a technique for distinguishing and segmenting a 3-D kidney shape using a line training dataset. This fast and effective strategy is applied to overcome images explicit problems, namely speckle noise, low boundary contrast, partial kidney occlusion, and probe misalignment, which limit the use of the solution. This paper offered another shape model called the complex-valued implicit shape model by consolidating prior information of prepared shapes and anatomical learning. After that, the recognized kidney is segmented utilizing a novel complex area-based level set methodology. However, there are three drawbacks to this methodology. First, the proposed kidney detection will most likely be unable to identify the kidney shape in low-quality ultrasound images. Second, the pre-processing module is unable to adequately isolate the voxels of the kidney shape from non-kidney voxels. Third, the enrolment system fails to fit the kidney shape shown on image.

Turco, Valinoti, & Martin et al. (2018) proposed a completely automated segmentation technique to compute the total kidney volume (TKV) from non-differentiated information in patients with autosomal dominant polycystic kidney disease (ADPKD). The proposed segmentation technique relies on deformable-models and level-set function development. The means as pursued: 1- The scope of the pixel forces in connection to the histogram of the kidney zone was investigated. This procedure enables the bones and different structures that are not targeted to be concealed. 2- Next, to lessen the noise by keeping the edge refinements, a non-local implicit-based channel was performed. 3- A K-means methodology was used to group the volumes. The kidney was distinguished in mechanically by considering the more noteworthy local regions. 4- Once the level set function was initiated, its advancement was guided by the image slope data, which laied

out the last renal shapes. 5- The automated strategy was actualized and connected manually according to the outcomes. 6- The kidney volumes from the mechanized and manual tracings were processed by summing up the results of the region inside the renal shape on each image and the thickness of the cut. 7- The understanding between the two techniques was assessed utilizing linear regression, and the Dice similarity coefficient. A Bland-Altman investigation presented a low bias (- 0.3%) and thin limit of understanding (11%), while the Dice coefficient showed a value of  $0.91 \pm 0.02$ , which was thought to be very high. This technique was tested on 21 patients. A bigger dataset is required to demonstrate the validity of the proposed methodology. Based on the underlying outcomes, future investigations should seek to improve the technique for further approval.

Currently, several different deep CNN models have been proposed: AlexNet, GoogleNet, DenseNet, and U-Net (Ronneberger, et al. 2015). These deep CNNs are applied in a range of different applications such as object detection, segmentation, and image classification. For kidney segmentation, Thong et al. (2018) proposed a kidney segmentation algorithm at variable pixel densities by using a convolutional networks approach. The method was evaluated using a collected dataset of 79 scans. However, while this method achieved accurate segmentation, it required high computation time.

Sharma, et al. (2017) presented a fully automated CNN made up of different layers, which learned features without using any handcrafted features. This model was tested using a patient dataset of 244 image acquisitions. However, this method suffered from the identification of false positives due to small, isolated noise, which was wrongly classified as foreground.

From the above review of the CNN models of kidney segmentation, it can be observed that most of these CNN models are based on the U-Net architecture, which works well with certain selected types of kidney images.

The problem considered in this thesis is complex as it involves poor-quality images affected by several adverse factors such as MRI system issues, noise, and different diseases. Therefore, the effect of each of these adverse factors on the images is unpredictable. In this situation, there is a need for generalized models that work well irrespective of these challenges. The current work is motivated by the challenge of proposing models that do not involve deep learning for enhancement and segmentation. This is because the performance of such deep learning models depends on the number of training samples used and the huge number of images involved in the training process. Further, it is uncertain whether the training samples include all the possible cases of the images, which limits generalization. In addition, collecting a huge number of images in the case of medical imaging is difficult. Therefore, using a deep learning-based model may not be robust enough for different datasets and applications compared to hand-crafted features that include fewer samples to determine the values for the conditions and parameters.

Over the last few years, the fuzzy technique has played an important role in image enhancement due to its ability to capture and represent uncertainty in the form of membership. Joshi, et al., (2018) proposed a fuzzy inference system (FIS) for enhancing contrast in low-resolution images. For each input image pixel value, the input membership function (Gaussian) fuzzified these pixels by assigning each pixel to the class with the highest membership value. Next, based on the rule IF-THEN, the input image is mapped to output. Finally, using the output member function, the defuzzified value obtained. However, obtaining image contrast enhancement using these stages is computationally expensive.

Fernandes et al. (2019), presented an adaptable contrast-enhancement technique employing fuzzy logic. Fuzzy common sense is relatively effective at handling ambiguous and vague data. Since contrast may also be considered to be a vague term,

fuzzy principles can be effectively applied to amplify the distinction of an image. Establishing an adaptable fuzzy inferencing system usually determines the pixels of the output depending on the contrast measure associated with the input image. This method can be applied to images requiring improvement in which excellent high-quality noise suppression should be present as well as lower illumination gain will be tolerable.

However, the above-mentioned methods may not work well for our kidney image enhancement task because kidney MRI images are affected by multiple adverse factors such as noise and low contrast. In this situation, deriving the fuzzy membership function is difficult because poor- quality input images are unpredictable. Therefore, generalized models (e.g., Gonzalez, Woods, & Eddins, 2012a; Gonzalez, Woods, & Eddins, 2012b) perform better than fuzzy-based models for enhancement in this thesis. This is because general methods can deal with different situations while methods developed for a specific purpose may not be sufficiently robust for complex images.

An overview of the state-of-the-art level set segmentation strategies is shown in Table 2.2.

**Table 2.2: Overview of Level-Set Segmentation Method. (ND = not defined)**

Reference	Method of segmentation	Method of initialization	UI	Validation	Limitation
(F. Yang et al., 2012)	level-set (DRLSE)  (Denominated distance Regularization level-set evolution)	-	ND	14 images	Lack of robustness to noisy area
(Lin Li et al., 2013)	Level-set	ND	ND	-	The restriction for this technique it's connected on 21 patients just to demonstrate legitimacy of the introduced methodology

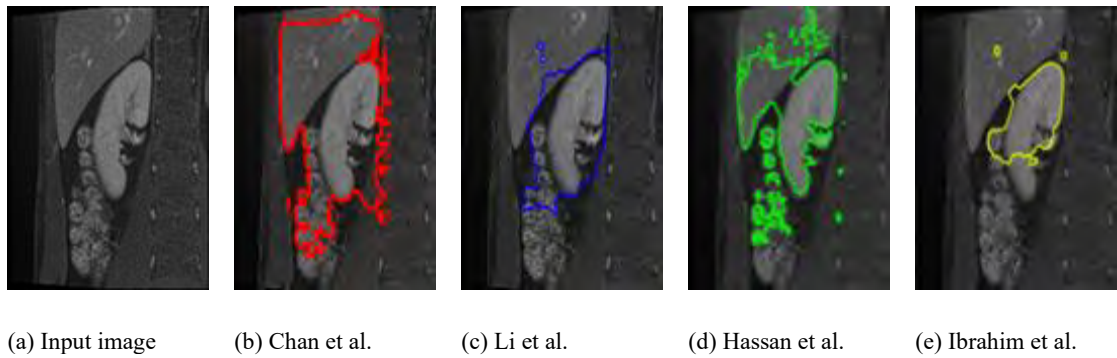
					bigger dataset required
(Noll et al., 2013)	Level-set and fast marching algorithm	Graph searching	I0	61 images	this method has low specificity may wrongly detect other structures.
(Song, Wang, Liu, & Li, 2015b)	DRLSE (Denominated distance Regularization level-set evolution)	-	I1	10 Images	Frame work the level set re-initialization caused numerical errors. This technique utilizes a manual initialization, which is then therefore refined towards the kidney boundary
(Hodneland et al., 2014)	Level-set and Registration	2D training masks	I1	20 images	require client interaction to intialization of section strategy
(Gloger et al., 2014) (Gloger et al., 2012) (Gloger, Tönnies, Laqua, et al., 2015) (Gloger, Tönnies, Mensel, et al., 2015)	level set and fuzzy clustering	Kidney probability map	I0	- 30 dataset 25 images 25 Images	This method is robust to changes in the parameterization
(Shehata et al., 2015b) (Shehata et al., 2015a)	Level set	Estimation of MGRF parameters	I2	40 datasets	Need to Estimate parameter
(Liu et al., 2015)	Level set	Estimation of MGRF parameters	I1,I2	50 datasets	Need to Estimate parameter

					And require client interaction to initialization of section strategy
(Khalifa et al., 2010)	Level set	Circular contour	I1	21 Images	This techniques were not designed to deal with low contrast
(Hufnagel et al., 2010)	Level set and SSM (Statistical Shape Model)	To place SSW in kidney with an evolutionary algorithm	I0	-	Need a prior shape knowledge
(Cuingnet et al., 2012)	Template deformation	Regression forests	I0	179 images	Overfit for dataset used with noisy segmentation
(Khalifa, Gimel'farb, et al., 2011)  (Khalifa, Elnakib, et al., 2011)  (Khalifa, Soliman, Takieldean, et al., 2016)	Level-set	ND	I1	14 datasets  29 Patients  36 datasets	This techniques were not designed to deal with low signal to noise ratio , low contrast , and diffusion boundaries

From the above discussion and review, the level set methods for kidney segmentation have many limitations such as lack of robustness towards noisy areas, and numerical errors resulting from the level set re-initialization. These techniques utilize manual initialization. Therefore, such methods cannot adequately isolate kidney shape voxels from non-kidney voxels. They are also robust to changes in the parameters and are designed to deal with low-contrast images.

### 2.3.3 Motivation of Kidney MR Segmentation - Active Contour Model

Many popular models have been proposed to address the issues that have been discussed. They can be categorized broadly as models that propose a generalized method for the segmentation of a region of interest in medical images. For example, an active contour model was established to segment brain tumours (Hasan et al., 2016). Ibrahim et al. (2016b) proposed a method for segmenting bacterial growth in microscopic images based on fractional operators. Since these methods use a generalized idea, they do not perform well in segmenting the kidney region from MRI images. The two methods shown in Figures 2.5(d) and 2.5(e) failed to segment the kidney region accurately. More robust methods for segmenting the kidney region from images have been proposed to overcome these limitations associated with active contours and models (Chan, Sandberg, & Vese, 2000; Chunming Li et al., 2010; L. Wang, Chen, & Shi, 2018) by using a level set (Chunming Li et al., 2010). Both models exploit the gradient descent for energy minimization in different ways. The gradient-based energy minimization model is not robust because of inhomogeneous intensity values and poor image quality. The input image in Figure 2.5(a) was affected by low contrast and degradations (i.e. poor-quality images). The active contour model (Chan et al., 2000) failed to segment the kidney correctly. Poor segmentation results are mainly attributed to the algorithm, which suffers from the tuning parameters of the model and local minimum problems. Therefore, models such as the Chan–Vese algorithm, which explores the gradient-based energy minimization function, may not work well on low-contrast and degraded images. Thus, the proposed work introduced a fractional Mittag–Leffler energy minimization function for kidney segmentation, which considers the advantages of fractional calculus. Further details can be found in the proposed methodology in Section 5.2.



(a) Input image (b) Chan et al. (c) Li et al. (d) Hassan et al. (e) Ibrahim et al.  
**Figure 2.5: Motivation for the Proposed Work on Kidney Segmentation**

### 2.3.4 Edge-based Method

A representation of the edges of an image will reduce the amount of information to be handled, while holding the basic data about the shape of object in the scene. This explanation of an image is easy to incorporate into a lot of object recognition algorithms utilized in computer vision alongside other image processing applications. The significant characteristic of the edge identification strategy is its ability to extract a definite edge line with great orientation, as shown by the increased literature about edge detection that has been accessible over the past three decades.

Edge detection is a basic tool for image segmentation. Edge detection techniques change the original images into edge images, which profit by the grey level progressions in the image. In the preparation of the images, particularly in PC visions, the edge recognition handles the restriction of critical varieties of a grey level image and the detection of the physical and geometrical properties of objects at the scene. It is a basic procedure that recognizes the frame of an object, its boundaries, and the background in the image. Edge detection is the most common methodology used for distinguishing critical discontinuities in intensity values. Edges are neighbourhood changes in the image intensity. Edges typically occur on the boundary between two regions. The main feature is that such intensities can be extracted from the edges of an image.

Edge detection is considered as an active research area in which it facilitates a higher level of image analysis. There are three unique kinds of discontinuities in the grey level,

namely, lines, edges and points. A spatial mask can be used to recognize all three kinds of discontinuities in an image. There are many edge detection techniques for image segmentation in the literature (Thong, Kadoury, Piché, & Pal, 2018; H. R. Torres et al., 2018).

Canny used as pre-processing step for our second proposed segmentation method, for this reason we considered Canny edge detection in literature review. A discontinuity-based edge detection procedure that is commonly used is the Canny edge detection technique. This is a standard edge detection strategy that was first introduced by John Canny in 1983, and it is still able to outperform many of the newer algorithms that have been created. It is an important method for finding edges. It first removes the noise from the image before detecting the edges of the image.

The Canny edge strategy (Canny 1986) attempts to enhance the image edge recognition by distinguishing the edges between various areas. The edge strategy has an advantage in that it radically reduces the amount of information to be processed, while saving auxiliary data about the boundary of the object (Shrimali, Anand et al., 2009). The execution of the Canny edge identification depends on a Gaussian filter to not only remove the image noise and smoothen the image details, but also weaken the edge data.

The Canny algorithm process can be broken down into 5 steps:

- Apply a Gaussian filter to get a smooth image by removing the noise.
- Calculate the intensity gradient of the image.
- Apply a non-maximal suppression to the gradient magnitude.
- Apply a threshold to locate the potential edges.
- Suppress all the weak edges and keep the strong ones.

Tomasi and Manduchi et al. (1998) adjusted a bilateral filter to perform edge recognition, which is the inverse of bilateral smoothing. The Gaussian domain kernel of a bilateral

filter is replaced by an edge location mask, and a Gaussian range piece is replaced by an inverted Gaussian kernel.

Chai et al. (2011) presented a speckle-reducing anisotropic diffusion (SRAD) system in the image de-noising portion of the Canny algorithm structure. The proposed technique removes speckle noise related to image details. A comparable methodology was presented by (Nikolic et al., 2016). However, in this method, diverse procedures and distinctive phantom images are used. In this study, Nikolic et al. (2016b) proposed a change in the Canny administrator by supplanting the Gaussian filter with an adjusted median filter and a weighted dynamic smoothing level.

Those strategies do not segment the kidney accurately. Thus, the models that investigate the Canny edge by using various filters may not function well for low-contrast and degraded images. As such, it is necessary to develop a potentially viable strategy for a kidney MRI segmentation model based on the use of kidney edge components, while preserving kidney-segmented edge information from low-contrast MRI images. An overview of state-of-the-art edge-based model segmentation strategies is shown in Table 2.3.

**Table 2.3: Overview of Edge based Model Segmentation.**

Reference	Category of segmentation	Limitation
(Tomasi & Manduchi, 1998a)	Canny (adjusted a bilateral filter)	Fail to precisely meet the desired boundary if the noise level in an image is high
(Shrimali, Anand, & Kumar, 2009)	Canny (Gaussian filter)	Gaussian filtering not only remove image noise and smoothers image details, but also weakens the edge data.
(Chai, Wee, & Supriyanto, 2011a)	Canny (SRAD filter)	Not work well for poor quality and degraded images
(Nikolic et al., 2016)	adjusted median filter	Not function well for low contrast and degraded images

There are many limitations to the edge-based segmentation method, according to the above discussion and review. It fails to precisely meet the desired boundary if the noise level in an image is high, and it does not work well for poor-quality and degraded images.

In view of the many limitations of the segmentation methods described in the above discussion and review, this study was carried out with the aim of proposing a generalized and new model for kidney segmentation from low-contrast MR images.

### **2.3.5 Motivation of Kidney MRI Segmentation - Edge based Model**

It should be noted that most edge recognition techniques require denoising strategies and the enhancement of the resolution of MRI images to decrease the image noise, whereby the signal sparse representation is utilized to evacuate unwanted structures in the region. The Canny edge detection, which was proposed by John Canny in 1983, is one of the standard edge detection strategies. It is mainly used to detect the edges of an image by first removing noise from the image.

The Canny edge detection strategy (Canny, 1986) attempts to illuminate the edges of an image by distinguishing them from various areas. The advantage of this strategy is that it can be used to investigate images by reducing the proceed information, while saving essential auxiliary data about the boundary of the object (Shrimali et al., 2009). However, the Canny edge detection strategy may still fail to precisely meet the desired boundary if the noise level in an image is high because noise and edges include high-frequency components.

Tomasi and Manduchi et al. (1998) adjusted a bilateral filter to perform edge recognition, which is the inverse of bilateral smoothing. The Gaussian domain kernel of a bilateral filter was replaced by an edge location mask, and a Gaussian range piece was replaced by an inverted Gaussian kernel.

Chai et al. (2011) presented a speckle-reducing anisotropic diffusion (SRAD) system in the image denoising portion of the Canny algorithm structure. The proposed technique

removes speckle noise related to image details. A comparable methodology was exhibited by (Nikolic et al., 2016). However, in this method, diverse procedures and distinctive phantom images are used, which means that a designed object is scanned or imaged in the field of medical imaging to analyse, evaluate, and tune the performance of different imaging devices. In this study, Nikolic et al. (2016b) proposed a change in the Canny main algorithm by replacing the Gaussian filter with an adjusted median filter.

The literature review of edge detection techniques demonstrated that numerous difficulties were encountered in kidney edge detection. The input image in Figure 2.6(a) was influenced by low contrast and corruptions. As such, Figure 2.6(b) presents the results of the traditional Canny method (Canny, 1986), Figure 2.6(c) illustrates the results of the SRAD method (Chai et al., 2011a), and Figure 2.6(d) shows the results of the bilateral-Canny method (Tomasi & Manduchi, 1998a). These strategies were unable to segment the kidney accurately. Thus, the models that investigated the Canny edge strategy by using various filters may not function well for low-contrast and degraded images. As such, it was proposed to develop a potentially viable strategy for a kidney MRI segmentation model based on the use of kidney edge components while preserving kidney-segmented edge information from low-contrast MRI images, in accordance with the applied Canny edge recognition calculation and other conditions.

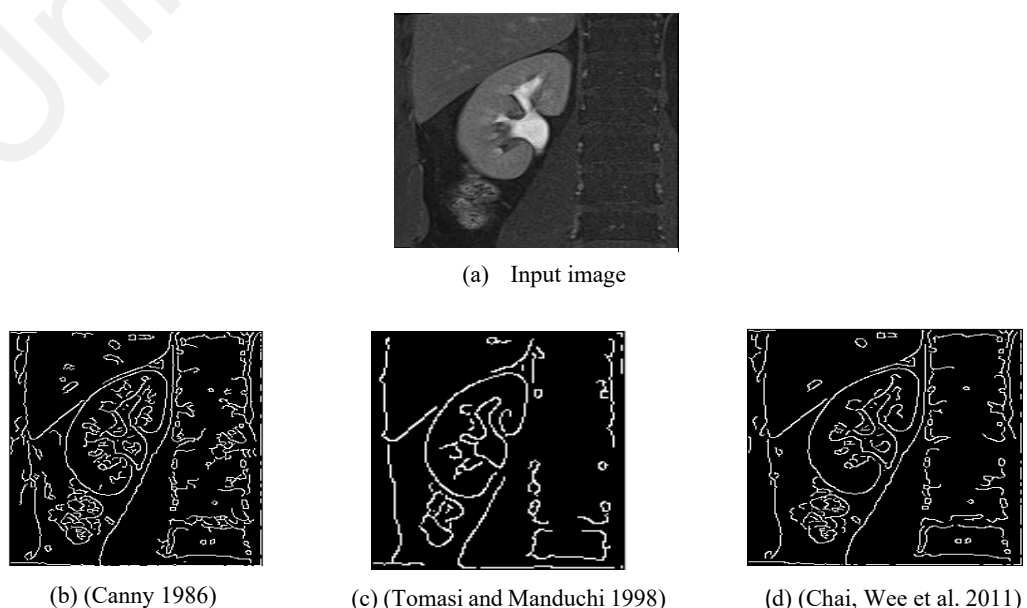


**Figure 2.6: Challenges of Kidney Boundary**

## 2.4 Evaluation Metrics

The progression and quality of medical imaging are essential for disease diagnosis. Some MRI images may present distortions during image acquisition, reproduction, pre-processing, and post-processing, possibly corrupting image quality. As such, image quality assessment (IQA) (Barrett, 1990) has emerged as an imperative issue in numerous fields and applications such as in image acquisition, compression, transmission, enhancement, and segmentation. IQA has become essential for assessing new software or hardware of imaging systems. IQA can be divided into two classes: objective and subjective evaluation. In an objective evaluation, a mathematical model is used to assess image quality, while in a subjective evaluation, image quality is assessed by a medical practitioner. Most image quality studies involve task-specific models for assessment and arrangement (Barrett, 1990); (Dutta, Ahn, & Li, 2013). The medical image quality is largely considered as a function of perceptibility of a specific illness or is causally linked to accuracy in diagnosis. Such task-specific model groups can distinguish between normal tissues and tumours that exist in the region of interest (ROI). An IQA considers the right classification as good image quality and the wrong classification as poor image quality. Nonetheless, an IQA of natural images has a distinctive methodology, and numerical models are used calculate a score that corresponds to the image quality that is conceivable to human judgment. Mathematical models reflect several factors, including contrast (Fang et al., 2015), luminance (Mittal, Moorthy, & Bovik, 2012), distortion (Moorthy & Bovik, 2011), complex measurement of an image (Ye & Doermann, 2012), texture measurement statistics (Tang, Joshi, & Kapoor, 2011), image highlights (Mittal et al., 2012), and natural scene statistics (NSS) (Mittal et al., 2012); (Moorthy & Bovik, 2011) (Saad, Bovik, & Charrier, 2012). Target techniques are additionally grouped into reduced reference (RR), full reference (FR) (Mittal, Soundararajan, & Bovik, 2013), and non-reference or blind

(NR) techniques (Mittal et al., 2013), depending on the amount of data accessible from an original image as a source of perspective:

- In FR strategies, a whole unique image is utilized as a reference image. This technique compares a distorted image with the original image. Some examples are mean squared error (MSE) and peak signal-to-noise ratio (PSNR), which are both the bases for a mathematically defined image quality.
- In RR techniques, the whole original image is inaccessible as a reference. Only some features about texture or other reasonable descriptive features of the original image are given.
- In blind or NR strategies, the original image is completely inaccessible. The pixel domain of a distorted image is used to search for artefacts.

FR and RR strategies require the accessibility of a reference image against the test image, classified as Jaccard's similarity coefficient (JSC) (Jaccard, 1901) and Dice's similarity coefficient (DSC) (Dice, 1945). In numerous applications, the reference image is inaccessible, so it cannot be compared with the test image. As such, the application of FR-IQA and RR-IQA algorithms is limited, and reliable NR-IQA calculations are required. NR-IQA depends on the rule that natural images have certain regular factual properties that are quantifiably adjusted by the presence of distortions. This technique is suitable for evaluating the nature of an image without a reference image.

The datasets for this research were collected from two different sources to evaluate the performance of the proposed and existing methods. The datasets included low contrast, low resolution, noise, complex background, inhomogeneity, and other surrounding tissues of MRI images.

### 2.4.1 Image Quality Assessment

Since no standard dataset for kidney image segmentation available in the literature, datasets collected. In order to measure the performance of the proposed enhancement model, the research adopted standard and no-reference measures to compare between the proposed method and other kidney enhancement methods (BRISQUE),(Mittal et al., 2012) and (NIQE)(Mittal et al., 2013) methods.

The BRISQUE, a no-reference image quality measure. The lower value of BRISQUE represents a better perceptual quality of an image. A BRISQUE score correlates well with the human perception of quality.

The naturalness image quality evaluator (NIQE) is also a no-reference image quality measure. A smaller score of NIQE specifies better perceptual image quality. However, a NIQE score does not correlate with the human perception of quality as reliably as the BRISQUE score. The NIQE model is not trained using subjective quality scores, so a NIQE score does not correlate as reliably as a BRISQUE score with the human perception of quality. The BRISQUE model is trained using subjective score opinions.

The proposed method was independent of datasets and applications. The proposed model can be applied to enhance other poor-quality images. Therefore, it can be deduced that the proposed model outperforms the existing methods in terms of application, as well as the BRISQUE and NIQE scores.

The standard measures, namely, sensitivity and accuracy, were used to measure the performance of the proposed model.

## 2.4.2 Segmentation Assessment

### Sensitivity:

The sensitivity coefficient was calculated from the results by using a manually segmented image. Sensitivity is the percentage of pixels recognized by the algorithm. It is provided by the following equation:

$$\text{Sensitivity} = \frac{TP}{TP+FN}, \text{ where} \quad 2.7$$

TP (True positive): number of pixels from A correctly classified like B

FN (False Negative): number of pixels from A incorrectly unclassified as B

A: Automatically MRI segmented

B: Manually MRI segmented

### Accuracy

Accuracy is the ratio of elements that correctly classify the variable elements, and it is calculated as follows:

$$\text{Accuracy} = \frac{TP+TN}{TP+TN+FP+FN}, \text{ where} \quad 2.8$$

TP (True positive): correctly segmented region as a kidney

FP (False positive): falsely segmented region as a kidney

TN (True negative): correct region detected as non-kidney

FN (False negative): false region detected as a non-kidney.

In the assessment of the segmentation process, both sensitivity and accuracy are not always significantly relevant because both methods of assessment depend on the segmented region. Evaluation is performed based on the segmented region but not the size of the region. The numerator and denominator of Equations (2.7) and (2.8) do not include the size of the kidney region. The numerator and denominator are simply the numeric values of the pixels compared with the ground-truth images under testing. For this reason, two additional metrics were used, namely, the Jaccard index and Dice coefficient (Hasan et al., 2016). The JSC and DSC were also used to compare between

the proposed method (kidney MR image segmentation-active contour model) and other kidney segmentation methods (such as active contour methods, level set functions), depending on the available ground truth for the input images.

### JSC

The Jaccard coefficient measures the similarity between two dataset samples and is defined as the size of the intersection features divided by the size of the union of sample sets.

JSC (Jaccard, 1901) is defined as  $Jaccard(I, G) = \frac{card(A \cap B)}{card(A \cup B)}$ , where 2.9

- A: Automatically segmented region.
- B: Manually segmented region (ground truth)
- Card (X): Indicates the pixel number in region X

### DSC

The DSC (Dice, 1945) is used to compare the similarity between two data sets: automatically-segmented region and manually-segmented region.

The DSC is defined as  $Dice(I, G) = 2 * \frac{|intersection(A,B)|}{|A|+|B|}$ , where 2.10

A: automatically segmented region

B: manually segmented region (ground truth)

The higher JSC and DSC values indicated that the proposed model was good and preserved the shape of the kidney. Further, a number of iterations were produced by the proposed model for kidney segmentation to measure the efficiency of the proposed model. Since the efficiency of the proposed segmentation method measures how fast this method can segment the kidney body correctly, this involves time complexity. The time complexity of the proposed segmentation method is a function that provides the running iteration time for kidney segmentation. Since the above-mentioned measures required ground truth, the kidney region had to be segmented manually by the user, where the

segmented regions were further verified by a doctor who was an expert radiologist. At the same time, the results given by the proposed and existing methods were verified by the same doctor to calculate the measures (JSC, DSC).

## **2.5 Summary**

This chapter reviewed the methods in relation to kidney enhancement and segmentation. Many enhancement and segmentation methods have been proposed for CT and MR images. It was noted from the review of the image enhancement and segmentation methods that most of the methods focused on a particular application and issue. Therefore, it is confirmed that a generalized method for kidney image enhancement and an efficient method for kidney region segmentation are still considered as open issues in the field of medical imaging.

Universiti Malaysia

## CHAPTER 3: RESEARCH METHODOLOGY

### 3.1 Background

The challenges in kidney image enhancement and segmentation were justified by reviewing the existing methods for the respective topics. This chapter presents the four main phases of the research methodology. Phase 1 presents the requirements and study analysis, and the three other phases are representing the design and implementation of three proposed algorithms for kidney image enhancement and segmentation. The description of each phase is given in the following subsections.

### 3.2 Research Phases

As shown in Figure 3.1, the implementation phase consisted of three methods. The first proposed algorithm presented a novel model for image enhancement of low-quality kidney MRI images using fractional entropy. The presented model evaluated the probability of the pixels representing the edge that was dependent on the entropy of the neighbouring pixels, thereby resulting in local fractional entropy. The details of the proposed method are discussed in Chapters 4, 5, and 6.

In the second proposed algorithm implementation, a modified active contour model driven by fractional-based energy minimization for kidney segmentation in MR images was presented. It consisted of a novel fractional Mittag-Leffler's function that replaced the standard gradient-descent minimization function. The proposed model exploited the special property of fractional calculus to preserve the high frequency features of processing contour.

In the third research stage, an algorithm was developed to remove the non-kidney components from the segmented kidney MRI images. The proposed algorithm was

designed in a way that it was able to remove the non-kidney components significantly, while preserving the kidney-segmented edge information in the MRI image.

The performances of the proposed algorithms were analysed using the (BRISQUE) (Mittal et al., 2012) and (NIQE) (Mittal et al., 2013) are used approaches to pre-processing operations (enhancement operation) and in terms of sensitivity and accuracy, the JSC, DSC and MNI were used for the segmentation process.

This work proposes an enhancement model for poor-quality kidney MRI images affected by geometrical transformation and noise. To achieve this, the proposed work applied two different quality measures, namely, BRISQUE and NIQE to determine the image quality. The measures are estimated for good- and poor-quality images, which are chosen randomly from different datasets. To determine the feasible values for the thresholds and parameters used in the proposed models for both enhancement and segmentation, we randomly chose 80 samples across the datasets for experimentation. The experimental results for different low-quality kidney MR images showed that the proposed models were effectively enhanced and segmented for removing the non-kidney components of low-quality kidney MRI images.

The main phases of the research methodology are the requirements, and implementation. The verification of the proposed algorithms by testing the different methods. However, a few stages of each developed scheme were formed within the first two steps of the methodological structure. The proposed algorithms were evaluated by testing each proposed scheme against two different datasets (i.e. dataset-1, which consisted of 230 MRI images collected from a hospital in Saudi Arabia, and dataset-2, which consisted of 20 images collected from Wikimedia Commons, as a standard dataset). Moreover, the scope was simplified in the requirements phase. The description will be in detail in the following chapters.

The proposed kidney enhancement and kidney segmentation developed and explained in the design phase.

Finally, the proposed algorithms were evaluated against two different datasets, which were collected from a hospital in Saudi Arabia and from Wikimedia Commons as a standard dataset, and the results were analysed.

The fractional calculus was used as a pre-processing stage, to enhance the low-contrast data. The main advantages of LEF (local entropy fractional) are its capability to detect edges through probability and local entropy if an image contains a minimal change in intensity values. When the intensity values in an image different, presented the edge details becomes easier. As such, when the intensity values change slightly because of various factors, including noise, disease, neighbouring tissues, and scanning systems, enhancing the edge details can be challenging. The local fractional entropy approach – which is inspired by the concept of fractional calculus – was further proposed to improve these processes (noise, disease, neighboring tissues), where fractional entropy is a generalization of Shannon entropy with fractional power ( $\alpha$ ). When  $\alpha=1$  the fractional entropy will become the Shannon entropy while fractional calculus is a generalization of ordinary calculus with fractional power ( $\alpha$ ). When  $\alpha=1$ , fractional calculus will become ordinary calculus and fractional entropy does not depend on fractional calculus. Then, after the enhancement stage was completed, the research proposed a novel energy minimization function called the fractional Mittag-Leffler's function (LFMLF) for kidney segmentation. Inspired by the ability of fractional calculus to handle non-linear problems such as inhomogeneous intensity values, poor quality (low contrast) and degradations (Al-Shamasneh et al., 2018; Jalab & Ibrahim, 2013, 2015), the research proposed the LFMLF for kidney segmentation from MRI images. The main contribution of this study from the investigation of the LFMLF is to provide different ways to address the complex

issue of kidney segmentation (noise, disease, neighbouring tissues, and scanning systems).

The gradient-descent energy minimization function suffers from inherent limitations such as sensitivity to inhomogeneous intensity values. Hence, methods that depend on the gradient-descent energy minimization function are not adequate to address the described issues associated with kidney segmentation. This limitation drove the motivation of this study to model an energy minimization function based on fractional calculus for kidney segmentation.

Universiti Malaya

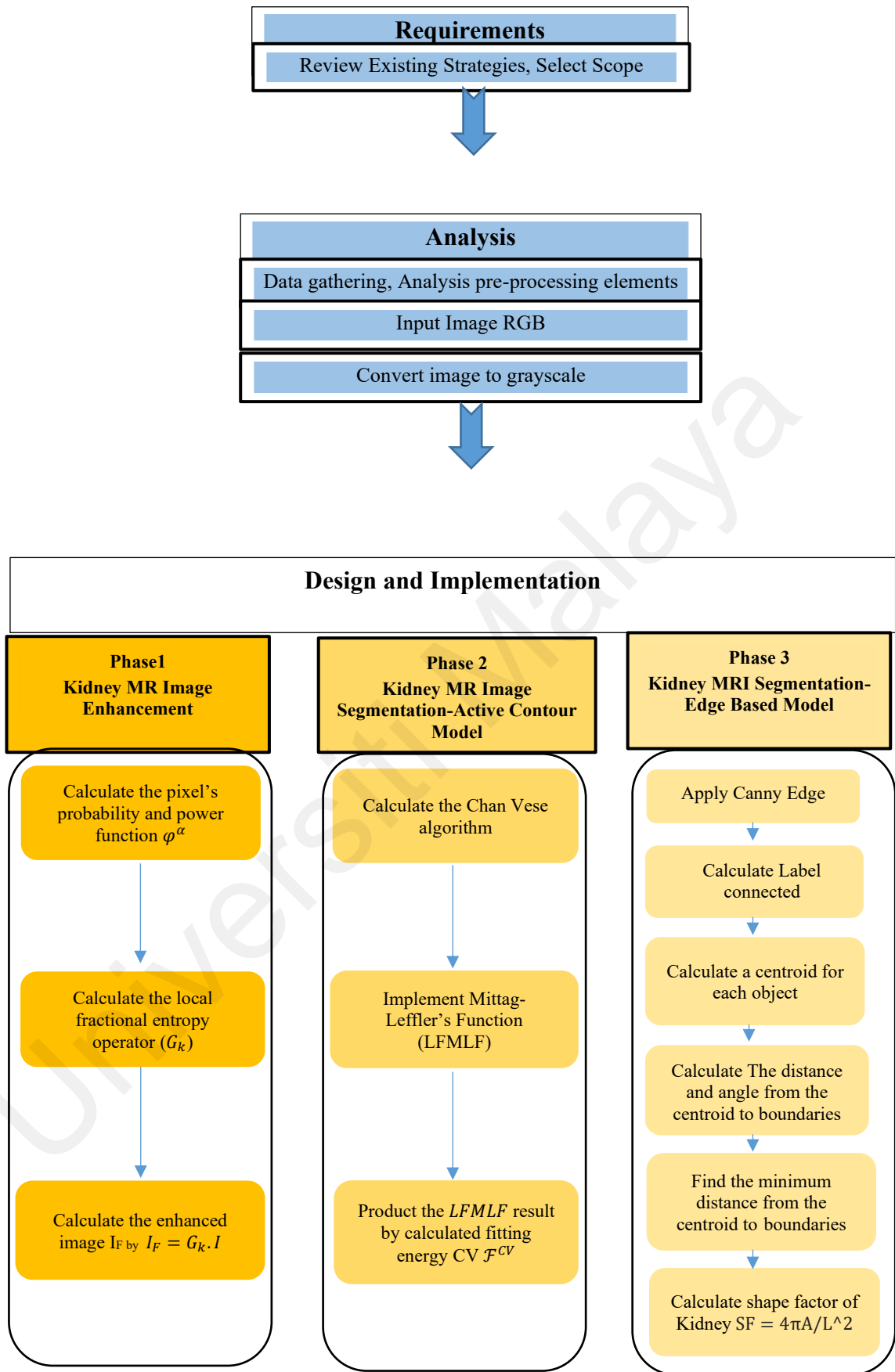


**Figure 3.1: General Flow of Proposed Methods**

Next, in the post-processing stage, which was the final stage, an algorithm was designed that was able to considerably remove the non-kidney components while preserving the kidney-segmented edge information in the MRI image-based Canny edge detection, with the application of some conditions, namely, the angle from the centroid to the boundary, the distance from the centroid to the boundary, and the shape factor of the kidney. The proposed methods (kidney MR image enhancement, kidney MR image segmentation-active contour model, kidney MR segmentation edge-based model) were evaluated.

### 3.2.1 Requirements Stage

The research methodology first three stages (i.e., requirements, system analysis and system design) had to be carried out before the proposed algorithms development. The first step of the proposed kidney enhancement and segmentation system was the requirements phase. The requirements phase was the main stage of each proposed phase. This step was comprised of the following activities.

**a) Review the Existing studies:** A comprehensive literature review was conducted to discover the problems with the enhancement and segmentation of low-contrast kidney MRI image schemes. The literature review, which were provided in Chapter 2, helped in finding the problem statement, and identifying the research objectives.

**b) Scope of Selection for Proposed Kidney Enhancement and Segmentation:**

The scope of the research was defined according to the explanation in the literature, and the structure of the enhancement and segmentation algorithms proposed by this research.

In terms of the application of the proposed algorithms, MATLAB language was chosen for the implementation of proposed enhancement and segmentation stages. The proposed enhancement and segmentation algorithms were identified to fulfil the following requirements:

1. Must be able to support grayscale and RGB images. A colored image is divided into three-channel images; namely, red, green, and blue. Each channel will produce a grayscale image. Hence, the proposed algorithm should be able to work with colored and grayscale images such as those in the MRI datasets.
2. Must be able to work on images with different format and dimensions such 2D and 3D images on different models (i.e. MRI, CT, US).
3. Must be able to accurately enhance and segment low-contrast MRI kidney images.
4. Must be robust towards input images different quality factors such as poor quality (low contrast), degradations, and contrast variations.
5. Must be effective for removing non-kidney components from segmented kidney MRI images.

### **3.3 Analysis Stage**

The suitable solutions to accomplish the scope identified in the requirements stage were considered. The result of the analysis phase helped in the construction of the most effective algorithms in order to achieve the objectives acknowledged by this research. In this section, the data collection for the proposed enhancement and segmentation algorithms is described. However, the analysis of this stage depended on the outcome of the proposed enhancement and segmentation algorithms. To confirm the results of the analysis stage, many experiments were carried out.

#### **3.3.1 Dataset Collection**

Since no standard dataset for kidney image segmentation available in the literature, datasets were collected from two different sources to evaluate the performance of the

proposed and existing methods. A hospital in Saudi Arabia was approached to collect a dataset of 230 MRI images from different patients. The dataset, called dataset-1 for experimentation, included MRI images with low contrast, low resolution, and noise. The images had a thickness of 1.7 mm, with dimensions of 256 x 256 pixels.

For disease identification (such as chronic kidney disease and acute kidney injury), as pre-processing steps, our proposed enhancing and segmentation methods are applied to poor-quality kidney images, the acquisition of image slices captured in different ways, and the capturing procedures do not significantly affect the overall performance of the models. Similarly, when images are captured for different image modalities, this also does not significantly affect the performance of all the proposed models.

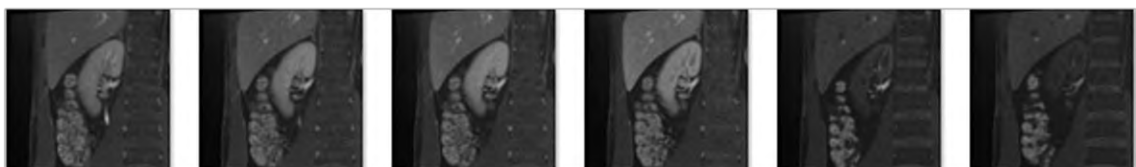
The medical device used for scanning the MRI images was the MRI-MAGNETOM Aera transforms 1.5T economics. The MRI image type used in this research was the MRI T1 vibe. The TR (repetition time) and TE (echo time) which are represent the basic pulse sequence parameters and are measured in milliseconds (ms). The TR (repetition time) is the cycle time between corresponding points, while the TE (echo time) is the time from the middle of the first pulse to the middle of the echo. The TR value was 3.4 ms and the TE value was 1.3 ms. The thickness of the image was 1.7 mm, and the dimensions were 256 x 256 pixels.

Images from Wikimedia Commons (an open-access repository), consisting of 20 MRI images, were also used. This was considered as the standard dataset and was called dataset-2 in this experiment. Since the dataset-2 images were collected from unknown sources that was made publicly available on the Wikimedia Commons repository for that not all parameters exist (the dimensions of the images were  $475 \times 512$  pixels, the file size was 43 KB, and the MIME type was image/jpeg), the images were much more complex than the images in dataset-1 due to the presence of a complex background, inhomogeneity and other surrounding tissues. In total, 250 images (i.e. 230 + 20 images) were used in

the experiment. It was estimated that the two datasets that were considered were adequate to evaluate the proposed and existing methods for kidney image segmentation because both the datasets had a different nature, which included the possible causes (low contrast, complex background, inhomogeneity and other surrounding tissues) of kidney image segmentation. The collected images were in the DICOM format. To avoid loss of information, the DICOM function in MATLAB 2018b, which is able to export images without affecting the quality of the original images, was used to display the images for processing.

### 3.3.1.1 Ground Truth Data

The Jaccard index and the Dice coefficient were employed as performance measures. A medical expert was contacted to determine the exact kidney in the input image, then the kidney regions were segmented manually under the supervision of clinical experts in the hospital. An experienced doctor was consulted for the manual segmentation of the kidney region. Furthermore, the ground truth was confirmed by two expert radiologists with over 20 years' experience, one of them the head of the radiology department from the same hospital where the new dataset was collected. Next, formal consent was obtained from the patients to use their MRI scans in this research. Samples from the two datasets with the ground truth are shown in Figures 3.2, while Figure 3.4 illustrates the samples from dataset-1 and dataset-2 to show the structure of the images in the datasets. Figure 3.3 and Figure 3.5, respectively, show the ground truth for both datasets. It was noticed that these input images were affected by multiple factors such as poor quality (low contrast), degradations, and contrast variations, as shown in Figure 3.2 and Figure 3.4.



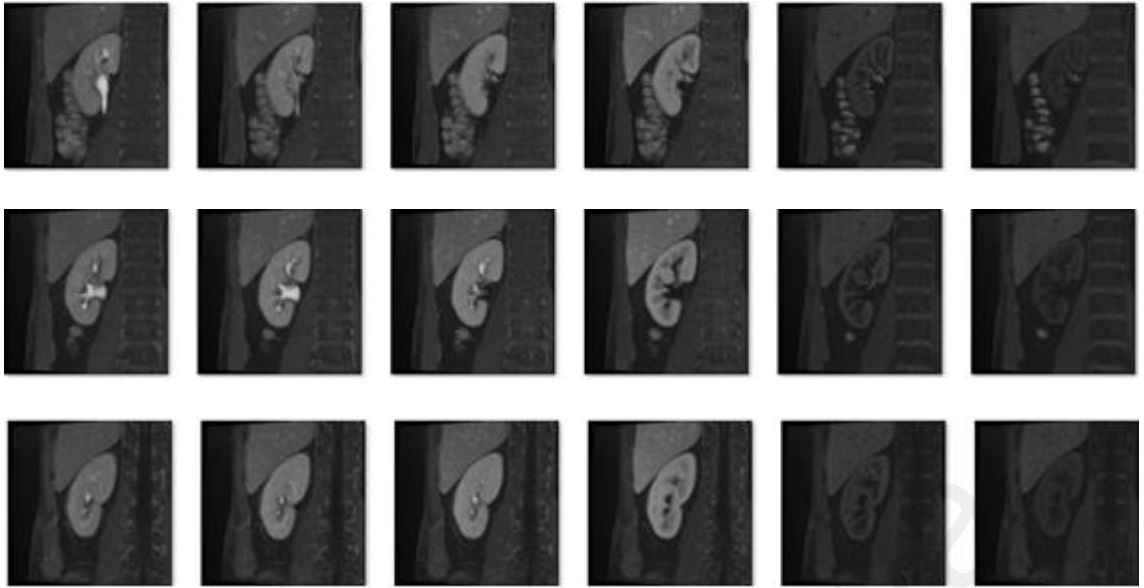


**Figure 3.2: Sample from Dataset-1 Which Consist 230 MRI Images Collected from Hospital in Saudi Arabia**

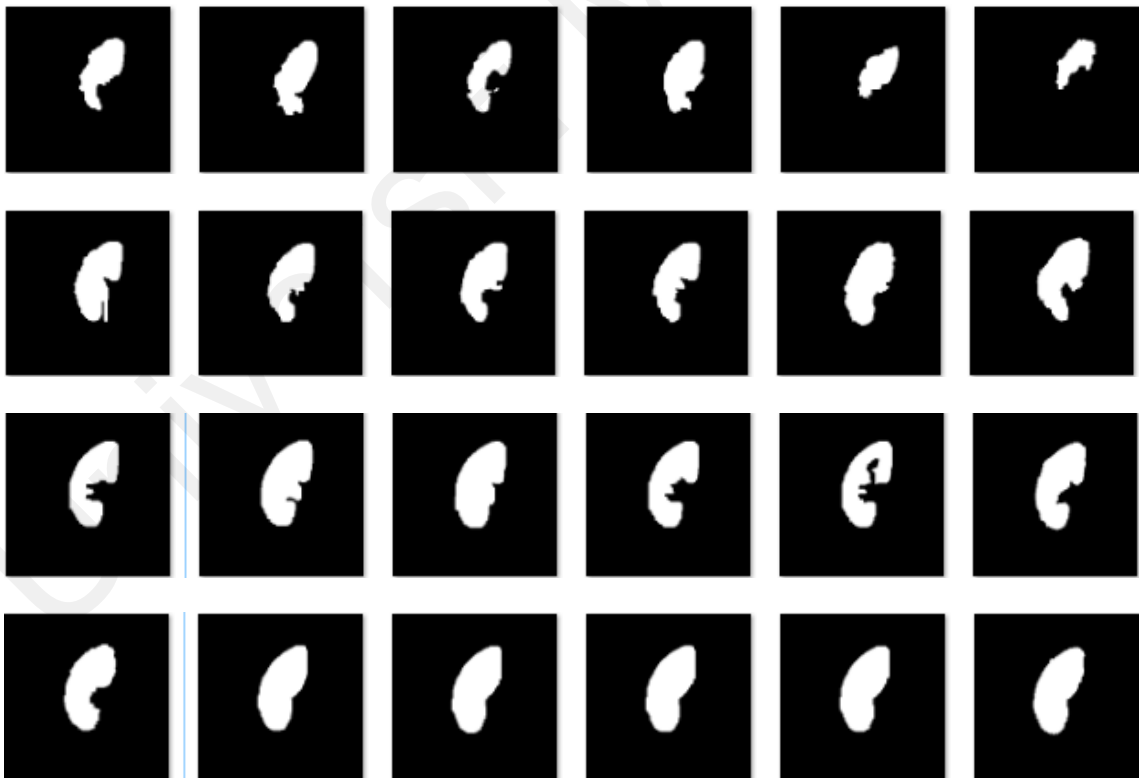


**Figure 3.3: Sample of Ground Truth for Dataset-1**

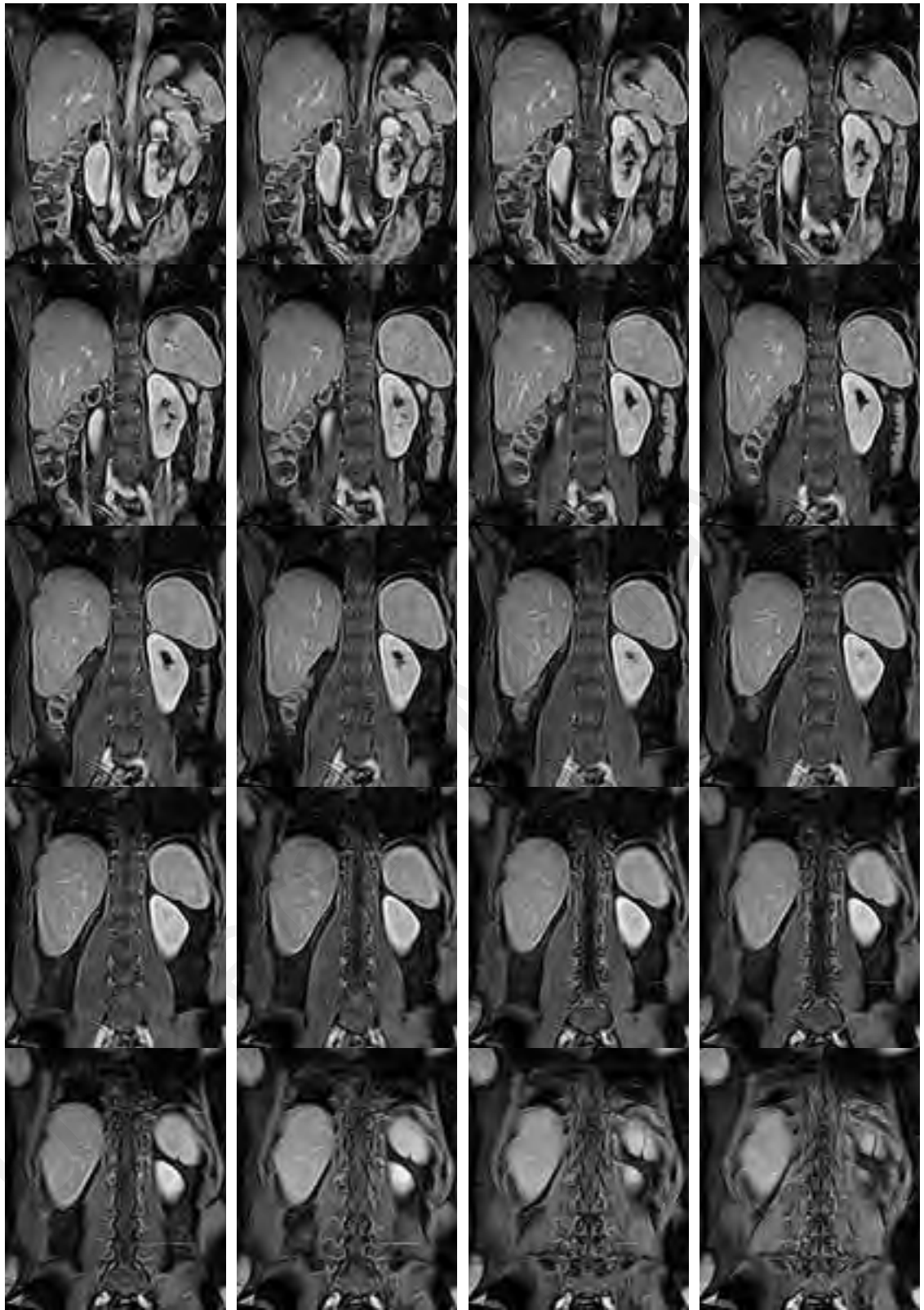


**Figure 3.4: Sample from Dataset-2 Which Consists of 20 Images Collected from Wikimedia Commons as Standard Dataset**

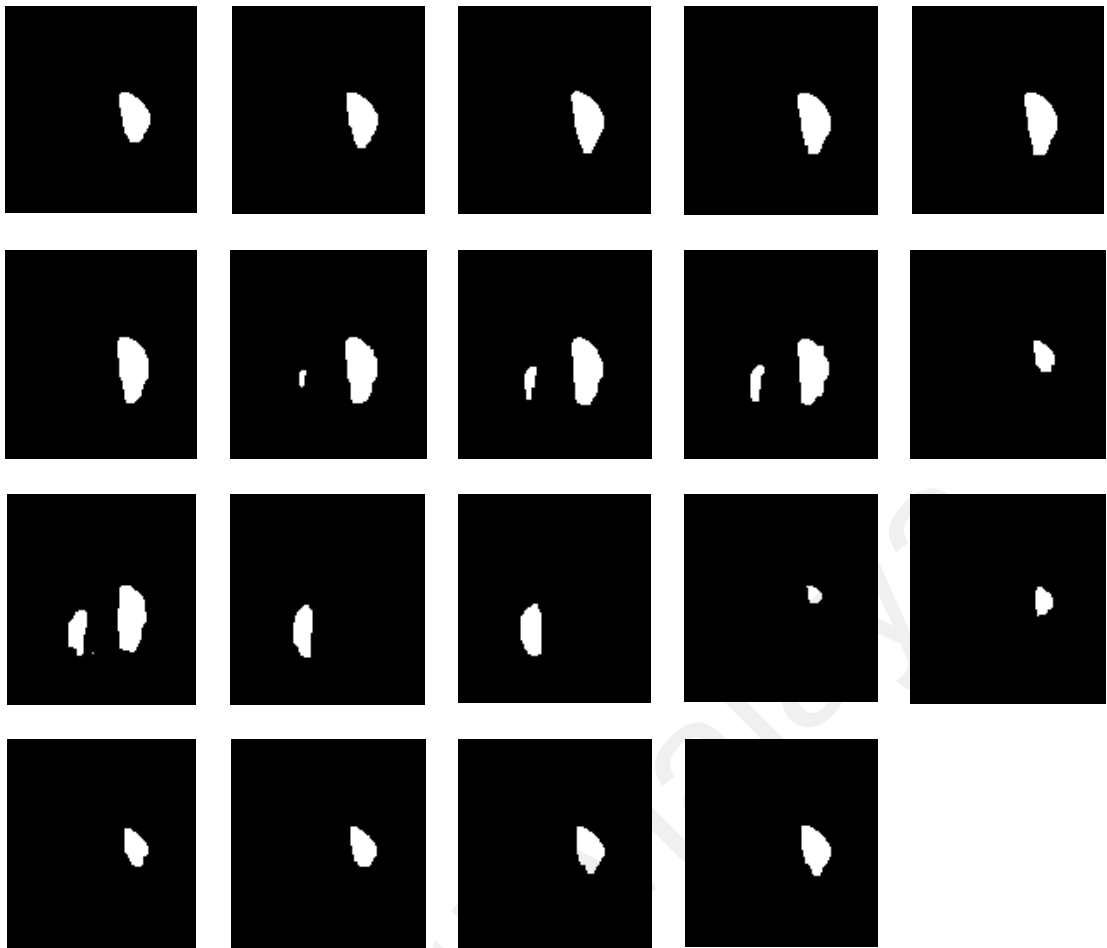


**Figure 3.5: Sample of Ground Truth for Dataset-2**

### **3.3.2 Hardware and Software Setup**

The experimental results were done using the MATLAB 2018b software using Intel Core i5 processor 2.40 GHz and 8 GB memory. A total of 250 experimental images were tested. The collected images were in DICOM format.

### **3.4 Summary**

The methodology was explained in this chapter. Each proposed phase was also described. Also, the requirements, analysis, primary design, and implementation, were explained.

## **CHAPTER 4: Fractional Entropy-based Method for Kidney Image Enhancement**

### **4.1 Background**

In the previous chapter, the research methodology stages were presented. This chapter proposes a new model for kidney image enhancement based on the fractional entropy approach. It is true that fractional entropy has the ability to solve complex issues, such as finding high-frequency values based on neighbouring information when the image is degraded and affected by distortions. This observation motivated the exploration of the same model in this chapter, which is organised as follows: In Section 4.2 the proposed method is explained, and in Section 4.3, the experimental results are presented.

### **4.2 Proposed Method**

As mentioned in the earlier chapters, when there is a critical distinction between intensity values in an image, it is simpler to enhance the edge information. However, if there is a slight change in the intensity values then enhancing the edge details can be challenging. Motivated by the strategies developed by (R. Ibrahim & Jalab, 2015; Raghunandan, Shivakumara, Jalab, Ibrahim, et al., 2017; S. Roy, Shivakumara, Jalab, & Ibrahim, 2016), where fractional calculus was investigated to improve text detection by using the local fractional entropy model.

The general flow of the proposed phases has been explained. As explained previously in Chapter 3, this research proposed a kidney enhancement algorithm. The following subsections define the structure of the proposed algorithm.

#### **4.2.1 Local Fractional Entropy**

The proposed model inferred that local fractional entropy is dependent on the pixel's frequency of the input. Subsequently, the presented model improved every pixel, where the grey-level changes were unimportant without influencing high frequency details. For

a consistent function,  $\varphi$  in  $[a, b]$ , and for a variable,  $u$  in  $[a, b]$ , the local fractional integral is clear defined (X.-J. Yang, 2011; X.-J. Yang, Baleanu, & Srivastava, 2015; X.-J. Yang & Srivastava, 2013):

$$I^{(\alpha)} \varphi(u) = \frac{1}{\Gamma(1+\alpha)} \int_a^b \varphi(u) (du)^\alpha, \quad 4.1$$

where  $\Gamma$  is the Euler gamma function. The fractional power operator is  $0 < \alpha \leq 1$ .

The discrete form of (4.1) is given by:

$$I^{(\alpha)} \varphi(u) = \frac{1}{\Gamma(1+\alpha)} \lim_{\Delta u_k \rightarrow 0} \sum_{k=0}^{n-1} \varphi(u_k) (\Delta u_k)^\alpha, \quad 4.2$$

where  $\Delta u_k = u_{k+1} - u_k$ ,  $u_0 = a$ .

The fractional entropies have been recommended by numerous researchers recently (see (Machado, 2014; Ubriaco, 2009)) for solving fractional nonlinear issues (see (X.- J. Yang, Baleanu, and Gao, 2017; X.- J. Yang, F. Gao, and H. Srivastava, 2017; X.- J. Yang, F. Gao, and H. M. Srivastava, 2017; X.- J. Yang, Machado, and Baleanu, 2017)).

The Tsallis entropy, as local fractional entropy, has been observed to improve the fractional integral operator. The probability of the pixels in the input image is indicated by  $\varphi$ . The Tsallis entropy is characterized as:

$$E_\alpha(\varphi(u)) = \frac{\int_a^b (\varphi(u))^\alpha du - 1}{1-\alpha} \quad 4.3$$

Hence, in the discrete form, it is:

$$E_\alpha(\varphi(u)) = \frac{1}{1-\alpha} \left( \sum_{k=0}^{n-1} \varphi^\alpha(u_k) - 1 \right) \quad 4.4$$

By applying the derivative with respect to  $\varphi$  in (4.4), the following is obtained

$$E_\alpha(\varphi(u)) = \frac{\alpha}{1-\alpha} \sum_{k=0}^{n-1} \varphi^{\alpha-1}(u_k) \quad 4.5$$

The power function  $\varphi^\alpha$  in (4.5) resulting the following local fractional integral:

$$I^{(\alpha)} \varphi^\alpha(u) = \frac{1}{\Gamma(1+\alpha)} \lim_{\Delta u_k \rightarrow 0} \sum_{k=0}^{n-1} \varphi^\alpha(u_k) (\Delta u_k)^\alpha \quad 4.6$$

In the examination by this study, the distance between pixels is regarded as being equivalent to 1. Consequently, the estimate of the limit part of (4.6) is as per the following:

$$\lim_{\Delta u_k \rightarrow 0} (\Delta u_k)^\alpha = 1.$$

Thus, the following is obtained

$$I^{(\alpha)} \varphi^\alpha(u) = \frac{1}{\Gamma(1+\alpha)} \lim_{\Delta u_k \rightarrow 0} \sum_{k=0}^{n-1} \varphi^\alpha(u_k) \quad 4.7$$

By taking the derivative regarding  $\varphi$  for the two sides of (4.7), the following is achieved

$$\dot{I}^{(\alpha)} \varphi^\alpha(u) = \frac{\alpha}{\Gamma(1+\alpha)} \lim_{\Delta u_k \rightarrow 0} \sum_{k=0}^{n-1} \varphi^{\alpha-1}(u_k) \quad 4.8$$

The local fractional entropy for images is the convolution of (4.5) and (4.8):

$$G = \dot{I}^{(\alpha)} \varphi^\alpha(u_k) * \dot{E}_\alpha(\varphi(u_k)) \quad 4.9$$

Consequently, the local fractional convolution operator is acquired

$$G = \frac{\alpha^2}{(1-\alpha)\Gamma(1+\alpha)} \left( \sum_{k=0}^{n-1} \frac{1}{\varphi^{1-\alpha}(u_k)} \right), \quad \varphi(u_k) \neq 0. \quad 4.10$$

From (4.10), the following improvement is obtained which is the contribution of the study:

$$G_k = \frac{\alpha^2}{(1-\alpha)\Gamma(1+\alpha)} \varphi_k^{\alpha-1}, \quad k = 0, 1, 2, \dots, n-1, \quad 4.11$$

where  $\varphi_k^{\alpha-1} = \varphi^{\alpha-1}(u_k)$  is the fractional probability of the pixels.

By utilizing the local fractional entropy operator ( $G_k$ ), the LFE is developed. The improved image,  $I_F$  is given by:

$$I_F = G_k \cdot I \quad 4.12$$

$G_k$  is calculated at every pixel, based on the image pixel's probability, and it is calculated in image spatial domain, while  $I_F$  represent the output enhanced image, and  $I$  is the input image.

The fractional power value ( $\alpha$ ) of the presented G operator is characterized by the scope of  $0 < \alpha \leq 1$ :

The above advanced function works well because the contrast enhancement is determined at every pixel, based on the pixel's probability. Figure 4.1 shows a low contrast input image with its improved counterpart, as well as diagrams of the probability distribution of their pixels. It was noted from the improved image shown in Figure 4.1 (a) that the contrast between the background and the pixels of the kidney was expanded and contrasted with the input image. This demonstrated that the proposed model improved the general quality of the image. It was apparent from Figure 4.1 (b) that the probability distribution of the pixels for the info image before the enhancement appeared to be too dense, while the probability distribution of the pixels in the enhanced image appeared to be dispersed. This implies that the contrast had been improved. Subsequently, it can be inferred that the low-contrast pixels representing the boundary of the kidney were improved and therefore, resulted in a dispersed probability distribution with similar frequencies of the input image. Figure 4.2 demonstrates the enhancing impact of the proposed model for a few more low contrast kidney images. The input images are shown in Figure 4.2(a), while the enhanced images are shown in Figure 4.2(b).

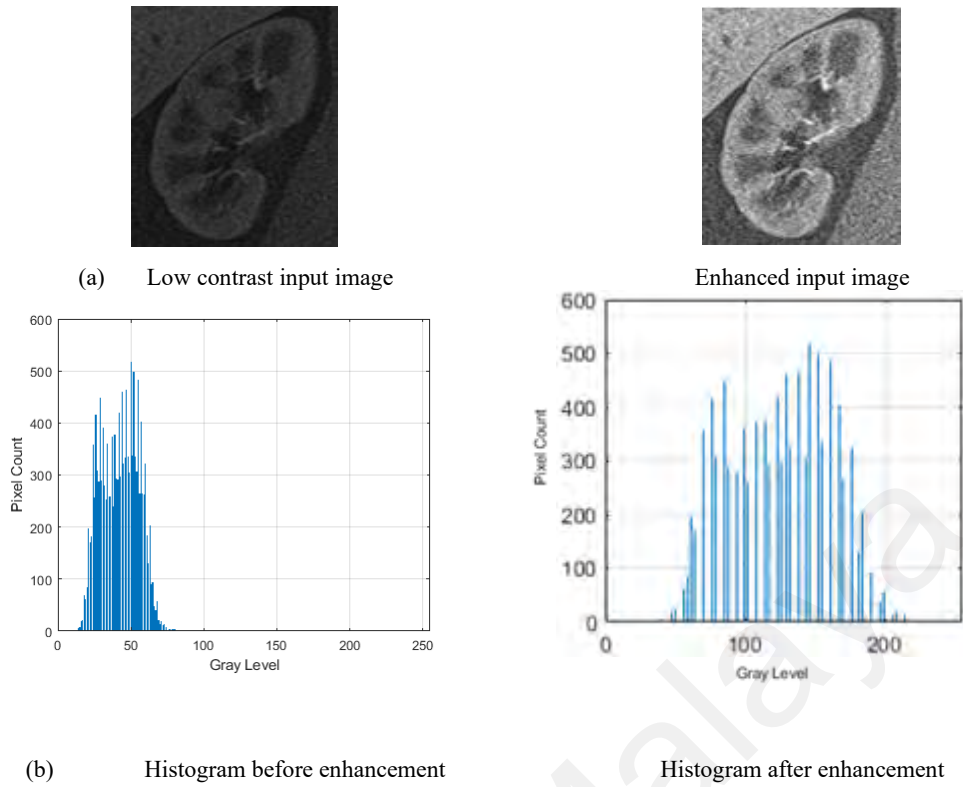


**Figure 4.1: Contrast is Increased after Enhancement**

In this approach, the proposed local fractional entropy algorithm was presented as a new model for enhancing low-quality kidney MRI images

The steps for the proposed algorithm as follow:

- 1 Low contrast kidney image generated by an MRI system (Refer to Figure 4.1)
- 2 Calculate the pixel's probability, as denoted by  $\varphi$  in the input image
- 3 Calculate the power function,  $\varphi^\alpha$
- 4 Calculate the local fractional entropy operator ( $G_k$ ), by dividing the power operator,  $\alpha^2$  by Gamma  $(1 - \alpha)\Gamma(1 + \alpha)$ , and then, multiply the result by the local fractional probability of the pixel,  $\varphi_k^{\alpha-1} = \varphi^{\alpha-1}(u_k)$ .
- 5 Calculate the enhanced image,  $I_F$  by the product of the local fractional entropy operator ( $G_k$ ), with  $I$  as the input image,  $I_F = G_k \cdot I$ .

- 6 Set the values of the fractional operator  $\alpha$ . The best value for the parameter,  $\alpha$  which gives a better perceptual quality of BRISQUE and NIQE is set experimentally to 0.7.
- 7 Calculate the BRISQUE and NIQE for the final enhanced images by the proposed LFE.
- 8 Image is enhanced using local fractional entropy (Refer to Figure 4.2).



(a) Input kidney images



(b) Enhanced counterpart of the input kidney images

**Figure 4.2: The Result of Proposed Enhancement Model on Different Kidney Images**

Two performance metrics which quantify the spread and flatness of the image histogram are calculated to show the effectiveness of proposed enhancement method.

These two metrics helped to differentiate between the low and high contrast images.

1- The histogram flatness measure (HFM) is the ratio of the geometric mean of  $h(x)$

to the arithmetic mean of  $h(x)$  and can be defined as:

$$\text{HFM} = \frac{\text{Geometric mean of histogram count}}{\text{Arithmetic mean of histogram count}} \quad 4.13$$

2- The histogram spread (HS) can be defined as (Tripathi, 2011)

$$HS = \frac{\text{Quartile distance of histogram}}{\text{Possible range of pixel values}} \quad 4.14$$

The histogram quartiles represent the amount of data spread. The quartile distance is the difference between the 3rd quartile and the 1st quartile of the extracted image histogram.

**Table 4.1: Histogram Flatness (HFM) and Histogram Spread (HS) Measures for Test Image of Figure 4.1**

	<b>low contrast image</b>	<b>Enhanced image</b>
HFM	0.2488	0.2962
HS	0.0086	0.0146

The results of Table 4.1, show that low contrast dark image shown in Figure 4.1, has HFM, and HS values less than the enhanced image by our proposed method. This performance metric conforms that the HFM, and HS depends not only on the intensity values of the histogram but also on the histogram bin positions, thus giving accurate results.

### **4.3 Experimental Results**

In this section, different low-contrast MRI kidney images were tested to determine the accuracy of the proposed method. As described in the previous chapters, the proposed method can be applied to datasets of different complexities, including those with low contrast, low resolution, noise, complex background, degradations and inhomogeneous contrast variations, and MRI images of other surrounding tissues. The proposed

enhancement scheme was examined against these datasets to evaluate the detection accuracy of the proposed method. To evaluate the accuracy of the method, evaluation metrics based on BRISQUE and NIQE were used. The performance of the method was evaluated on the dataset of collected images. As far as it is known, at present, there is no standard dataset available in the existing literature for the enhancement of kidney images. The measures mentioned in Chapter 3 were used to evaluate the proposed enhancement method, namely, the BRISQUE (A. Mittal, A. K. Moorthy, and A. C. Bovik, 2012a) and NIQE (A. Mittal, R. Soundararajan, and A. C. Bovik, 2013a).

In general, a smaller score of BRISQUE and NIQE indicate a better perceptual image quality. In the presented model, the key parameter was  $\alpha$ , where the performance of the proposed model changed, as indicated by its value. Consequently, the normal BRISQUE scores for predefined test images were computed from the dataset by differing the values of  $\alpha$ . Changes in  $\alpha$  values will affect the probability of the enhanced image and the BRISQUE score. The proposed model picked the value of  $\alpha$  when the BRISQUE score reached the lowest value. As shown in Figure 4.3, BRISQUE gave the most reduced score of  $\alpha$  at 0.7. A similar value was considered for all the experiments in this work. Note that the estimations of BRISQUE changed quickly with respect to small changes in  $\alpha$ . This changing behaviour reflected the impact of fractal entropy on the value of every pixel of the enhanced image.

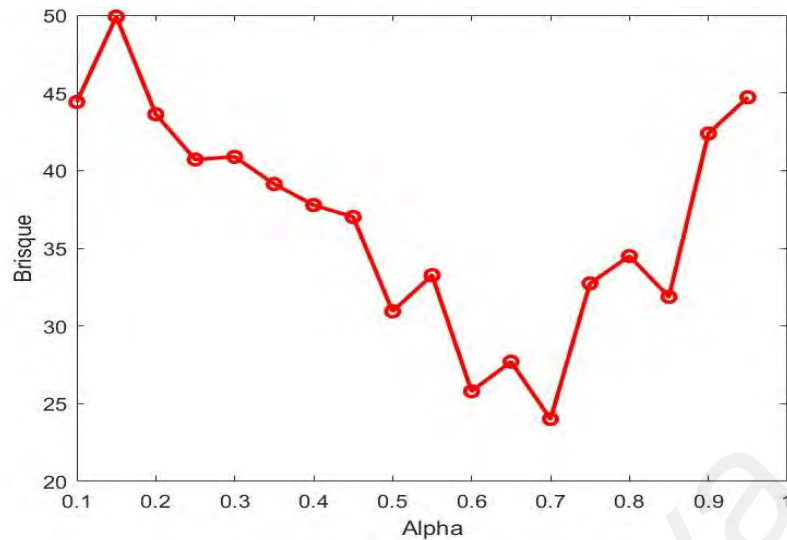


**Figure 4.3: Determining the Value for  $\alpha$  with the average BRISQUE Measure**

To demonstrate the adequacy of the proposed model, the essential and recent techniques were implemented for a comparative study. It was speculated that if the fundamental strategy functions work well, the most recent techniques should work well as well. Thus, the proposed strategy was evaluated against the outcomes from the traditional techniques (Gonzalez and Woods, 2012), specifically the adjusted intensity values (AIV) to a specified range, the contrast-limited adaptive histogram equalization (CLAHE), and the histogram equalization (HISTEQ). These are very basic methods for image enhancement. In addition, the Tsallis entropy technique (Jalab, Ibrahim, and Ahmed, 2017) proposed another scientific model by utilizing the convolution of the fractional Tsallis entropy for image denoising. Raghunandan et al. (2017) presented the fractional Riesz model for enhancing licence plate images. This technique explores fragmentary calculus for enhancing licence plate images. This method has also been proposed for enhancing license plate number and text enhancement in natural-scene images, although it has not yet been used for kidney image enhancement. In addition, this method is different from the proposed model; this is because the objective of the existing method is different and so the method suffers from inherent limitations. Although the

existing method was developed based on fractionals, the concept and the parameters used in the method are different from the proposed method.

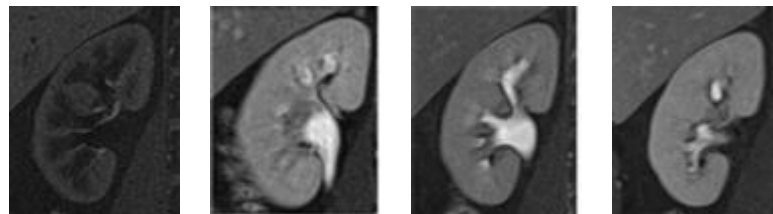
#### **4.3.1 Qualitative Results of Proposed and Existing Methods**

To show the effectiveness of the proposed algorithm, we implement the recent Tsallis entropy technique and the fractional Riesz model, basic models with adjusted intensity values (AIV) to a specified range, contrast-limited adaptive histogram equalization (CLAHE), and histogram equalization (HISTEQ), for comparative study. The latest models should work effectively because they use the same basic idea for enhancement. The qualitative test results for the presented and current existing strategies for various low-contrast MRI kidney images are shown in Figure 4.4.

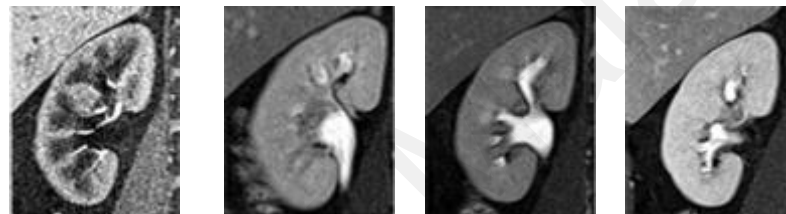
For qualitative comparison, we used a comparison with appropriate image-enhancing methods whose MATLAB codes are publicly available (AIV, CLAHE, and HISTEQ). It was hypothesized that if the fundamental strategy functions work well, the most recent techniques should also work well. The qualitative test results for the presented and current existing strategies for various low-contrast MRI kidney images are shown in Figure 4.4.

When comparing the results of the proposed enhancing method with the basic techniques such as adjusted intensity values (AIV) to a specified range, the contrast-limited adaptive histogram equalization (CLAHE), and the histogram equalization (HISTEQ), these are very basic methods for image enhancement, In addition, in comparison to the Tsallis entropy technique and fractional Riesz model, the proposed model produced better outcomes. This was valid because all the basic enhancing methods enhance the entire image globally and work well for images with similar intensity values and applied for specific applications such as the Riesz model. Also, the proposed model is appropriate for enhancing images that are affected by numerous factors such as MRI system, noise, and diseases. These factors cause differentiations in quality in various regions of an image. This is because the proposed model considers local data to enhance the pixels of

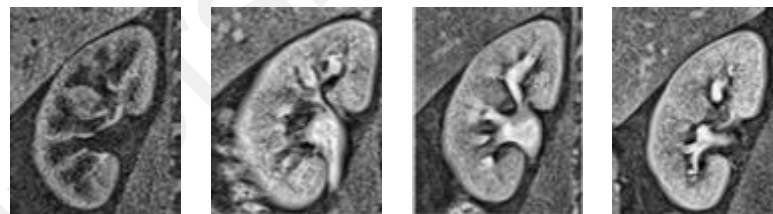
a given image. Moreover, the proposed enhanced method reduces the similarities between the kidney region and the surrounding tissue because the proposed model considers local information for enhancing pixels. Therefore, increase the contrast between the background and kidney edge that's mean sharpen edge of the kidney.



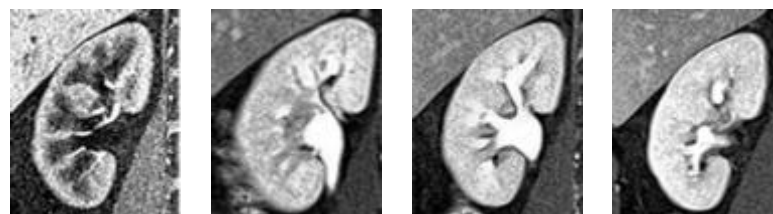
(a) Input Kidney images



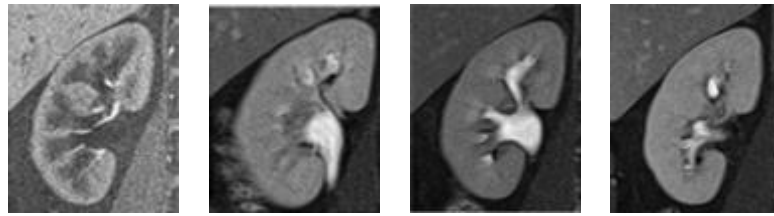
(b) Adjust Intensity Values to Specified Range (AIV) (Gonzalez, R. Et al. 2012)



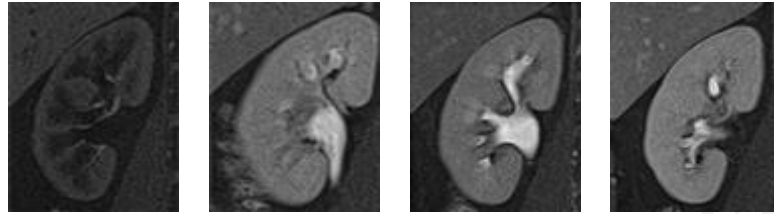
(c) Contrast-Limited Adaptive Histogram Equalization (CLAHE) (Gonzalez, R. Et al. 2012)



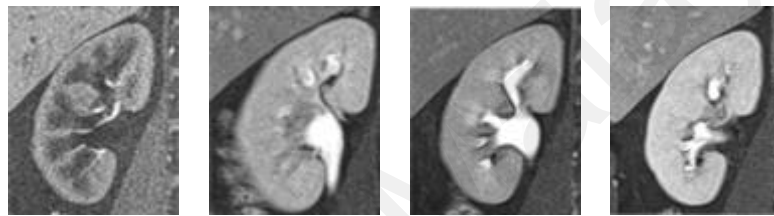
(d) Histogram Equalization (HISTEQ) (Gonzalez, R. Et al. 2012)



(e) Tsallis entropy (Jalab, Ibrahim et al. 2017)



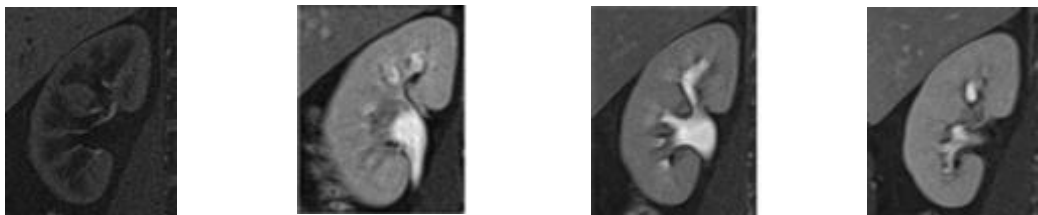
(f) Riesz Fractional (Raghunandan, Shivakumara et al. 2017)



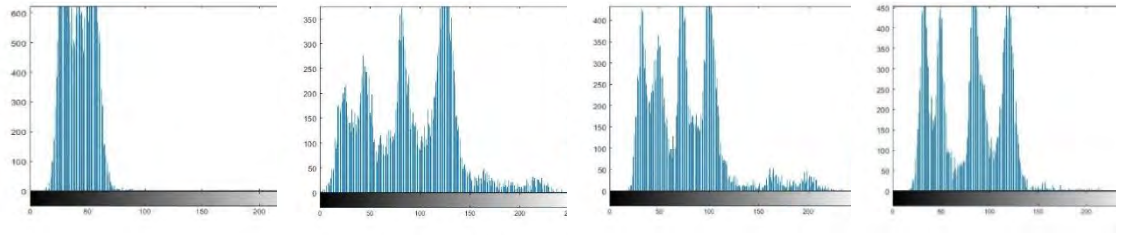
(g) Proposed method

**Figure 4.4: Enhancement Results of the Proposed and Existing Methods**

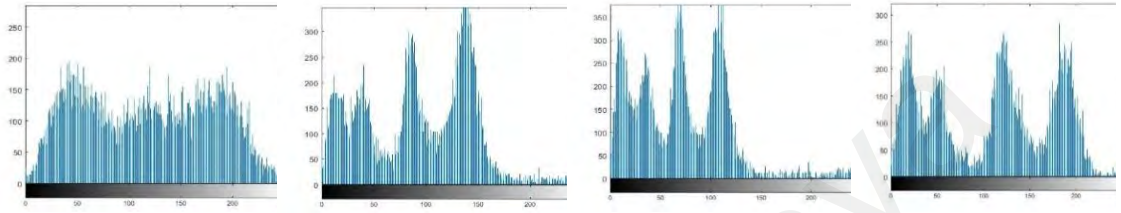
Contrast enhancement techniques are used to improve the quality of an image to make it more legible for human vision. Contrast manipulation involves changing the range of values in an image to increase contrast. The motivation behind image enhancement is to improve the contrast of an image and remove noise to enhance image quality.



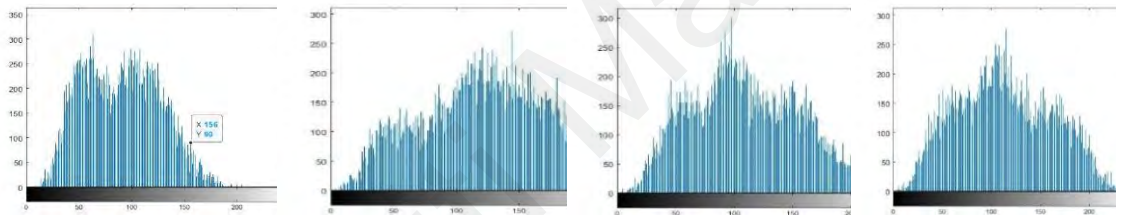
(a) Input Kidney images



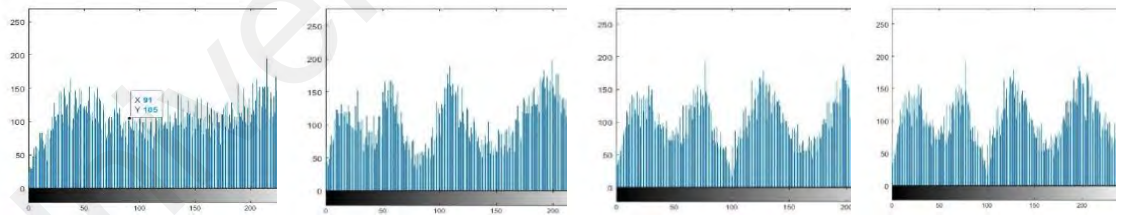
(b) Histogram for Input Kidney images histogram



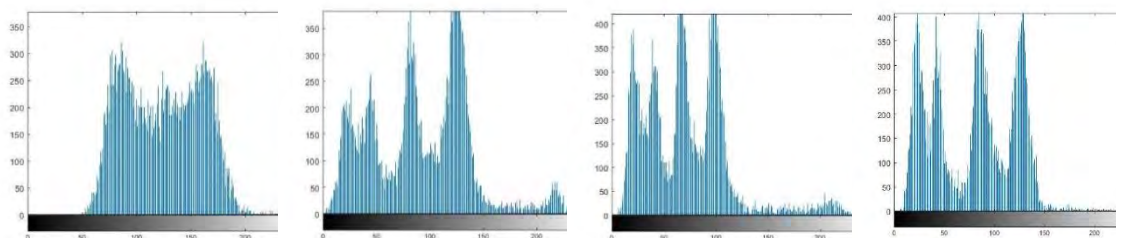
(c) Histogram for Adjust Intensity Values to Specified Range (AIV) (Gonzalez, R. Et al. 2012) histogram



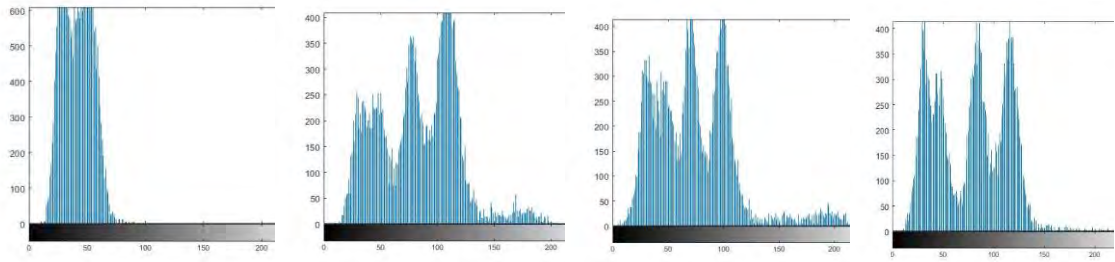
(d) Histogram of Contrast-Limited Adaptive Histogram Equalization (CLAHE) (Gonzalez, R. Et al. 2012)



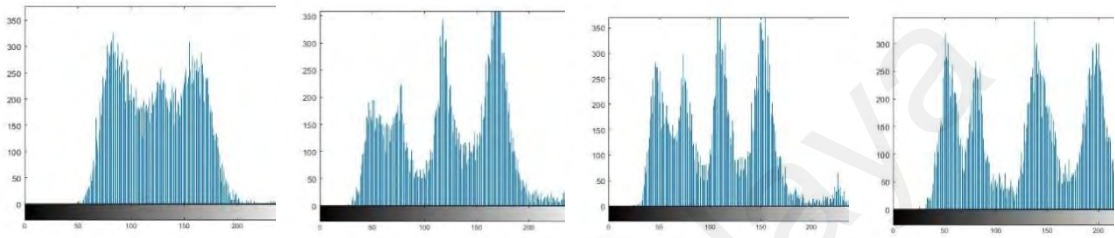
(e) Histogram of Equalization (HISTEQ) (Gonzalez, R. Et al. 2012)



(f) Histogram of Tsallis entropy (Jalab, Ibrahim et al. 2017)



(g) Histogram of Riesz Fractional (Raghunandan, Shivakumara et al. 2017)



(H) Histogram of Proposed method

**Figure 4.5: Histogram for Enhancement Results of the Proposed and Existing Methods Where X Line Refer to Gray Level and Y Line Refer to Pixel Count**

The contrast-enhancement method maps values of the intensities of an image to a new range. Figure 4.5 (a and b) shows the low contrast of an original image with its histogram. Notice that the histogram of the image (Figure 4.5(b)) shows all the values of intensity (where the X line refers to the gray level and the Y line refers to pixel count), which are unevenly distributed throughout the range.

Various image enhancement techniques have been implemented in the MATLAB environment as mentioned before in Chapter 4 Section 4.3. These techniques are the Intensity Adjustment Technique (`imadjust`), the Histogram Equalization Technique (`histeq`), and the Adaptive Histogram Equalization technique (`adapthisteq`). As described below, all of these techniques are applied to kidney images to investigate the effects of these enhancement techniques on MRI images.

The Intensity Adjustment Technique is one of several image-enhancement approaches and is particularly suitable for image enhancement. Figure 4.5 (c) shows the histogram

for an adjusted enhanced image. The level of contrast is increased in the image, and the histogram now fills the entire range [0,250], mostly, the histogram is present on the left. The histogram for the contrast-limited adaptive histogram equalization (Adapthisteq) technique operates on small regions in the image, called tiles. This technique enhances the contrast for each tile; it is used to avoid amplifying any noise that might be present in the image and Figure 4.5, (d) shows this histogram image. Adapthisteq produces an output image with values distributed throughout the range [0,250].

Histogram Equalization is a computer image-processing method used to enhance contrast in images. Figure 4.5 (e) shows the histogram for enhancement-tested images. The Histeq histogram produces an output image with values evenly distributed throughout the range (i.e., stretching out the intensity range of the image to enhance contrast).

In the Intensity Adjustment Technique (imadjust), Histogram Equalization Technique (histeq), and Adaptive Histogram Equalization technique (adapthisteq), the enhancement histogram is produced for the kidney edges in the same way as for other regions; the enhancement is achieved globally way not locally.

In addition, the Tsallis entropy technique and fractional Riesz model are used for enhancing license plate images. However, neither of these techniques work well for kidney-image enhancement, as shown in Figure 4.5 (f, g), as the histogram appears to be almost the same as the histogram for the input image.

State-of-the-art methods focus on denoising and speckle noise removal to enhance kidney images. While these methods work well for enhancing the entire image globally, they do not work well for local information. Moreover, one cannot expect or predict the global effect of different causes because kidney images contain different quality levels in different regions. Therefore, the enhancement is performed for both kidney boundaries and other regions.

The proposed method shown in Figure 4.5(h) produces an output histogram image with values distributed throughout the range [0,250]. The proposed method works to increase the contrast between the background and the kidney edges. By sharpening the edge details of the kidney, our proposed enhancement model is designed for images affected by multiple adverse factors and different poor-quality considerations, and it outperforms other state-of-the-art methods. This achievement is because fractional calculus can solve the non-linear problem, and overcome poor-quality, low contrast images.

#### **4.3.2 Quantitative Results**

The quantitative results are reported in Table 4.2. The best BRISQUE and NIQE scores were obtained by the proposed model in contrast to the current strategies. This demonstrated that the proposed model was superior to the current strategies. In reference to BRISQUE, the AIV was the second best compared with the proposed model, and the CLAHE was the second best for NIQE compared with the proposed model. Similarly, the HISTEQ and the Riesz fractional reported the worst outcomes as far as the BRISQUE and NIQE values were concerned in comparison to the other techniques. This was because these fundamental strategies suffered from the effects of inherent constraints such as global thresholding. As for the Riesz fractional-based technique, the parameters were tuned by the content of the licence plate images. Moreover, the proposed model did not depend much on the specific content of the image. Rather, it investigated the probability of the pixels utilizing nearby data. In this way, this technique was independent of datasets and applications. In other words, the presented model can be utilized to enhance other poor-quality medical images. In this way, it was found that the proposed model outperformed the existing techniques in terms of its applications, and BRISQUE and NIQE scores.

**Table 4.2: The Enhancement Performance of the Proposed and Existing Methods.**

Methods	BRISQUE	NIQE
Histogram Equalization (Gonzalez & Woods, 2012)	41.35	8.65
CLAHE (Gonzalez & Woods, 2012)	38.85	7.08
AIV (Gonzalez & Woods, 2012)	25.95	7.10
Tsallis entropy (Jalab, Ibrahim, & Ahmed, 2017)	37.03	6.04
Riesz Fractional (Raghunandan, Shivakumara, Jalab, & Ibrahim, 2017)	41.93	10.01
<b>Proposed method</b>	<b>22.37</b>	<b>6.32</b>

#### 4.4 Discussion

Medical imaging is an important tool used for the screening, detection, and diagnosis of diseases affecting the internal organs and tissues of the human body. However, most of these images suffer from quality-related problems such as blurring, low resolution, noise, system acquisition problems, and the challenge of detecting different diseases. All of these issues make it difficult to extract suitable data from such images. This makes image enhancement a complex challenge. To address this, the current chapter focuses on kidney-image enhancement by proposing a new local fractional entropy approach by estimating the probability of pixels which represent the edge of the kidney based on the entropy of the neighbouring pixels, since if there are small changes in the values, this indicates the edge of the kidney tissue. As mentioned in the literature review, as no standard dataset is available for kidney image enhancement, our dataset is collected from two different resources. The dataset includes low contrast, low resolution, and noise so both datasets are suitable for evaluation. To demonstrate the adequacy of the proposed model, the essential recent techniques were implemented for a comparative study of adjusted intensity values (AIV) to a specified range, contrast-limited adaptive histogram

equalization (CLAHE), and histogram equalization (HISTEQ). These are relatively basic methods for image enhancement. In addition, the Tsallis entropy technique (Jalab, Ibrahim, and Ahmed, 2017) proposed another scientific model by utilizing the convolution of the fractional Tsallis entropy for image denoising. Raghunandan et al. (2017) presented a fractional Riesz model for enhancing licence plate images. Most of these methods focus on denoising and speckle noise removal for enhancing kidney images. These methods work well for enhancing the entire image globally but not locally as well as being applied for specific applications like Riesz, which are used for text detection and recognition in other fields (not for kidney images). State-of-the-art enhancement methods are effective at globally enhancing kidney images, moreover, one cannot expect or predict the global effects of different causes because kidney images contain different quality levels in different regions. Therefore, the enhancement is performed for both kidney boundaries and other regions. For this application, there is an urgent need to develop a model that considers local information to enhance the edge details for kidney images. The proposed method works by increasing the contrast between the background and the edges of the kidney by sharpening edge details. The Blind/Referenceless Image Spatial Quality Evaluator (BRISQUE) (Mittal et al. 2012) and the naturalness image quality evaluator (NIQE) (Mittal et al. 2013) are used for evaluating our proposed enhancement method. Lower value scores indicate a better quality image. The qualitative and quantitative evaluation results illustrated that our proposed enhancement model for images affected by multiple adverse factors and different poor quality outperformed the other state-of-the-art methods. This was because the fractional calculus used can solve the non-linear problem in poor-quality, low-contrast images. However, despite its merits, the proposed approach is subject to several limitations. For example, when the input images are affected by several factors such as noise, it is difficult to analyze the image content by eye and so the enhancement method does not work well.

This is because the proposed model cannot distinguish between the actual values and the noise pixel values. Also, while the proposed model involves few parameters to achieve better results, on occasion, the parameters fail to obtain the correct values to obtain good results in different situations. Therefore, it is necessary to reduce the model's dependency on these parameters.

#### **4.5 Chapter Summary**

This chapter presented a description of each step of the proposed research method for the novel research stage; namely, the enhancement of MRI kidney images. The proposed algorithm presented local fractional entropy as a new model for enhancing low-quality MRI kidney images. The results of the experiments on different low-quality kidney MRI images demonstrated that the proposed model effectively enhanced the images. The next chapter presents the proposed fractional-based minimization function method for kidney-image segmentation and the experimental results.

## CHAPTER 5: FRACTIONAL-p-BASED MINIMIZATION FUNCTION FOR KIDNEY IMAGE SEGMENTATION

### 5.1 Background

In the previous chapter, a new method for enhancing low quality MRI kidney images based on fractional entropy was presented. However, due to the adverse effects of kidney images, there are chances of enhancing other details along with the details of kidney region. Therefore, this chapter proposes a new model for segmentation of the kidney region from the enhanced images. The segmentation method presents a modified active contour model driven by fractional-based energy minimization for MRI kidney segmentation.

This chapter is organised as follows: Section 5.1 presents the study background, Section 5.2 outlines the proposed method, and Section 5.3 describes the experimental results of the segmentation.

### 5.2 Proposed Method

As mentioned in the previous chapters, the limitation of the gradient-descent energy minimization function drove the motivation to model an energy minimization function based on fractional calculus for kidney segmentation. The proposed work has been divided into two steps – the first section provides an overview of the gradient-based energy minimization function, while the following section proposes a new fractional Mittag-Leffler energy minimization function for kidney segmentation from MRI images.

As mentioned in Chapter 3, this research proposed a kidney segmentation algorithm. The following sub-sections explain in detail the proposed algorithm.

### 5.2.1 Overview of Chan–Vese (CV) Algorithm

According to the literature on kidney segmentation and general object segmentation, the gradient-based energy minimization function approach to image segmentation is popularly known as the Chan–Vese (CV) algorithm (Chan et al., 2000). Therefore, this section presents an overview of the CV algorithm before the proposed LFMLF is described. The theoretical analysis of the CV algorithm for kidney segmentation is as follows: The CV algorithm refers to energy minimization as the “fitting energy” for segmentation. The minimizing level set function,  $\phi$  is defined in Equation (5.1) as

$$\begin{aligned} \mathcal{F}^{CV}(C, c_1, c_2) = & \mu \text{Length}(C) + \nu \text{Area}(\text{inside}(C)) \\ & + \lambda_1 \int_{\text{inside}(C)} |I(x, y, z) - c_1|^2 dx dy dz \\ & + \lambda_2 \int_{\text{outside}(C)} |I(x, y, z) - c_2|^2 dx dy dz \end{aligned} \quad 5.1$$

where  $\lambda_1$  and  $\lambda_2$  are the internal and external control forces, respectively, while  $\mu$  and  $\nu$  are used to control the smoothness of the curve  $C$  which define the boundary of the object where  $c_1, c_2$  are the internal and external smoothness, respectively. More details for fixing the parameters can be found in (Friedman, 2010).  $\delta_o$  is a 2D Dirac function,  $\nabla$  is the gradient operator, and  $H$  is the Heaviside function.

The Chan-Vese energy function,  $\mathcal{F}^{CV}$ , in the form of  $\phi$  is given as follows:

$$\begin{aligned} \mathcal{F}^{CV}(\phi(x, y, z)) = & \mu \int_{\Omega} \delta_o(\phi(x, y, z)) |\nabla \phi(x, y, z)| dx dy dz + \\ & \nu \int_{\Omega} H(\phi(x, y, z)) dx dy dz + \lambda_1 \int_{\text{inside}(C)} |I(x, y, z) - \\ & c_1|^2 H(\phi(x, y, z)) dx dy dz + \\ & \lambda_2 \int_{\text{outside}(C)} |I(x, y, z) - c_2|^2 (H(\phi(x, y, z))) dx dy dz \end{aligned} \quad 5.2$$

The alternative updating of  $c_1, c_2$ , and  $\emptyset$  are used to minimize the Chan-Vese function,  $\mathcal{F}^{CV}$ . The values of  $c_1$  and  $c_2$  are defined in Equation 5.3 and Equation 5.4, respectively.

$$c_1(\emptyset(x, y, z)) = \frac{\int_{\Omega} I(x, y, z) \cdot H(\emptyset(x, y, z)) dx dy dz}{\int_{\Omega} H(\emptyset(x, y, z)) dx dy dz} \quad 5.3$$

$$c_2(\emptyset(x, y, z)) = \frac{\int_{\Omega} I(x, y, z) \cdot (1 - H(\emptyset(x, y, z))) dx dy dz}{\int_{\Omega} (1 - H(\emptyset(x, y, z))) dx dy dz} \quad 5.4$$

The associated Euler-Lagrange for  $\emptyset$ , with the proposed LFMLF $_{\alpha}$  is defined in Equation 5.5

$$\begin{cases} \frac{\partial \emptyset}{\partial t} = LFMLF_{\alpha} \left[ \mu \operatorname{div} \left( \frac{\nabla \emptyset}{|\nabla \emptyset|} \right) - v - \lambda_1 (I(x, y) - c_2)^2 + \lambda_2 (I(x, y) - c_2)^2 \right] \text{ in } \Omega \\ \frac{\delta(\emptyset)}{|\nabla \emptyset|} \frac{\partial \emptyset}{\partial \vec{n}} = 0 \text{ on } \partial \end{cases} \quad 5.5$$

where  $\frac{\partial \emptyset}{\partial \vec{n}}$  indicates the exterior normal derivative of  $\emptyset$ .

### 5.2.2 The LFMLF Energy Minimization Function for Kidney Segmentation

It was noted from the theory presented in Section 5.3.1 that the concept of CV can be modified to derive a fractional-based energy minimization function to improve the performance of the CV algorithm for kidney segmentation. This observation motivated the introduction of a new fractional Mittag-Leffler (LFML) energy minimization function for kidney segmentation, which is presented formally as follows:

Let  $f \in L^p(X)$  be the space of the Lebesgue integral functions with the norm

$$\|f\|_X = [\int |f|^p dm + \inf \int (\nabla f)^p dm]^{1/p} < \infty, p \geq 1, \quad 5.6$$

where  $m$  satisfies  $m(B(2r)) \leq Km(B(r))$ ,  $K > 0$ , and  $B(r)$  is a set of radii,  $r$ . The capacity  $C_p$  of the set  $E$  in  $X$  is defined in Equation 5.7 as

$$C_p(E) = \inf \|f\|_X^p \quad 5.7$$

Finding a stable fixed boundary is deeply connected to the study of energy minimization.

For  $f \in B(X)$ , the differential fractional operator is defined in Equation 5.8 as

$$D^\alpha f(x) = \lim_{x \rightarrow x_0} \frac{\Gamma(\alpha+1) [f(x) - f(x_0)]}{(x-x_0)^\alpha} \quad 5.8$$

where  $0 < \alpha < 1$  is the fractal measure (Hausdorff measure) of  $x$  and  $x_0$  in  $X$ .

By applying Equation 5.8, the fractional gradient can be derived as defined in Equation 5.9 below

$$\nabla^\alpha f(x) = e[D^\alpha f(x)] = \sum_{i=1}^n D^\alpha f_i e_i \quad 5.9$$

where  $f$  is an  $n$ -dimensional function, and  $e$  is the unit vector. The generalized fractional norm is derived by substituting Equation 5.9 into Equation 5.6, as defined in Equation 5.10.

$$\|f\|_{X,\alpha} = \inf_{f \in X} \int (|f| + \nabla^\alpha f)(x) dx \quad 5.10$$

Equation 5.9 is substituted into Equation 5.6 to obtain the generalized fractional norm as follows.

$$\|f\|_{X,\alpha} = [ \int |f^{(\alpha)}|^p dm + \inf \int (\nabla^\alpha f^{(\alpha)})^p dm ]^{1/p} < \infty, p \geq 1. \quad 5.11$$

To minimize the energy term, as defined in Equation 5.11, a special function based on the fractional Mittag-Leffler function (LFMLF) for kidney segmentation in MRI images was proposed. Therefore, the proposed LFMLF was instantly linked to the diffusion process (Mainardi, Mura, & Pagnini, 2010), as defined in Equation 5.12.

$$E_\alpha(x^\alpha) = \sum_{n=0}^{\infty} \frac{x^{n\alpha}}{\Gamma(1+\alpha n)} \quad 5.12$$

In image processing, the difference  $(x - x_0)^\alpha = 1$ . Therefore, applying Equation 5.12 in Equation 5.8 gives the following, as defined in Equation 5.13.

$$E^{(\alpha)}_{\alpha}(x^{\alpha}); = D^{\alpha} E_{\alpha}(x^{\alpha}) = \lim_{x \rightarrow x_0} \frac{\Gamma(\alpha+1) [E_{\alpha}(x^{\alpha}) - 1]}{(x-x_0)^{\alpha}} \quad 5.13$$

In this study, the LFMLF was implemented as a minimization function, as defined in Equation 5.14.

$$LFMLF_{\alpha} = \Gamma(\alpha + 1) * [E_{\alpha}(x^{\alpha}) - 1] \quad 5.14$$

In this approach, the proposed LFMLF presented a new model for the segmentation of the edges of the kidney from low-quality kidney MRI images.

The steps for the proposed algorithm as follow:

- 1 Low-contrast image generated by an MRI system (Refer to Figure 5.1)
- 2 Calculate the Chan-Vese (CV) algorithm, which refers to energy minimization as “fitting energy” for segmentation, and the minimizing level set function,  $\varphi$ , as defined in the equation

$$\begin{aligned} \mathcal{F}^{CV}(C, c_1, c_2) = & \mu \text{Length}(C) + v \text{Area}(\text{inside}(C)) + \\ & \lambda_1 \int_{\text{inside}(C)} |I(x, y, z) - c_1|^2 dx dy dz + \lambda_2 \int_{\text{outside}(C)} |I(x, y, z) - \\ & c_2|^2 dx dy dz \end{aligned} \quad 5.15$$

where  $\lambda_1$  and  $\lambda_2$  are the internal and external control forces, while the smoothness of  $C$  is controlled by  $\mu$  and  $v$ .

- 3 Implement a minimization function to minimize the energy term by minimizing 2 factors,  $\alpha$  and  $\theta$ , by using the Mittag-Leffler function (LFMLF)
- 4 Set the values of the fractional operator,  $\alpha$ . The best values for the parameter,  $\alpha$  which give the best results for kidney segmentation are the Jaccard similarity coefficient (JSC) and the Dice coefficient set experimentally to 0.35.
- 5 Implement the LFMLF, which is defined in Equation 5.16

$$LFMLF_{\alpha} = \frac{1}{\theta^{\alpha}} \frac{\Gamma(\alpha) (\Gamma(\alpha+1))^2}{\Gamma(\alpha^2)} - \Gamma(\alpha + 1) \quad 5.16$$

where  $\theta$  is the diffusion constant,  $\alpha$  the fractional power.

- 6 Multiply the *LFMLF* result with the calculated fitting energy CV  $\mathcal{F}^{CV}$  algorithm as in Equation 5.17

$$\begin{cases} \frac{\partial \phi}{\partial t} = LFMLF_{\alpha} \left[ \mu \operatorname{div} \left( \frac{\nabla \phi}{|\nabla \phi|} \right) - v - \lambda_1 (I(x, y) - c_2)^2 + \lambda_2 (I(x, y) - c_2)^2 \right] \text{ in } \Omega \\ \frac{\delta(\phi)}{|\nabla \phi|} \frac{\partial \phi}{\partial \vec{n}} = 0 \text{ on } \partial \end{cases} \quad 5.17$$

- 7 Calculate the sensitivity, accuracy, Jaccard, and Dice coefficient for the final segmented images using the proposed LFMLF (Refer to Figure 5.2).

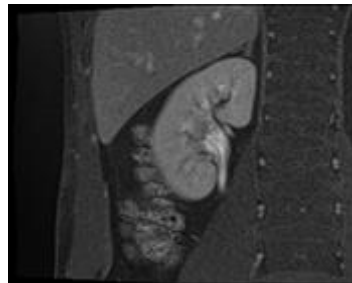


**Figure 5.1: Low Contrast Input Image**

**Figure 5.2: Segmented Image using the Proposed Algorithm**

### 5.3 Experimental Results

The datasets for this study were collected from two different sources to evaluate the performance of the proposed and existing methods. A dataset consisting of 230 images of different patients was collected. The dataset, called dataset-1 for the experiment, included images with low contrast, low resolution, and noise. Images were also collected from Wikimedia Commons, which consisted of 20 images. This was considered as a standard dataset and was called dataset-2 in this experiment. Since the images in dataset-2 were collected from unknown sources, the images were much more complex than the images in dataset-1 due to the presence of a complex background, inhomogeneity, and other surrounding tissues. In total,  $230 + 20 = 250$  images were considered for the experiments. The two datasets were adequate for the evaluation of kidney image segmentation because both datasets had different characteristics. The collected images

were in DICOM format. In order to avoid the loss of information, the DICOM function in MATLAB 2018b was used to display the images for processing, where the images were exported without affecting the quality of the original images.

The proposed method was tested using the standard measures, as mentioned in Chapter-3, namely, sensitivity and accuracy, which measured whether the proposed model was able to segment the kidney sections correctly or not.

In the assessment of the segmentation process, both sensitivity and accuracy are not always significantly relevant because both methods of assessment depend on the image size. For this reason, two additional metrics were used, namely the Jaccard index and the Dice coefficient (Hasan et al., 2016).

The higher JSC and DSC values indicated that the proposed model was good and preserved the shape of the kidney. Further, the efficiency of the proposed model was measure by the number of iterations consumed by the model for the kidney segmentation. Since the above-mentioned measures required ground truth, the kidney regions were manually segmented, where the segmented regions were further verified by a doctor, who was an expert radiologist. At the same time, the results given by the proposed and existing methods were verified by the same doctor to calculate the measures. The ground truth and segmentation results of the samples using the proposed method for dataset-1 and dataset-2 are shown in Figure 5.5 and Figure 5.6, respectively.

To show the effectiveness and usefulness of the proposed model, it was compared to the following state-of-the-art methods by: (Chan et al., 2000), who used an active contour criteria for segmentation, (Hasan et al., 2016), who proposed an automated segmentation method to segment the tumour regions in volumetric MRI brain scans, (R. W. Ibrahim, Nashine, & Kamaruddin, 2017), who proposed a generalized hybrid time-space dynamic system to segment medical images based on a local regional active contour model, and Li et al. (2010), who explored a level set for kidney segmentation. The reason for

choosing the method by (Chan et al., 2000) for the comparative study was to show that energy minimization alone is not sufficient to achieve better results for kidney segmentation in complex images affected by multiple adverse factors. Similarly, the reason for choosing the methods of (Hasan et al., 2016; R. W. Ibrahim et al., 2017) was that these methods explore the generalized model for segmenting the region of interest in medical images. Similarly, a comparison was performed to demonstrate that the generalized models may not be adequate to achieve enhanced results for kidney image segmentation.

In the proposed fractional Mittag-Leffler function (LFMLF),  $\alpha$  is a key parameter, according to Equation 5.17. To determine a feasible value for  $\alpha$  to achieve better results for kidney segmentation, experiments were conducted on 60 images selected randomly from dataset-1 and dataset-2 to calculate the mean accuracy by varying the  $\alpha$  value, as illustrated in Figure 5.3. It was noticed in Figure 5.3 that the mean accuracy scores showed the highest results for the value at 0.35. Hence, the same value was considered as the optimal value for experimentation. Similarly, the number of iterations of the proposed model was taken as another key parameter to indicate better results. In order to determine the feasible values for the thresholds and parameters used in the proposed models for both enhancement and segmentation, we choose 100 samples across datasets randomly for experimentation. Therefore, in the thesis, only the number of testing sample are mentioned, for experimentation to calculate the mean accuracy scores by varying the number of iterations, as illustrated in Figure 5.4. It was observed in Figure 5.4 that the mean accuracy score reached the highest peak at 600 iterations for dataset-1 and 300 iterations for dataset-2. Thus, 600 and 300 were the feasible values for the iterations of dataset-1 and dataset-2, respectively. Then, the same values were used for all the experiments in this work. In the same way, the values for the parameters, namely,  $\lambda_1 = \lambda_2 = 1$ , length penalty,  $\mu = 10^6$  and  $\mu_F = 0.01$ , were determined in this study.

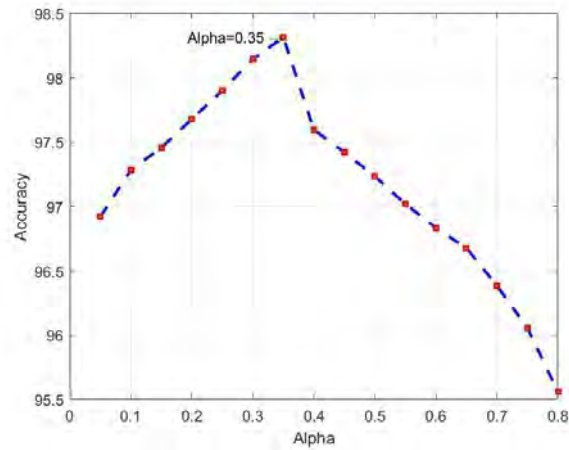


**Figure 5.3: Determining the Optimal Value for The Alpha to Segment the Kidney Images by Varying Fractional Power  $\alpha$  and Calculating Mean Accuracy.**

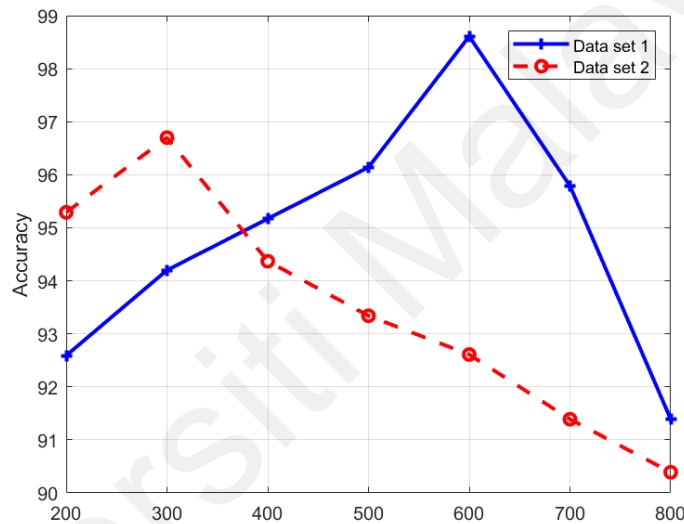


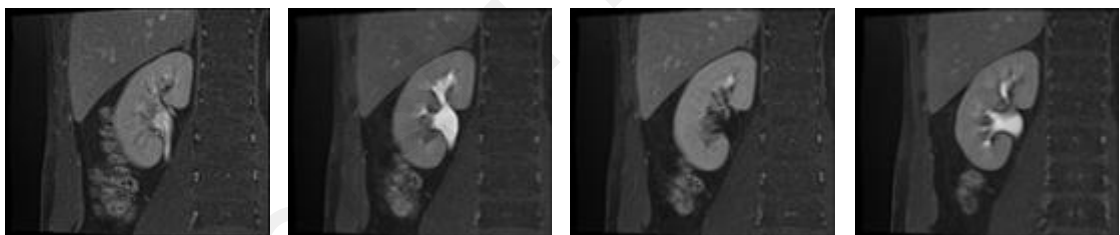
**Figure 5.4: Determining the Number Optimal Iterations for Kidney Segmentation for Dataset-1 And Dataset-2 By the Proposed Method.**

### 5.3.1 Qualitative Results

The qualitative results of the proposed segmentation model for dataset-1 and dataset-2 are shown in Figure 5.5 and Figure 5.7, respectively. It can be observed that the input images were affected by multiple factors such as poor quality (low contrast), degradations and contrast variations, as shown in Figure 5.5(a) and Figure 5.7(a), and the proposed model was able to successfully segment the kidney regions, as shown in Figure 5.5(c) and Figure 5.7 (c). This was evident from the comparison of the segmentation results of the

proposed model with the ground truth, where the results of the proposed method were almost the same as the ground truth. This showed that the proposed model, which combines fractional calculus with the active contour model, is able to handle images affected by various complexities. This is the advantage of the proposed fractional-based model for segmentation.

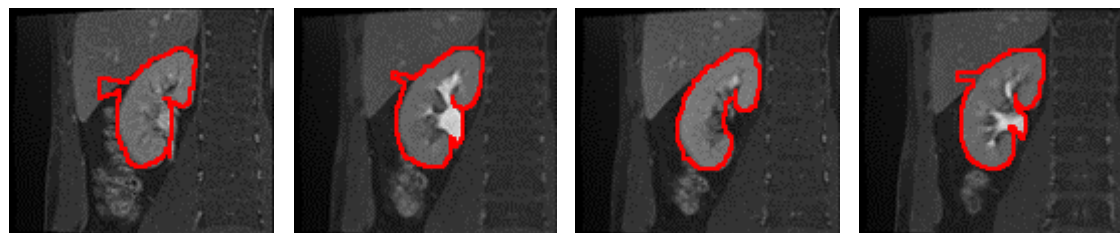
The segmentation results for state-of-the-art techniques with proposed segmentation model for dataset-1 and dataset-2 are shown in Figure 5.6 and Figure 5.8, respectively. It can be observed that the existing method fail to segment kidney in proper way since the boundary covers extra background. This is because existing method sensitive to poor quality and inhomogeneous intensities. The Proposed method can segment kidney region successfully due to its, ability to handle complex situation.



(a) Input images



(b) Ground truth

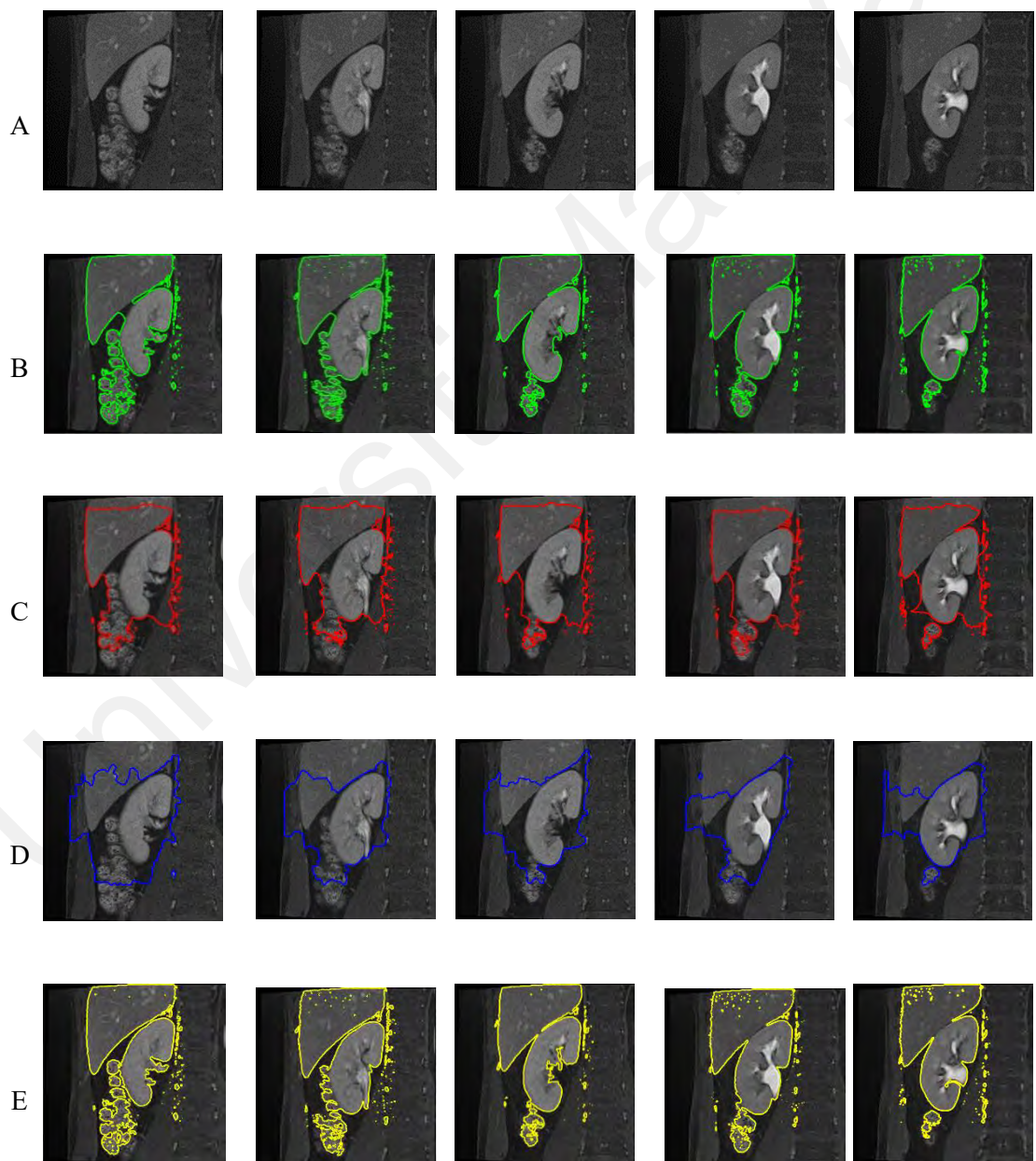


(c) Proposed kidney segmentation



(d) Binary image of proposed kidney segmentation

**Figure 5.5: Examples of Kidney Segmentation Using the Proposed Kidney Segmentation for Dataset-1**



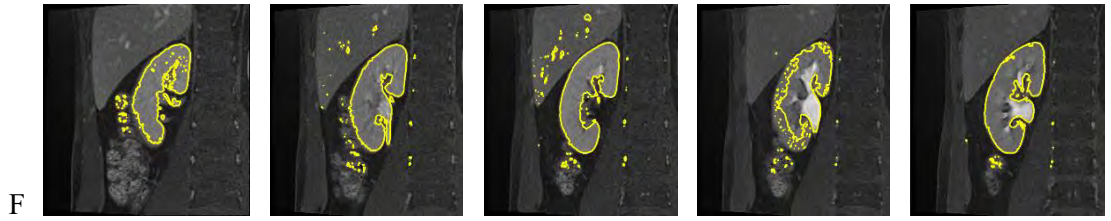
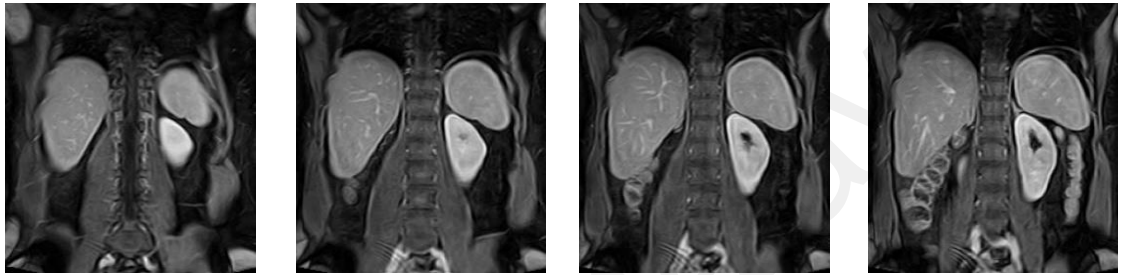
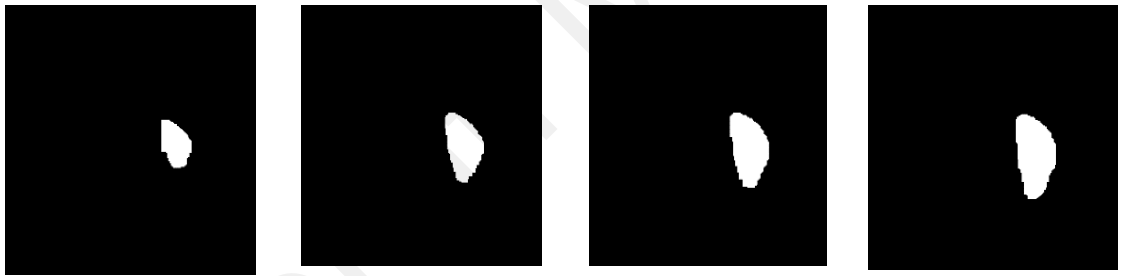


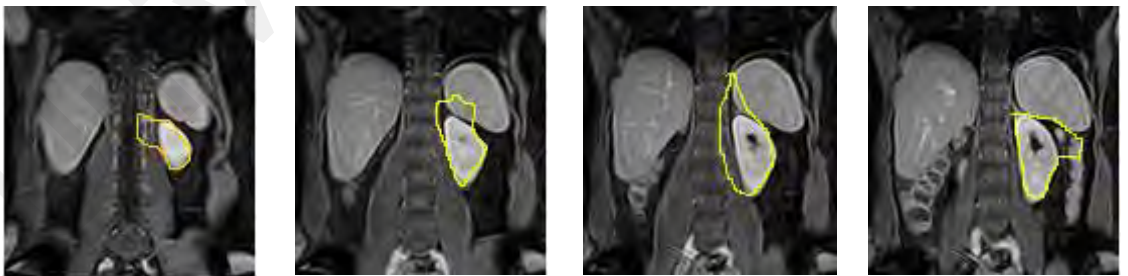
**Figure 5.6: The experimental results of the proposed and existing models for kidney segmentation dataset1. (A) Input images, (B) Hasan et al. (C) Chan et al. (D) Li et al. (E) Ibrahim et al. (F) Proposed Method**



(a) Input images



(b) Ground truth

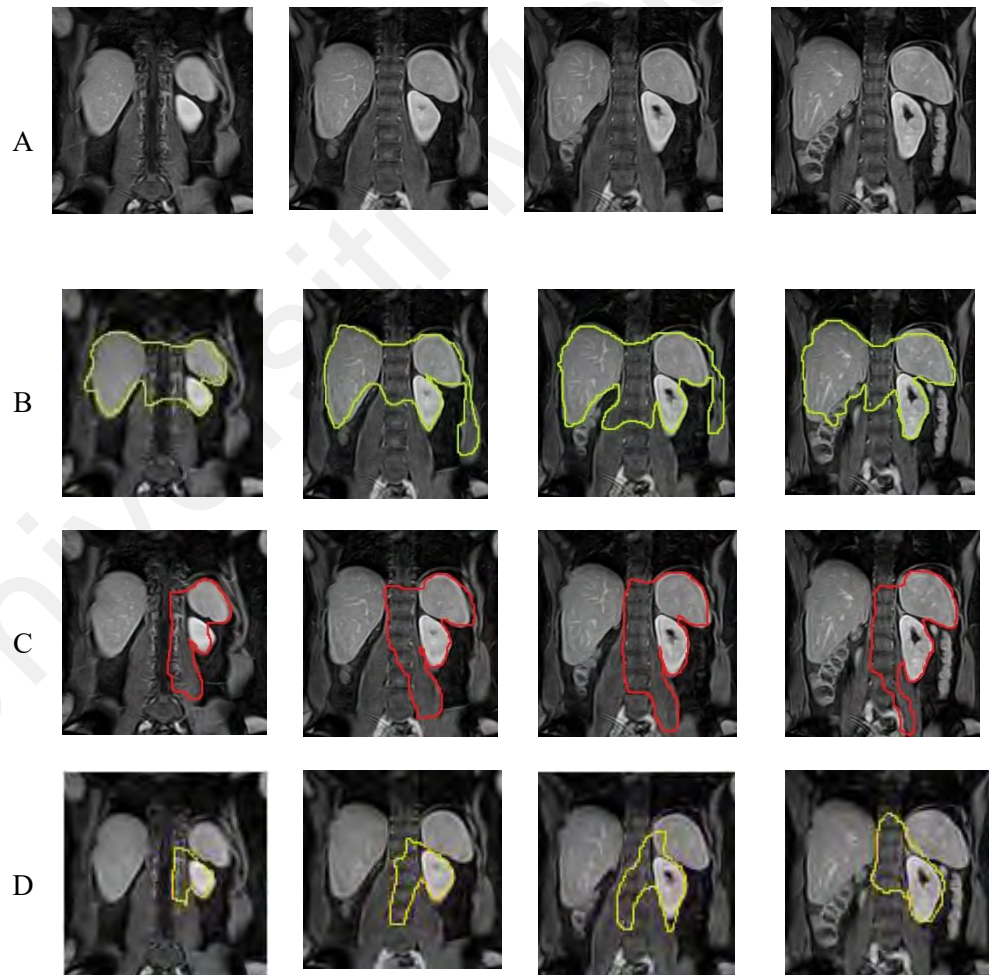


(c) Proposed kidney Segmentation



(d) Binary image of proposed kidney segmentation

**Figure 5.7: Example of Kidney Segmentation Using the Proposed Method for Dataset-2**



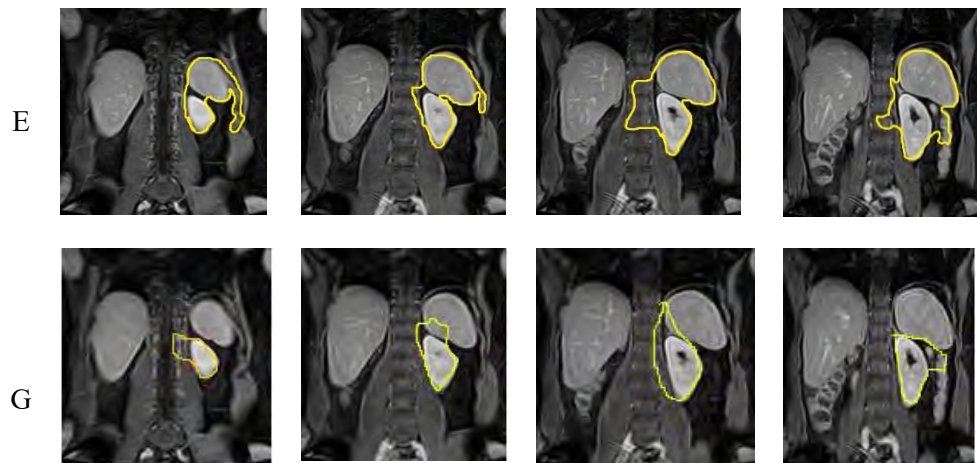


**Figure 5.8** The experimental results of the proposed and existing models for kidney segmentation. (A) Input images, (B) Hasan et al, (C) Chan et al, (D) Li et al, (E) Ibrahim et al, (G) Proposed Method

### 5.3.2 Quantitative Results

The quantitative results for dataset-1 and dataset-2 are described in Table 5.1 and Table 5.2, respectively. It is evident that the proposed model shown best in using the following metrics for evaluation the kidney segmentation: sensitivity, accuracy, JSC, and DSC when compared with other existing models. The number of iterations with dataset-1 was the highest due to the nature and size of the images it contained. The number of computations was insufficient to determine the computational time required, as this depends on several factors, such as the method, coding, logic, and implementation. In general, if the method requires a greater number of iterations, the process will involve a greater number of operations. Therefore, the number of computations may be high but not necessarily time-consuming. Therefore, it can be asserted that the proposed model outperformed the existing models in terms of segmentation, shape preservation and efficiency. When the results of the proposed and existing models on dataset-1 and dataset-2 were compared, the proposed and existing methods reported poorer results for dataset-2 compared to the results for dataset-1. This was justifiable because dataset-2 was much

more complex than dataset-1, as described in the previous section. Table 5.1 and Table 5.2 show that the methods of (Hasan et al., 2016; R. W. Ibrahim et al., 2017), which involved generalized models for segmentation, achieved better results than the other methods, except for the proposed model for kidney image segmentation, in terms of sensitivity. This is true because generalized models have the ability to tackle the different adverse factors of an image, while methods developed for specific purposes may not be robust enough for complex images. However, the results of the generalized methods were poorer than the proposed method for all measures. This showed that the proposed model is suitable for complex and simple images.

The results in Table 5.2 showing the measures of kidney segmentation for Dataset-2. The measures are affected by the overlapping of kidney and background tissues. It was noted from Table 5.2 that the sensitivity of the proposed model was lower than the JSC. This was due to the occasional inclusion of additional background information in the segmentation results produced by the proposed model. Hence, there was the possibility that the model missed counting a result for sensitivity, while this did not occur for the JSC. This was because in the case of sensitivity, the segmentation results with extra information might have been classified as a false negative, while this did not occur for the JSC.

**Table 5.1: Performance of the Proposed and Existing Methods for Dataset-1**

Methods	Sensitivity (%)	Accuracy (%)	JSC (%)	DSC (%)	Iterations
(Li et al., 2010)	93.60	98.64	87.06	92.77	700
(Chan et al., 2000)	86.56	91.25	86.23	84.75	800
(R. W. Ibrahim et al., 2017)	90.89	89.90	84.10	87.92	700
(Hasan et al., 2016)	88.17	90.73	86.69	82.84	700
<b>Proposed Method</b>	<b>94.79</b>	<b>98.95</b>	<b>93.11</b>	<b>94.70</b>	<b>600</b>

**Table 5.2: Performance of the Proposed and Existing Methods for Dataset-2**

<b>Methods</b>	<b>Sensitivity(%)</b>	<b>Accuracy(%)</b>	<b>JSC(%)</b>	<b>DSC(%)</b>	<b>Iterations</b>
(Li et al., 2010)	61.17	66.73	61.69	60.84	500
(Chan et al., 2000)	60.56	67.95	61.23	65.75	500
(R. W. Ibrahim et al., 2017)	73.28	75.37	67.50	73.32	500
(Hasan et al., 2016)	72.91	69.03	70.86	75.78	500
<b>Proposed Method</b>	<b>83.14</b>	<b>85.99</b>	<b>86.38</b>	<b>83.86</b>	<b>500</b>

#### 5.4 Discussion

The current chapter focused on our proposed method for segmenting kidney images from enhancement input MRI images, which contain enhanced information about other neighboring organs and background information. Accurate segmentation is challenging due to intensity inhomogeneity caused by imperfections during the image acquisition process. Most state-of-the-art kidney segmentation methods are developed for use with high-quality images, not poor-quality images. To overcome this, our motivation was to propose a new model for segmenting kidney images from low-contrast MRI images. This chapter presented a model consisting of a novel fractional energy minimization for segmenting kidney images from low-contrast MRI images. Existing methods such as the active-contour model, which uses gradient-based energy minimization, are sensitive to inhomogeneous intensity values. Therefore, it is important to propose a new fractional Mittag-Leffler function for energy minimization to maintain the high-frequency contour features while enhancing low-frequency texture details in smooth areas. The dataset was collected from two different resources; the images were complex with the presence of complex backgrounds, and featured inhomogeneity and surrounding tissues, as well as including all the causes of kidney segmentation. The proposed model was compared to the following state-of-the-art methods (e.g., Hasan et al., 2016), who explored active contours for segmenting brain tumor MRI brain images. Ibrahim, Nashine, & Kamaruddin (2017) proposed a method for segmenting bacteria growth from a microscopic image based on a fractional operator. However, these methods depend on

generalized segmentation approaches, which under-perform in segmenting kidney regions from MRI images. To overcome these limitations, more robust methods for segmenting kidney details from images have been proposed. For example, Chan et al. (2000) used an active contour criteria for segmentation while Li et al. (2010) explored a level set for kidney segmentation. Both methods used gradient descent for energy minimization, which is not robust for inhomogeneous intensity values and poor-quality images. Using energy minimization alone is not sufficient to achieve optimal results for kidney segmentation in complex images affected by multiple adverse factors. To overcome this, the proposed fractional Mittag-Leffler-minimization method for kidney segmentation offers the advantages of fractional calculus which can deal with low-contrast and degraded images. Also, to assess if the proposed method segmented kidney images effectively or not, sensitivity and accuracy measures are applied. Based on the qualitative and quantitative results, the proposed method outperformed the existing models in terms of sensitivity, accuracy, JSC, and DSC, and can segment images of the kidney region successfully. The good segmentation results achieved by our proposed model were due to applying fractional calculus in an active contour. However, the key limitation of this method is that it is computationally expensive.

## **5.5 Chapter Summary**

This chapter presented a detailed description of each step of the proposed research method for the novel research stage, namely, segmentation. The segmentation method presented a modified active contour model driven by fractional-based energy minimization for MRI kidney segmentation. The experimental results for different low-quality kidney MR images showed that the proposed model effectively segmented the kidney boundary of low-quality kidney MR images.

## CHAPTER 6: Edge-based Method for Kidney Image Segmentation

### 6.1 Background

In the earlier chapter, a new method for the segmentation of the kidney edge from low-quality MRI kidney images using a modified active contour model driven by fractional-based energy minimization for MRI kidney segmentation was presented. However, since the method involves an active contour model, the method is said to be computationally expensive. Therefore, this chapter proposes an efficient method based on edge information for an accurate segmentation of the kidney region from enhanced images.

This chapter is organised as follows: Section 6.1 presents the background, Section 6.3 outlines the proposed edge-based method for kidney segmentation, while Section 6.4 describes the experimental results.

### 6.2 Proposed Edge-Based Method for Kidney Segmentation

Edge features is one of the most important features in image processing applications. The purpose is to detecting discontinuities of object boundary in the levels of brightness. The edge detection has been used extensively in many applications, so that it is important to design an efficient edge detector which influence the image analysis. This study presented a new method of extracting kidney edges from low quality MRI images. The proposed algorithm was designed to remove significant non-kidney elements while preserving kidney-segmented edge information from low-contrast MRI images.

Canny edge information is used for segmenting the kidney region in the images as shown in Figure 6.2. However, the Canny-based output does not provide segmentation results directly. Therefore, to reduce the complexity of the background, Canny edge information is used as it eliminates background information and provides finely detailed images of the kidney region. The information given by the Canny for the kidney region is considered

as input for the subsequent steps to segment the kidney region. In other words, the Canny information is used as a pre-processing result to segment the kidney region in the images. The proposed edge-based method for kidney image segmentation was applied to the MRI image-based Canny edge detection under three applicable conditions, namely:

Condition (1): Angle from the centroid to boundaries

Condition (2): Distance from the centroid to boundaries

Condition (3): Shape factor of the kidney

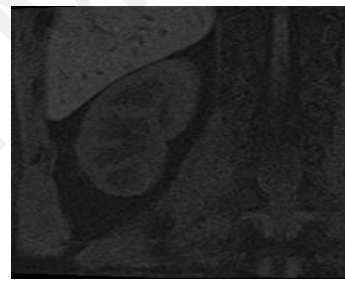
The first step was to apply the Canny edge detection to the input image,  $I(x, y)$ . The input images are shown in Figure 6.1 and the Canny edge images are shown Figure 6.2.

The detailed steps for the proposed algorithm were as follows:

a) Input MRI image



Example (1) MRI input image



Example (2) MRI input image

**Figure 6.1: Samples of MRI Kidney Images**

b) Apply Canny edge



Example (1) Canny Edge Map



Example (2) Canny Edge Map

**Figure 6.2: Canny Edge Image**

c) Label connected components

Connected-component labelling in 2-D binary images was used to label each blob. The total number of objects in the image in Example 1 was 152 objects, while the image in Example 2 had 215 objects. Some objects were chosen from both examples, as shown in Figure 6.3 and Figure 6.4.

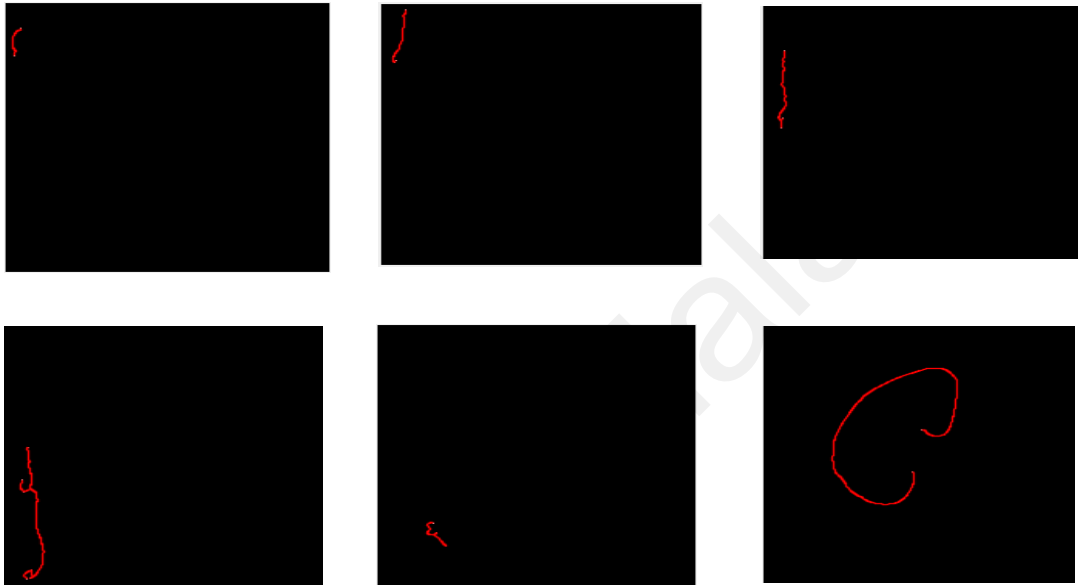


Figure 6.3: Label Object Sample Example 1

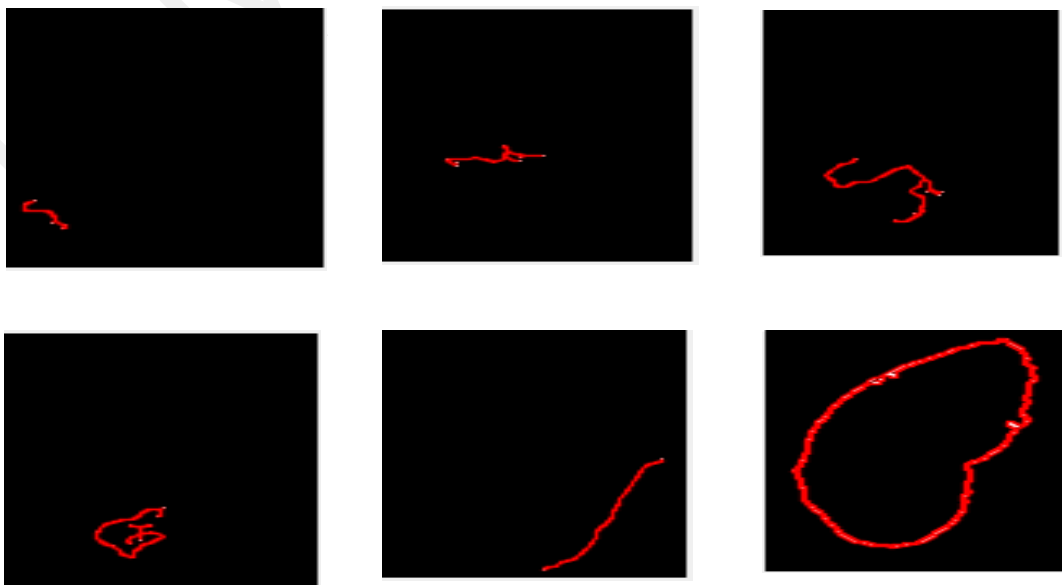


Figure 6.4: Label Object Sample Example 2

- d) Find the centroid for each object using the region props function (see Figure 6.5).
- e) In Figure 6.6, the centroid is marked as a star. Then, the boundary (BW) is used to trace the region boundary in the binary image and to calculate the boundary point  $(x, y)$ .

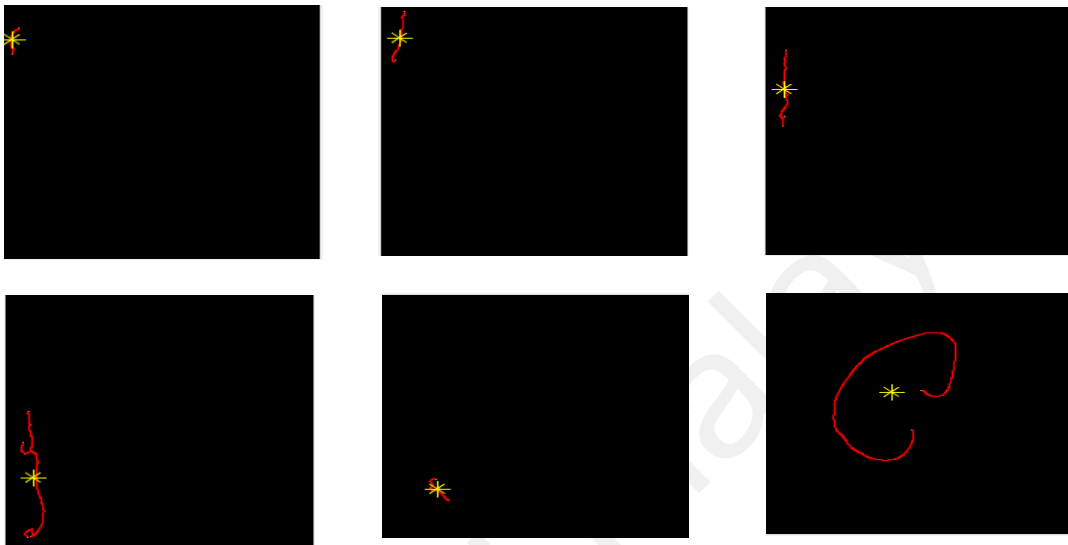


Figure 6.5: Object Centroid Example 1

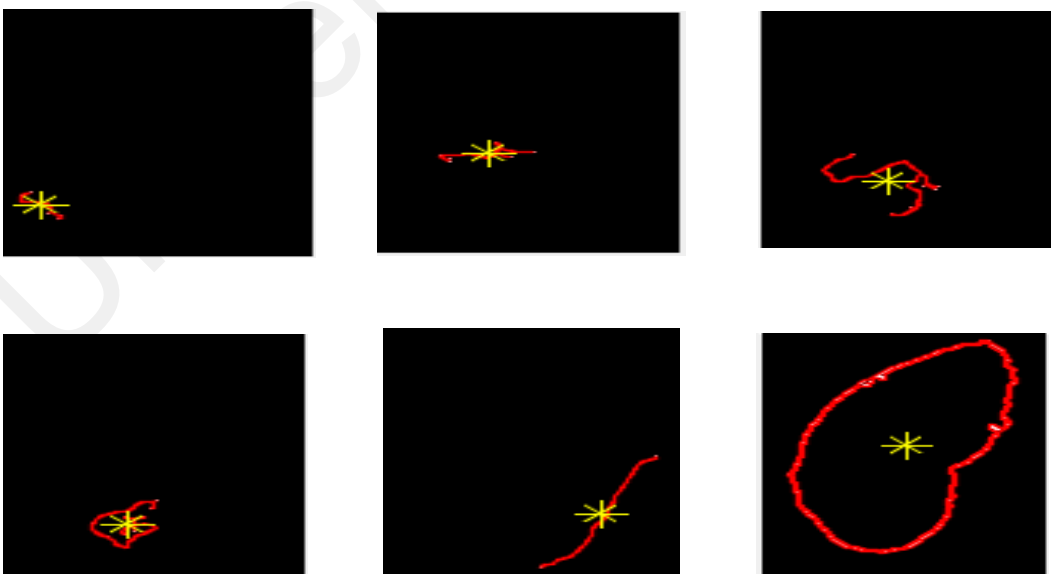


Figure 6.6: Object Centroid Example 2

- f) The distance from the centroid to the boundary is calculated using the equation

$$\text{distance} = \sqrt{(x - x_{\text{Centroid}})^2 + (y - y_{\text{Centroid}})^2} \quad 6.1$$

- g) Then the angle from the centroid to the boundary is calculated using the next equation

$$\text{Angle} = \text{atan2d}(y - y_{\text{Centroid}}, x - x_{\text{Centroid}}) \quad 6.2$$

- h) Then, the angle from the centroid to the boundary is calculated as the max angle and max distance found for each object. To extract the kidney edge without any non-kidney component, hence the max angle and max distance represent the kidney components.
- i) The minimum distance from the centroid to the boundary is found. Then, the object is removed or otherwise kept.
- j) If there is still any non-kidney component in the final result, the shape factor of the kidney is calculated to remove any non-kidney component and keep kidney edges to get final result as:

$$\text{SF} = 4\pi A/L^2 \quad 6.3$$

A: area of region

L: is the number of boundaries which is equal to the number of x.

For the kidney, the SF will be the min value.

The final result extracted for the kidney edge is shown in Figure 6. 7 for Example1 and Example 2.



**Figure 6. 7: The Result of Proposed Segmentation Model on Different Kidney Images**

### 6.3 Experimental Results

A dataset, consisting of 230 images, was collected of different patients. The dataset included low-quality image characteristics such as low contrast, low resolution, and noise. The dataset was considered adequate enough to evaluate the proposed and existing methods for kidney image segmentation because the nature of the dataset varied in terms of low-quality characteristics that included the possible causes of kidney image segmentation.

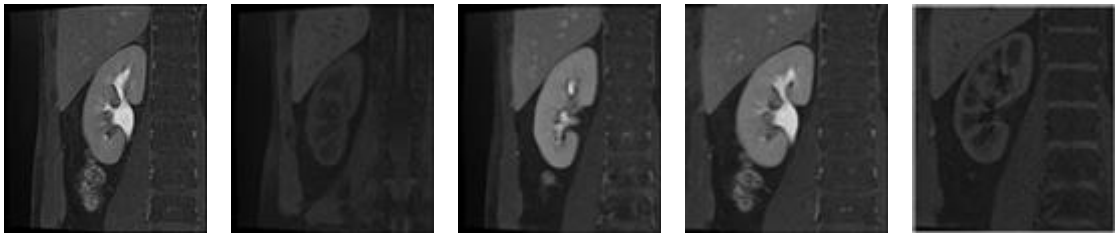
In order to measure whether the proposed model was able to segment kidney parts correctly or not, standard measures, namely, sensitivity and accuracy, were used. Kidney regions were segmented manually, and the segmented regions were further verified by a doctor who was an expert radiologist. At the same time, the results given by the proposed and existing methods were verified by the same doctor to calculate the measures. The ground truth samples and segmentation results of the proposed edge-based method for kidney segmentation for the dataset are shown in Figure 6. 8.

To show the effectiveness and usefulness of the proposed model, it was compared with the following state-of-the-art methods: Canny edge strategy (Canny, 1986), which uses Gaussian filtering for segmentation. However, the Canny edge detection may still fail to precisely meet the desired boundary if the noise level in the image is high because the noise and edges both include high frequency components. The execution of the Canny edge identification depends on Gaussian filtering. Gaussian filtering does not just remove image noise and smothers image subtleties, but also weakens the edge data. Tomasi and Manduchi (1998) adjusted the bilateral filter to do edge recognition, which is the inverse of bilateral smoothing. Chai, Wee et al. (2011) presented the speckle-reducing anisotropic diffusion (SRAD) system in the image denoising part of the Canny algorithm structure. The proposed technique is able to remove speckle noise while maintaining image subtleties.

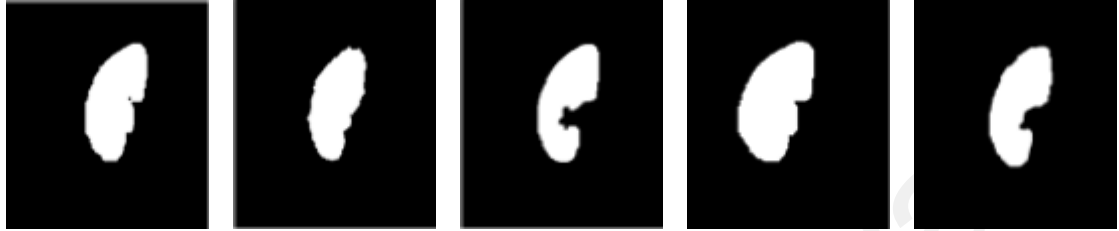
These strategies do not segment the kidney accurately. Thus, this may be the reason why the models which investigated the Canny edge with various filters on their own may not function well for low-differentiation and degraded images. In this way, a viable strategy for removing the non-kidney part from low-complexity MRI images was developed according to the Canny edge recognition calculations with the application of a few conditions, namely, the angle from the centroid to the boundaries, the distance from the centroid to the boundaries, and the shape factor of the kidney.

### **6.3.1 Qualitative Results**

The qualitative results of the proposed segmentation model for the dataset1 and dataset2 are shown in Figure 6.8 and Figure 6.9, respectively. It was observed that the input images were affected by multiple factors, such as poor quality (low contrast), degradations, and contrast variations, as shown in Figure 6.8(a) and 6.9(a). The proposed model was able to successfully segment the kidney regions, as shown in Figure. 6.8(c) and Figure 6.9(c). This was evident from the comparison of the segmentation results of the proposed model and the ground truth, where the results of the proposed edge-based method for kidney segmentation were almost the same as the ground truth. This shows that the proposed model has the ability to handle complex situations (i.e., kidney diseases). This is the advantage of the proposed model for segmentation.



(a) Input images



(b) Ground truth



(c) Proposed Edge-based kidney segmentation



(d) Binary image of proposed Edge-based kidney segmentation

**Figure 6.8: Examples of Kidney Segmentation Using the Proposed Edge-Based Method for Kidney Segmentation**

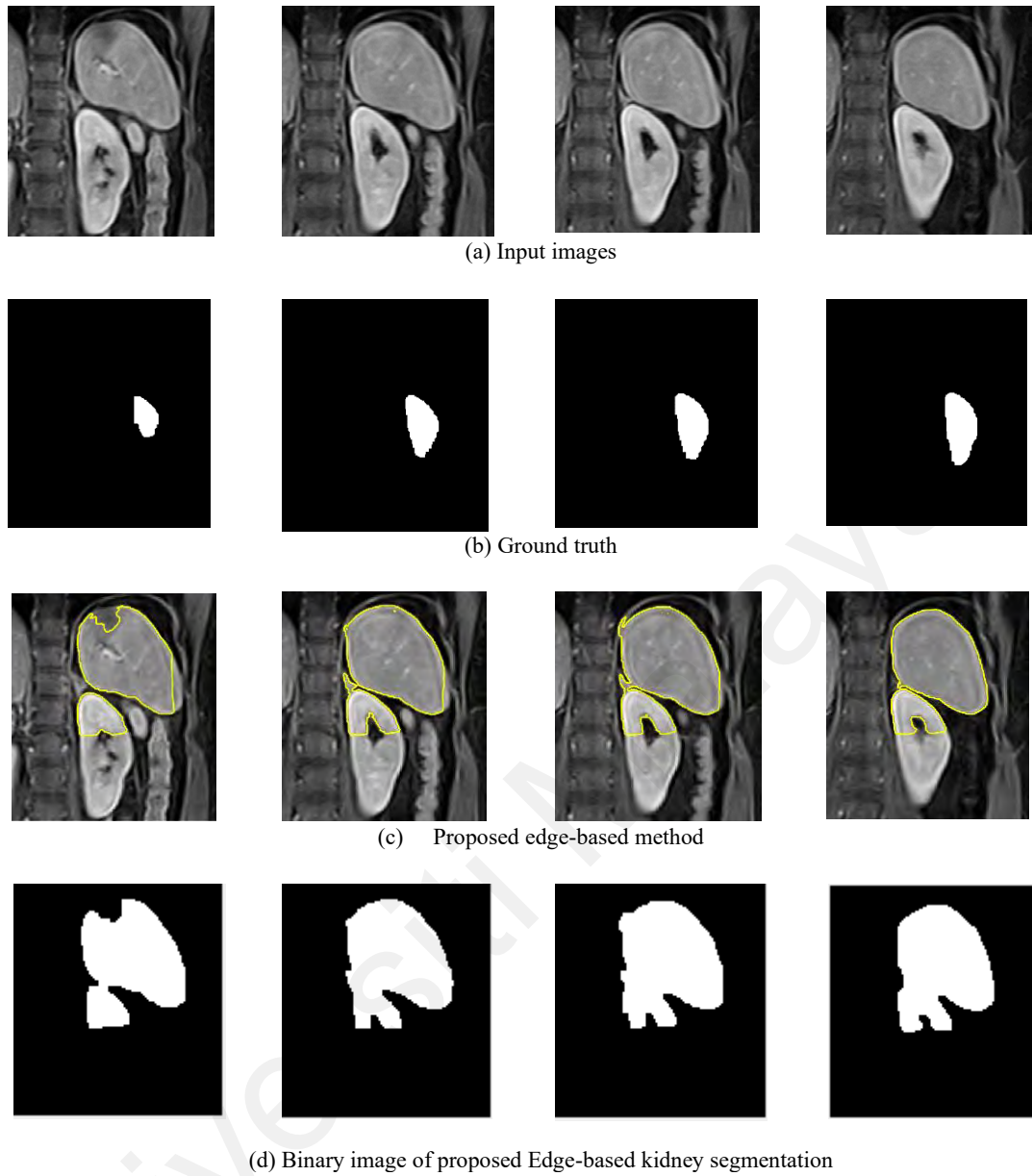


**Figure 6.9: Samples of Kidney Segmentation Using Proposed Edge-Based Method on Dataset-2**

### 6.3.2 Quantitative Results

The quantitative results for the tested dataset are reported in Table 6.1 and Table 6.2, where it was evident that the proposed model produced the best results in terms of sensitivity and accuracy, JSC, DSC compared to other existing models.

Therefore, it can be asserted that the proposed model outperformed the existing models in terms of segmentation, shape preservation and efficiency. Table 6.1 and Table 6.2 show that the proposed model was suitable for complex images as well as simple images.

**Table 6.1: Perform of The Proposed and Existing Methods for Dataset-1**

Methods	Sensitivity (%)	Accuracy (%)	JSC (%)	DSC (%)
(Tomasi & Manduchi, 1998b)	30.28	63.788	49.55	68.92
(Chai, Wee, & Supriyanto, 2011b)	33.28	59.865	45.79	56.32
<b>Proposed</b>	<b>98.14</b>	<b>94.656</b>	<b>90.55</b>	<b>93.92</b>

**Table 6.2: Performance of the proposed edge-based method for kidney image segmentation on Dataset-2**

Methods	Sensitivity (%)	Accuracy (%)	JSC (%)	DSC (%)
(Tomasi & Manduchi, 1998b)	39.58	41.788	41.95	42.79
(Chai, Wee, & Supriyanto, 2011b)	38.28	39.85	40.79	37.32
<b>Proposed</b>	<b>48.34</b>	<b>48.68</b>	<b>47.85</b>	<b>46.52</b>

#### 6.4 Evaluating two proposed segmentation methods

To support the first proposed segmentation algorithm (Fractional-Based Minimization Function for Kidney Image Segmentation) this method overcomes the limitations of the second proposed segmentation method which is the edge-based method for kidney image segmentation. A qualitative and quantitative evaluation is provided using dataset-1 in Sections 6.5.1 and 6.5.2.

### 6.4.1 Qualitative Results

The qualitative results of both proposed segmentation models for dataset-1 are shown in Figure 6.10. It was observed that the input images were affected by multiple factors, as shown in Figure 6.10(a). Each proposed model was able to successfully segment the kidney regions, with more accurate results for proposed segmentation 1 (fractional-based minimization function) compared to the proposed segmentation 2 (edge-based method) as shown in Figure 6.10(c) and Figure 6.10(d).

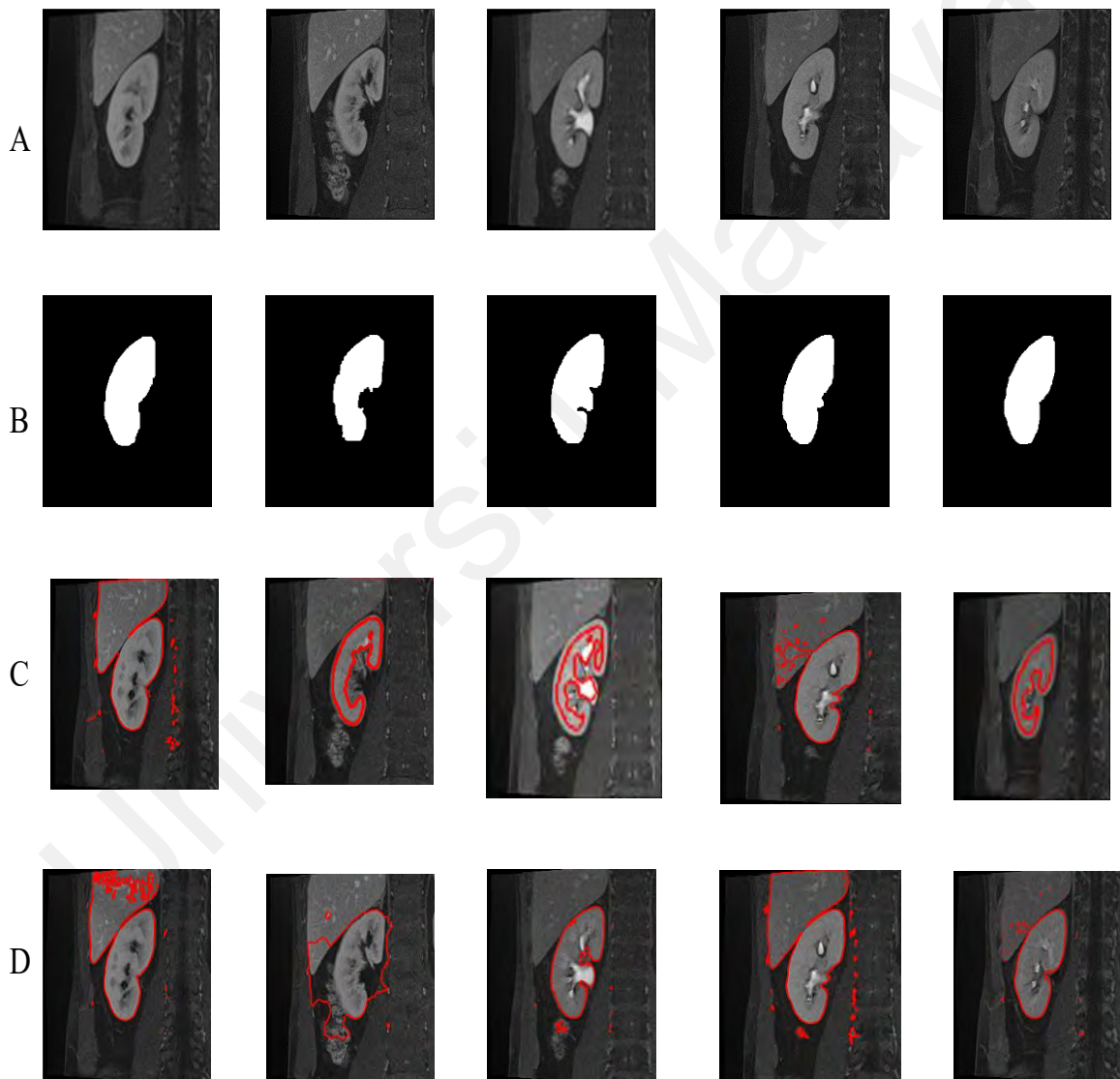


**Figure 6.10: The Comparison results between the two proposed segmentation methods using dataset 1 (A) Input images, (B) Ground Truth, (C) Proposed segmentation 1, (D) Proposed segmentation 2**

## 6.4.2 Quantitative Results

The quantitative results for the tested dataset are reported in Table 6.3 and Table 6.4, where it was evident that both proposed segmentation models produced good results in terms of accuracy, with lower computational time for the edge-based method. This is because after implementing the edge-based method, the active contour-based method is computationally expensive because it involves a large number of iterations. However, the motivation for using the active contour-based method is to develop a generalized method to obtain accurate results. Although the active contour-based method is computationally expensive, it achieves better results compared to the edge-based method. In contrast, while the edge-based method is more efficient, it is not as accurate as the active contour-based method.

The proposed enhancement model enhanced images of the kidney region that included other body parts. This made the segmentation of the kidney region difficult. The proposed work explored a fractional calculus-based method for segmenting the kidney region in the enhanced images. Since fractional calculus has the ability to handle uncertainty between the prominent pixels and background pixels, the proposed method exploited this property to segment the kidney region in the enhanced images. According to the experiments, the above method is computationally expensive, which means that the method requires a greater number of operations. As the number of operations increases, the processing time also increases. The second segmentation method proposed was developed using an edge-based method. It is true that the pixels, which represent the contours of the kidney, share unique spatial relationships. Based on this, the proposed model achieved better results than the existing models.

**Table 6.3: The Comparison results between the two proposed segmentation methods using dataset 1**

Method	Accuracy of dataset1	Time (sec)
Proposed segmentation1	98.95	3.26
Proposed segmentation 2	94.65	0.76

**Table 6.4: The Comparison results between the two proposed segmentation methods using dataset 2**

Method	Accuracy of dataset2	Time (sec)
Proposed segmentation1	80.55	4.66
Proposed segmentation 2	50.21	1.88

## 6.5 Discussion

According to the experimental results in Chapter 5, the proposed active contour-segmentation method is computationally expensive. To develop an efficient method for segmenting the kidney based on enhanced images, the proposed work developed an edge-based method. Edges are important features in such images to separate key data, and it represents the basic tools for segmentation. However, edges of such regions can be hard to determine because the MRI input images are affected by multiple factors, such as poor quality, degradation, and contrast variation. The state-of-the-art developed methods work by segmenting high-quality images; additionally, the performance of these methods is affected when the shape of the kidney changes. To overcome this, we developed a strategy for segmenting kidney-edge components by preserving kidney segmentation edge information from low-contrast MRI input images. The Canny edge detection strategy (Canny, 1986; Tomasi and Manduchi, 1998; Chai, 2011), did not segment the kidney accurately. These methods are mainly used to determine edges by removing noise from images before edge detection to simplify the information to be processed while maintaining edge information.

However, this can still fail to accurately designate the boundaries if the noise level in the image is too high; also, the Canny method depends on Gaussian filters, which not only remove noise but also smooth the image, which affects edge data. To measure the performance of our proposed method, we used standard measures; namely, sensitivity, accuracy, JSC, and DSC. The proposed edge-based method for kidney-image segmentation was applied to the MRI image-based Canny edge detection under three applicable conditions; namely: (i) angle from the centroid to boundaries; (ii) the distance from the centroid to boundaries, and (iii) the shape factor of the kidney. According to qualitative and quantitative results, the proposed method outperforms existing methods and is useful in the terms of accuracy, sensitivity, JSC, and DSC. Moreover, the proposed method achieved this performance with a minimum of computational expense. However, when the proposed enhancement method does not enhance the details properly over the entire image, the proposed segmentation method fails to perform well.

## **6.6 Chapter Summary**

This chapter presented the description of each step of the proposed edge-based method for kidney image segmentation. The experimental results on different low-quality kidney MR images showed that the proposed model was able to carry out the effective segmentation of kidney MRI images based on the use of kidney edge components while preserving kidney-segmented edge information from low-contrast MRI images.

## CHAPTER 7: CONCLUSIONS AND FUTURE WORK

### 7.1 Background

In this research, three novel approaches for enhancing and segmenting kidney components from low-contrast kidney MRI images, namely, an active contour model and edge-based methods for kidney image segmentation, were proposed. This chapter describes the summary, contributions and limitations of the proposed methods and recommendations for future work.

### 7.2 Summary of the Proposed Work

According to the objectives mentioned in Chapter-1, the proposed thesis work achieved the following, as described below.

A new model based on fractional entropy was proposed for kidney image enhancement. This was the first objective of the thesis. The results showed that the proposed model is effective and useful for enhancing the fine details of the kidney region in the input images. It was also shown that the proposed model works well for images affected by noise, blurring and poor quality (low contrast). In addition, the results of a comparative study of the proposed model and existing models showed that the proposed model is effective.

To achieve the second objective, the proposed work introduced a novel local fractional Mittag-Leffler function (LFMLF) as an energy minimization function to swap the standard gradient-descent minimization function in an active contour segmentation. The proposed model exploited the special property of fractional calculus, namely, its capability to not only preserve high-frequency contour features, but also to improve the low-frequency texture details in a smooth area to overcome the challenges. The results of the proposed model showed that it works well for images posed with different challenges.

For achieving the third objective, the proposed work developed an edge-based method for segmenting the kidney region in enhanced images. The proposed method extracted the unique information of the pixels, which represent the contours of the kidney for segmenting the region. The results of the proposed method and existing methods showed that the proposed method is accurate compared to the existing methods.

### **7.3 Contributions of the Proposed Work**

This thesis made three contributions, namely, a fractional entropy model for MRI kidney image enhancement, a fractional calculus-based method for kidney image segmentation, and an edge-based method for efficient kidney image segmentation.

The proposed work explored the fractional entropy information in a new way to achieve better results, and this was the main contribution compared to the existing models. Since the kidney images that were considered in this thesis were complex in nature in terms of low contrast, resolution, degradation and poor quality, the proposed fractional entropy enhanced the pixels based on the neighbouring information, irrespective of the above challenges.

Similarly, due to complex images, the proposed enhancement model enhanced other information along with the kidney region. This made the segmentation of the kidney region difficult. The proposed work explored a fractional calculus-based method for segmenting the kidney region in the enhanced image. Since fractional calculus has the ability to handle uncertainty between the prominent pixels and background pixels, the proposed method exploited this property to segment the kidney region in the enhanced image.

According to the experiments, the above method is computationally expensive. To develop an efficient method for segmenting the kidney region from the enhanced images, the proposed work developed an edge-based method. It is true that the pixels, which represent the contours of the kidney, share some unique spatial relationship. Based on this, the

proposed model achieved better results. The main contribution of the proposed method was the achievement of results with acceptable efficiency.

#### **7.4 Limitations of the Proposed Work**

Although the methods proposed in this thesis worked well for the different situations, there were some limitations as follows:

When the input images are affected by noise, and are severely blurred, where one cannot see the content in the image with the naked eye, the enhancement method does not work well. This is because the proposed model gets confused with the actual pixel values and the noise pixel values. The proposed model involves many parameters to achieve better results. Sometimes, the parameters fail to get the correct values to obtain good results for different situations. It is necessary to reduce the dependency on the parameters.

In the case of segmentation, the success of the proposed model depends on the success of the proposed enhancement model. If the enhancement model fails to classify the pixels of the kidney from the background pixels, the proposed segmentation will fail. This shows that there is a need to develop a method that works well without depending on the enhancement.

Although the proposed edge-based method is efficient for segmenting the kidney region from enhanced images, the method is sensitive to a complex background and low-contrast images. When the proposed enhancement method does not enhance the details properly for the whole image, the proposed segmentation method fails to perform well. When the image contains different regions with different contrast qualities, the edge-based method does not perform well. In addition, if the image loses the details of the kidney contours, the edge-based method fails to segment the kidney region from the enhanced images.

## **7.5 Recommendations for Future Work**

In view of the listed drawbacks of the proposed models of each topic, there is scope for the improvement of the proposed models. At times, the input image is expected to be affected by several causes, such as noise, blurring and other distortions. Therefore, it is necessary to developing a model that can cope effectively with many challenges. This is one major issue that should be considered in future work.

The current trend is to explore deep learning-based models for solving complex issues. Future studies can explore a combination of feature extraction and deep learning for image enhancement and segmentation. In this context, one more work in the future can be to generate ground truth and collect a large number of images for the learning and training of the deep network.

Future works can combine both the enhancement and segmentation steps into one method for evaluating the proposed system. Next, the proposed work can be extended to identify the related diseases in kidney images.

## REFERENCES

- Abdulahi, W. A., & Tapamo, J. R. (2015, September). Fast Chan-Vese without edges and connected component analysis for kidney segmentation in MRI images. In *AFRICON 2015* (pp. 1-5). IEEE.
- Agrawal, O. P. (2002). Formulation of Euler–Lagrange equations for fractional variational problems. *Journal of Mathematical Analysis and Applications*, 272(1), 368-379.
- Al-abayechi, A. A. A., Jalab, H. A., Ibrahim, R. W., & Hasan, A. M. (2017, November). Image Enhancement Based on Fractional Poisson for Segmentation of Skin Lesions Using the Watershed Transform. In *International Visual Informatics Conference* (pp. 249-259). Springer, Cham.
- Al-Shamasneh, A., Jalab, H., Palaiahnakote, S., Obaidellah, U., Ibrahim, R., & El-Melegy, M. (2018). A new local fractional entropy-based model for kidney MRI image enhancement. *Entropy*, 20(5), 344.
- assanpour, H., Samadiani, N., & Salehi, S. M. (2015). Using morphological transforms to enhance the contrast of medical images. *The Egyptian Journal of Radiology and Nuclear Medicine*, 46(2), 481-489.
- Barrett, H. H. (1990). Objective assessment of image quality: effects of quantum noise and object variability. *JOSA A*, 7(7), 1266-1278.
- Baselice, F., Ferraioli, G., Ambrosanio, M., Pascazio, V., & Schirinzi, G. (2018). Enhanced Wiener filter for ultrasound image restoration. *Computer methods and programs in biomedicine*, 153, 71-81.
- Bavu, É., Gennisson, J. L., Couade, M., Bercoff, J., Mallet, V., Fink, M., ... & Pol, S. (2011). Noninvasive in vivo liver fibrosis evaluation using supersonic shear imaging: a clinical study on 113 hepatitis C virus patients. *Ultrasound in medicine & biology*, 37(9), 1361-1373.
- Beland, M. D., Walle, N. L., Machan, J. T., & Cronan, J. J. (2010). Renal cortical thickness measured at ultrasound: is it better than renal length as an indicator of renal function in chronic kidney disease?. *American Journal of Roentgenology*, 195(2), W146-W149.
- Bellomo, R., Kellum, J. A., & Ronco, C. (2012). Acute kidney injury. *The Lancet*, 380(9843), 756-766.
- Bhadauria, H. S., Dewal, M. L., & Anand, R. S. (2011, February). Comparative analysis of curvelet based techniques for denoising of computed tomography images. In 2011 International Conference on Devices and Communications (ICDeCom) (pp. 1-5). IEEE.
- Blackwell, D. L., Lucas, J. W., & Clarke, T. C. (2014). Summary health statistics for US adults: national health interview survey, 2012. *Vital and health statistics. Series 10, Data from the National Health Survey*, (260), 1-161.

- Bokacheva, L., Rusinek, H., Zhang, J. L., & Lee, V. S. (2008). Assessment of renal function with dynamic contrast-enhanced MR imaging. *Magnetic resonance imaging clinics of North America*, 16(4), 597-611.
- Borges, E. P., & Roditi, I. (1998). A family of nonextensive entropies. *Physics Letters A*, 246(5), 399-402.
- Bottrill, M., Kwok, L., & Long, N. J. (2006). Lanthanides in magnetic resonance imaging. *Chemical Society Reviews*, 35(6), 557-571.
- Brown, D. F., Rosen, C. L., & Wolfe, R. E. (1997). Renal ultrasonography. *Emergency medicine clinics of North America*, 15(4), 877-893.
- Butzer, P. L., & Westphal, U. (2000). An introduction to fractional calculus. In *Applications of Fractional Calculus in Physics* (pp. 1-85): World Scientific.
- Campbell, F. W., & Robson, J. G. (1968). Application of Fourier analysis to the visibility of gratings. *The Journal of physiology*, 197(3), 551.
- Canny, J. (1986). A computational approach to edge detection. *IEEE Transactions on pattern analysis and machine intelligence*, (6), 679-698.
- Cao, J. (2018). An Image Enhancement Method Based on Fractional Calculus and Retinex. *Journal of Computer and Communications*, 6(11), 55.
- Caselles, V., Kimmel, R., & Sapiro, G. (1997). Geodesic active contours. *International Journal of computer vision*, 22(1), 61-79.
- Chai, H. Y., Wee, L. K., & Supriyanto, E. (2011, July). Edge detection in ultrasound images using speckle reducing anisotropic diffusion in canny edge detector framework. In *Proceedings of the 15th WSEAS international conference on Systems* (pp. 226-231). World Scientific and Engineering Academy and Society (WSEAS).
- Chan, T. F., Sandberg, B. Y., & Vese, L. A. (2000). Active contours without edges for vector-valued images. *Journal of Visual Communication and Image Representation*, 11(2), 130-141.
- Chehab, M., & Bratslavsky, G. (2016). Kidney Imaging. In *Interventional Urology* (pp. 221-232). Springer, Cham.
- Chen, G. H., Tang, J., & Leng, S. (2008). Prior image constrained compressed sensing (PICCS): a method to accurately reconstruct dynamic CT images from highly undersampled projection data sets. *Medical physics*, 35(2), 660-663.
- Chen, Y., Chen, H., & Shi, J. (2013). In vivo bio-safety evaluations and diagnostic/therapeutic applications of chemically designed mesoporous silica nanoparticles. *Advanced Materials*, 25(23), 3144-3176.
- Clapp, W. (2009). Renal anatomy. In: New York: Cambridge Univ. Press.

- Cohen, L. D. (1991). On active contour models and balloons. *CVGIP: Image understanding*, 53(2), 211-218.
- Cohen, L. D., & Cohen, I. (1993). Finite-element methods for active contour models and balloons for 2-D and 3-D images. *IEEE Transactions on Pattern Analysis & Machine Intelligence*, (11), 1131-1147.
- Couser, W. G., Remuzzi, G., Mendis, S., & Tonelli, M. (2011). The contribution of chronic kidney disease to the global burden of major noncommunicable diseases. *Kidney international*, 80(12), 1258-1270.
- Cuingnet, R., Prevost, R., Lesage, D., Cohen, L. D., Mory, B., & Ardon, R. (2012, October). Automatic detection and segmentation of kidneys in 3D CT images using random forests. In *International Conference on Medical Image Computing and Computer-Assisted Intervention* (pp. 66-74). Springer, Berlin, Heidelberg.
- Dice, L. R. (1945). Measures of the amount of ecologic association between species. *Ecology*, 26(3), 297-302.
- Dutta, J., Ahn, S., & Li, Q. (2013). Quantitative statistical methods for image quality assessment. *Theranostics*, 3(10), 741.
- Erdt, M., & Sakas, G. (2010, March). Computer aided segmentation of kidneys using locally shape constrained deformable models on CT images. In *Medical Imaging 2010: Computer-Aided Diagnosis* (Vol. 7624, p. 762419). International Society for Optics and Photonics.
- Evangelin, M. J., & Suresh, L. P. (2015, March). Segmentation driven image application to 2D-MRI of kidney. In *2015 International Conference on Circuits, Power and Computing Technologies [ICCPCT-2015]* (pp. 1-5). IEEE.
- Fang, Y., Ma, K., Wang, Z., Lin, W., Fang, Z., & Zhai, G. (2015). No-reference quality assessment of contrast-distorted images based on natural scene statistics. *IEEE Signal Processing Letters*, 22(7), 838-842.
- Frederico, G. S., & Torres, D. F. (2007). A formulation of Noether's theorem for fractional problems of the calculus of variations. *Journal of Mathematical Analysis and Applications*, 334(2), 834-846.
- Fernandes, S., Vashi, H., Shetty, A., & Kelkar, V. (2019, December). Adaptive Contrast Enhancement using Fuzzy Logic. In *2019 International Conference on Advances in Computing, Communication and Control (ICAC3)* (pp. 1-6). IEEE.
- Gloger, O., Liebscher, V., Tönnies, K. D., & Völzke, H. (2014). Fully Automatic Renal Parenchyma Volumetry in LDA-based Probability Maps Using Variational Outer Cortex Edge Alignment Forces. In *IWBBIO* (pp. 1207-1218).
- Gloger, O., Tönnies, K. D., Liebscher, V., Kugelmann, B., Laqua, R., & Völzke, H. (2011). Prior shape level set segmentation on multistep generated probability maps of MR datasets for fully automatic kidney parenchyma volumetry. *IEEE transactions on medical imaging*, 31(2), 312-325.

- Gonzalez, R. C., Woods, R. E., & Eddins, S. L. (2012). Image processing place. *Diambil kembali dari Image Database: [http://www.imageprocessingplace.com/downloads\\_V3/root\\_downloads/image\\_databases/standard\\_test\\_images.zip](http://www.imageprocessingplace.com/downloads_V3/root_downloads/image_databases/standard_test_images.zip)*
- Guan, J., Ou, J., Lai, Z., & Lai, Y. (2018). Medical image enhancement method based on the fractional order derivative and the directional derivative. *International Journal of Pattern Recognition and Artificial Intelligence*, 32(03), 1857001.
- Gungor, M. A., & Karagoz, I. (2015). The homogeneity map method for speckle reduction in diagnostic ultrasound images. *Measurement*, 68, 100-110.
- Hart, T. C., Gorry, M. C., Hart, P. S., Woodard, A. S., Shihabi, Z., Sandhu, J., ... & Bleyer, A. J. (2002). Mutations of the UMOD gene are responsible for medullary cystic kidney disease 2 and familial juvenile hyperuricaemic nephropathy. *Journal of medical genetics*, 39(12), 882-892.
- Hasan, A., Meziane, F., Aspin, R., & Jalab, H. (2016). Segmentation of brain tumors in MRI images using three-dimensional active contour without edge. *Symmetry*, 8(11), 132.
- Herrmann, R. (2008). Gauge invariance in fractional field theories. *Physics Letters A*, 372(34), 5515-5522.
- Hodneland, E., Hanson, E. A., Lundervold, A., Modersitzki, J., & Eikefjord, E. (2014). Segmentation-driven image registration-application to 4D DCE-MRI recordings of the moving kidneys. *IEEE Transactions on Image Processing* 23(5), 2392-2404.
- Huang, A. J., Lee, V. S., & Rusinek, H. (2004). Functional renal MR imaging. *Magnetic Resonance Imaging Clinics*, 12(3), 469-486.
- Huang, G., Xu, L., Chen, Q., & Men, T. (2015). Image Enhancement Using a Fractional-Order Differential. In *Proceedings of the 4th International Conference on Computer Engineering and Networks* (pp. 555-563). Springer, Cham.
- Huang, J., Yang, X., Chen, Y., & Tang, L. (2013). Ultrasound kidney segmentation with a global prior shape. *Journal of Visual Communication and Image Representation*, 24(7), 937-943.
- Hufnagel, H., Ehrhardt, J., Pennec, X., Schmidt-Richberg, A., & Handels, H. (2010, March). Coupled level set segmentation using a point-based statistical shape model relying on correspondence probabilities. In *Medical Imaging 2010: Image Processing* (Vol. 7623, p. 762318). International Society for Optics and Photonics.
- Ibrahim, R., & Jalab, H. (2015). Existence of Ulam stability for iterative fractional differential equations based on fractional entropy. *Entropy*, 17(5), 3172-3181.

- Ibrahim, R. W., Nashine, H. K., & Kamaruddin, N. (2017). Hybrid time-space dynamical systems of growth bacteria with applications in segmentation. *Mathematical biosciences*, 292, 10-17.
- Jaccard, P. (1901). Étude comparative de la distribution florale dans une portion des Alpes et des Jura. *Bull Soc Vaudoise Sci Nat*, 37, 547-579.
- Jackson, D. O., Fukuda, T., Dunn, O., & Majors, E. (1910). *On  $q$ -definite integrals*. Paper presented at the Quart. J. Pure Appl. Math.
- Jalab, H. A., & Ibrahim, R. W. (2013). Texture enhancement based on the Savitzky-Golay fractional differential operator. *Mathematical Problems in Engineering*, 2013.
- Jalab, H. A., & Ibrahim, R. W. (2015). Fractional Alexander polynomials for image denoising. *Signal Processing*, 107, 340-354.
- Jalab, H. A., Ibrahim, R. W., & Ahmed, A. (2017). Image denoising algorithm based on the convolution of fractional Tsallis entropy with the Riesz fractional derivative. *Neural Computing and Applications*, 28(1), 217-223.
- James, A. P., & Dasarathy, B. V. (2014). Medical image fusion: A survey of the state of the art. *Information Fusion*, 19, 4-19.
- Jha, V., Garcia-Garcia, G., Iseki, K., Li, Z., Naicker, S., Plattner, B., ... & Yang, C. W. (2013). Chronic kidney disease: global dimension and perspectives. *The Lancet*, 382(9888), 260-272.
- Johal, R. S. (1998).  $q$  calculus and entropy in nonextensive statistical physics. *Physical Review E*, 58(4), 4147.
- Joshi, S., & Kumar, S. (2018). Image contrast enhancement using fuzzy logic. arXiv preprint arXiv:1809.04529.
- Jun, L., Xiaodong, Z., & Erping, L. (2006). Study on differential diagnosis of renal column hypertrophy and renal tumors by pulsed subtraction contrast-enhanced ultrasonography. *Chinese Journal of Ultrasound in Medicine*, 4, 039.
- Kallel, F., & Hamida, A. B. (2017). A new adaptive gamma correction based algorithm using DWT-SVD for non-contrast CT image enhancement. *IEEE transactions on nanobioscience*, 16(8), 666-675.
- Kang, J., Lee, J. Y., & Yoo, Y. (2016). A new feature-enhanced speckle reduction method based on multiscale analysis for ultrasound b-mode imaging. *IEEE Transactions on Biomedical Engineering*, 63(6), 1178-1191.
- Khalifa, F., El-Baz, A., Gimel'farb, G., Ouseph, R., & El-Ghar, M. A. (2010, August). Shape-appearance guided level-set deformable model for image segmentation. In *2010 20th international conference on pattern recognition* (pp. 4581-4584). IEEE.
- Khalifa, F., Elnakib, A., Beache, G. M., & Gimel'farb, G. (2011). *3D kidney segmentation from CT images using a level set approach guided by a novel stochastic speed*

*function*. Paper presented at the International Conference on Medical Image Computing and Computer-Assisted Intervention.

- Khalifa, F., Gimel'farb, G., El-Ghar, M. A., Sokhadze, G., Manning, S., McClure, P., ... & El-Baz, A. (2011, September). A new deformable model-based segmentation approach for accurate extraction of the kidney from abdominal CT images. In *2011 18th IEEE International Conference on Image Processing* (pp. 3393-3396). IEEE.
- Khalifa, F., Soliman, A., Dwyer, A. C., Gimel'farb, G., & El-Baz, A. (2016, September). A random forest-based framework for 3D kidney segmentation from dynamic contrast-enhanced CT images. In *2016 IEEE International Conference on Image Processing (ICIP)* (pp. 3399-3403). IEEE
- Koff, S. A., Binkovitz, L., Coley, B., & Jayanthi, V. R. (2005). Renal pelvis volume during diuresis in children with hydronephrosis: implications for diagnosing obstruction with diuretic renography. *The Journal of urology*, *174*(1), 303-307.
- Koyuncu, H., & Ceylan, R. (2017, April). A hybrid tool on denoising and enhancement of abdominal CT images before organ & tumour segmentation. In *2017 IEEE 37th International Conference on Electronics and Nanotechnology (ELNANO)* (pp. 249-254). IEEE.
- Lausch, A., Ebrahimi, M., & Martel, A. (2011, March). Image registration for abdominal dynamic contrast-enhanced magnetic resonance images. In *2011 IEEE International Symposium on Biomedical Imaging: From Nano to Macro* (pp. 561-565). IEEE.
- Lavagno, A., Scarfone, A. M., & Swamy, P. N. (2007). Basic-deformed thermostatics. *Journal of Physics A: Mathematical and Theoretical*, *40*(30), 8635.
- Les, T., Markiewicz, T., Dziekiewicz, M., & Lorent, M. (2018, September). Automatic recognition of the kidney in CT images. In *19th International Conference Computational Problems of Electrical Engineering* (pp. 1-4). IEEE.
- Li, B., & Xie, W. (2015). Adaptive fractional differential approach and its application to medical image enhancement. *Computers & Electrical Engineering*, *45*, 324-335.
- Li, C., Xu, C., Gui, C., & Fox, M. D. (2010). Distance regularized level set evolution and its application to image segmentation. *IEEE transactions on image processing*, *19*(12), 3243-3254
- Li, L., Gu, J., Wen, T., Qin, W., Xiao, H., & Yu, J. (2014, April). Multiscale Geometric Active Contour Model and Boundary Extraction in Kidney MR Images. In *International Conference on Health Information Science* (pp. 212-219). Springer, Cham.
- Li, L., Ross, P., & Kruusmaa, M. (2013, September). Ultrasound image segmentation by Bhattacharyya distance with Rayleigh distribution. In *2013 Signal Processing: Algorithms, Architectures, Arrangements, and Applications (SPA)* (pp. 149-153). IEEE.

- Lima, E., Rodrigues, P. L., Mota, P., Carvalho, N., Dias, E., Correia-Pinto, J., ... & Vilaca, J. L. (2017). Ureterscopy-assisted percutaneous kidney access made easy: first clinical experience with a novel navigation system using electromagnetic guidance (IDEAL stage 1). *European urology*, 72(4), 610-616
- Liu, N., Soliman, A., Gimel'farb, G., & El-Baz, A. (2015, October). Segmenting Kidney DCE-MRI Using 1<sup>st</sup>-Order Shape and 5<sup>th</sup>-Order Appearance Priors. In *International Conference on Medical Image Computing and Computer-Assisted Intervention* (pp. 77-84). Springer, Cham.
- Lucké, B., & Schlumberger, H. G. (1958). Tumors of the kidney, renal pelvis, and ureter. *Annals of Surgery*, 148(2), 293.
- Mainardi, F., Mura, A., & Pagnini, G. (2010). The *M*-Wright Function in Time-Fractional Diffusion Processes: A Tutorial Survey. *International Journal of Differential Equations*, 2010
- Marsousi, M., Plataniotis, K. N., & Stergiopoulos, S. (2017). An automated approach for kidney segmentation in three-dimensional ultrasound images. *IEEE journal of biomedical and health informatics*, 21(4), 1079-1094
- Mittal, A., Moorthy, A. K., & Bovik, A. C. (2012). No-reference image quality assessment in the spatial domain. *IEEE Transactions on image processing*, 21(12), 4695-4708.
- Mittal, A., Soundararajan, R., & Bovik, A. C. (2012). Making a “completely blind” image quality analyzer. *IEEE Signal Processing Letters*, 20(3), 209-212.
- Mohamed, E. A., & Rashed, E. A. (2016). *Blood vessels reconstruction in CT with shape prior approach*. Paper presented at the Biomedical Engineering Conference (CIBEC), 8th Cairo International.
- Moorthy, A. K., & Bovik, A. C. (2011). Blind image quality assessment: From natural scene statistics to perceptual quality. *IEEE transactions on Image Processing*, 20(12), 3350-3364.
- Mounier-Vehier, C., Lions, C., Devos, P., Jaboureck, O., Willoteaux, S., Carre, A., & Beregi, J. P. (2002). Cortical thickness: an early morphological marker of atherosclerotic renal disease. *Kidney international*, 61(2), 591-598.
- Nikken, J. J., & Krestin, G. P. (2007). MRI of the kidney—state of the art. *European radiology*, 17(11), 2780-2793.
- Nikolic, M., Tuba, E., & Tuba, M. (2016, November). Edge detection in medical ultrasound images using adjusted Canny edge detection algorithm. In *2016 24th Telecommunications Forum (TELFOR)* (pp. 1-4). IEEE.
- Noble, V. E., & Brown, D. F. M. (2004). Renal ultrasound. *Emergency Medicine Clinics of North America*, 22(3), 641-659.

- Noll, M., Li, X., & Wesarg, S. (2013, September). Automated kidney detection and segmentation in 3d ultrasound. In *Workshop on Clinical Image-Based Procedures* (pp. 83-90). Springer, Cham.
- Osher, S., & Paragios, N. (Eds.). (2003). *Geometric level set methods in imaging, vision, and graphics*. Springer Science & Business Media.
- Osher, S., & Sethian, J. A. (1988). Fronts propagating with curvature-dependent speed: algorithms based on Hamilton-Jacobi formulations. *Journal of computational physics*, 79(1), 12-49.
- Petitjean, C., & Dacher, J. N. (2011). A review of segmentation methods in short axis cardiac MR images. *Medical image analysis*, 15(2), 169-184.
- Poon, C. S., Braun, M., Fahrig, R., Ginige, A., & Dorrell, A. (1994, September). Segmentation of medical images using an active-contour model incorporating region-based image features. In *Visualization in Biomedical Computing 1994* (Vol. 2359, pp. 90-97). International Society for Optics and Photonics.
- Prevost, R., Mory, B., Correas, J. M., Cohen, L. D., & Ardon, R. (2012, May). Kidney detection and real-time segmentation in 3D contrast-enhanced ultrasound images. In 2012 9th IEEE International Symposium on Biomedical Imaging (ISBI) (pp. 1559-1562). IEEE.
- Qiao, X., Lu, W., Su, X., & Chen, Y. W. (2015). Automatic segmentation method for kidney using dual direction adaptive diffusion flow. In *Innovation in Medicine and Healthcare 2015* (pp. 299-307). Springer, Cham.
- Qin, L., Zhu, C., Zhao, Y., Bai, H., & Tian, H. (2013). Generalized gradient vector flow for snakes: new observations, analysis, and improvement. *IEEE Transactions on Circuits and Systems for Video Technology*, 23(5), 883-897.
- Raghunandan, K. S., Shivakumara, P., Jalab, H. A., Ibrahim, R. W., Kumar, G. H., Pal, U., & Lu, T. (2017). Riesz fractional based model for enhancing license plate detection and recognition. *IEEE Transactions on Circuits and Systems for Video Technology*, 28(9), 2276-2288
- Rahman, T., & Uddin, M. S. (2013, May). Speckle noise reduction and segmentation of kidney regions from ultrasound image. In *2013 International Conference on Informatics, Electronics and Vision (ICIEV)* (pp. 1-5). IEEE.
- Remuzzi, G., Benigni, A., Finkelstein, F. O., Grunfeld, J. P., Joly, D., Katz, I., ... & Antiga, L. (2013). Kidney failure: aims for the next 10 years and barriers to success. *The Lancet*, 382(9889), 353-362.
- Rodrigues, P. L., Rodrigues, N. F., Fonseca, J., Lima, E., & Vilaça, J. L. (2013). Kidney targeting and puncturing during percutaneous nephrolithotomy: recent advances and future perspectives. *Journal of endourology*, 27(7), 826-834.
- Ronneberger, O., Fischer, P., & Brox, T. (2015, October). U-net: Convolutional networks for biomedical image segmentation. In *International Conference on Medical image computing and computer-assisted intervention* (pp. 234-241). Springer, Cham.

- Roy, A., & Maity, S. P. (2014, December). CS Reconstructed MR Image Segmentation Using Morphological Enhancement and FCM. In *2014 Fourth International Conference of Emerging Applications of Information Technology* (pp. 228-232). IEEE.
- Roy, S., Shivakumara, P., Jalab, H. A., Ibrahim, R. W., Pal, U., & Lu, T. (2016). Fractional poisson enhancement model for text detection and recognition in video frames. *Pattern Recognition*, *52*, 433-447
- Saad, M. A., Bovik, A. C., & Charrier, C. (2012). Blind image quality assessment: A natural scene statistics approach in the DCT domain. *IEEE transactions on Image Processing*, *21*(8), 3339-3352.
- Sharma, K., Rupprecht, C., Caroli, A., Aparicio, M. C., Remuzzi, A., Baust, M., & Navab, N. (2017). Automatic segmentation of kidneys using deep learning for total kidney volume quantification in autosomal dominant polycystic kidney disease. *Scientific reports*, *7*(1), 1-10.
- Shehata, M., Khalifa, F., Soliman, A., Alrefai, R., El-Ghar, M. A., Dwyer, A. C., ... & El-Baz, A. (2015, September). A level set-based framework for 3D kidney segmentation from diffusion MR images. In *2015 IEEE International Conference on Image Processing (ICIP)* (pp. 4441-4445). IEEE.
- Shehata, M., Khalifa, F., Soliman, A., Alrefai, R., El-Ghar, M. A., Dwyer, A. C., ... & El-Baz, A. (2015, April). A novel framework for automatic segmentation of kidney from DW-MRI. In *2015 IEEE 12th International Symposium on Biomedical Imaging (ISBI)* (pp. 951-954). IEEE.
- Shrimali, V., Anand, R. S., & Kumar, V. (2009). Current trends in segmentation of medical ultrasound B-mode Images: A Review. *IETE technical review*, *26*(1), 8-17.
- Siemer, S., Lahme, S., Altziebler, S., Machtens, S., Strohmaier, W., Wechsel, H. W., ... & Becker, H. (2007). Efficacy and safety of TachoSil® as haemostatic treatment versus standard suturing in kidney tumour resection: a randomised prospective study. *European urology*, *52*(4), 1156-1163.
- Song, Y., Wang, H., Liu, Y., Li, C., Tasian, G. E., Gong, Z., & Zhao, D. (2015). An improved level set method for segmentation of renal parenchymal area from ultrasound images. *Journal of Medical Imaging and Health Informatics*, *5*(7), 1533-1536.
- Song, Y., Wang, H., Liu, Y., Li, C., Tasian, G. E., Gong, Z., & Zhao, D. (2015). An improved level set method for segmentation of renal parenchymal area from ultrasound images. *Journal of Medical Imaging and Health Informatics*, *5*(7), 1533-1536.
- Stevens, L. A., Coresh, J., Greene, T., & Levey, A. S. (2006). Assessing kidney function—measured and estimated glomerular filtration rate. *New England Journal of Medicine*, *354*(23), 2473-2483.

- Supriyanto, E., Tahir, N. A., Nooh, S. M., Arooj, A., & Hafizah, W. (2011, July). Automatic ultrasound kidney's centroid detection system. In *Proceedings of the 15th WSEAS international conference on Computers* (pp. 160-165). World Scientific and Engineering Academy and Society (WSEAS).
- Tang, H., Joshi, N., & Kapoor, A. (2011, June). Learning a blind measure of perceptual image quality. In *CVPR 2011* (pp. 305-312). IEEE
- Thong, W., Kadoury, S., Piché, N., & Pal, C. J. (2018). Convolutional networks for kidney segmentation in contrast-enhanced CT scans. *Computer Methods in Biomechanics and Biomedical Engineering: Imaging & Visualization*, 6(3), 277-282.
- Tomasi, C., & Manduchi, R. (1998, January). Bilateral filtering for gray and color images. In *Iccv* (Vol. 98, No. 1, p. 2).
- Torres, H. R., Oliveira, B., Queirós, S., Morais, P., Fonseca, J. C., D'hooge, J., ... & Vilaça, J. L. (2016, May). Kidney Segmentation in 3D CT Images Using B-Spline Explicit Active Surfaces. In *2016 IEEE International Conference on Serious Games and Applications for Health (SeGAH)* (pp. 1-7). IEEE
- Torres, H. R., Queiros, S., Morais, P., Oliveira, B., Fonseca, J. C., & Vilaca, J. L. (2018). Kidney segmentation in ultrasound, magnetic resonance and computed tomography images: A systematic review. *Computer methods and programs in biomedicine*, 157, 49-67
- Trinh, D. H., Luong, M., Rocchisani, J. M., Pham, C. D., & Dibos, F. (2011, September). Medical image denoising using kernel ridge regression. In *2011 18th IEEE International Conference on Image Processing* (pp. 1597-1600). IEEE.
- Turco, D., Valinoti, M., Martin, E. M., Tagliaferri, C., Scolari, F., & Corsi, C. (2018). Fully Automated Segmentation of Polycystic Kidneys From Noncontrast Computed Tomography: A Feasibility Study and Preliminary Results. *Academic radiology*, 25(7), 850-855.
- Ubricco, M. R. (2001). Quantum group invariant, nonextensive quantum statistical mechanics. *Physics Letters A*, 283(3-4), 157-162.
- Wang, H., Pulido, J. E., Song, Y., Furth, S. L., Tu, C., Zhang, C., ... & Tasian, G. E. (2014, August). Segmentation of renal parenchymal area from ultrasound images using level set evolution. In *2014 36th Annual International Conference of the IEEE Engineering in Medicine and Biology Society* (pp. 4703-4706). IEEE.
- Wang, L., Chen, G., Shi, D., Chang, Y., Chan, S., Pu, J., & Yang, X. (2018). Active contours driven by edge entropy fitting energy for image segmentation. *Signal Processing*, 149, 27-35.
- Wang, Y., Wu, Y., & Jia, Y. (2014). Shape constraints for the left ventricle segmentation from cardiac cine mri based on snake models. In *Shape Analysis in Medical Image Analysis* (pp. 373-412). Springer, Cham.
- Will, S., Martirosian, P., Würslin, C., & Schick, F. (2014). Automated segmentation and volumetric analysis of renal cortex, medulla, and pelvis based on non-contrast-

- enhanced T1-and T2-weighted MR images. *Magnetic Resonance Materials in Physics, Biology and Medicine*, 27(5), 445-454
- Wu, Y., Wang, Y., & Jia, Y. (2013). Segmentation of the left ventricle in cardiac cine MRI using a shape-constrained snake model. *Computer Vision and Image Understanding*, 117(9), 990-1003
- Xu, J., Kochanek, K. D., Murphy, S. L., & Tejada-Vera, B. (2016). Deaths: final data for 2014.
- Yang, F., Qin, W., Xie, Y., Wen, T., & Gu, J. (2012). A shape-optimized framework for kidney segmentation in ultrasound images using NLTV denoising and DRLSE. *Biomedical engineering online*, 11(1), 82.
- Yang, X. J. (2011). *Local Fractional Functional Analysis & Its Applications*. Hong Kong: Asian Academic Publisher Limited.
- Yang, X. J., Baleanu, D., & Srivastava, H. M. (2015). Local fractional similarity solution for the diffusion equation defined on Cantor sets. *Applied Mathematics Letters*, 47, 54-60.
- Yang, X. J., Srivastava, H. M., He, J. H., & Baleanu, D. (2013). Cantor-type cylindrical-coordinate method for differential equations with local fractional derivatives. *Physics Letters A*, 377(28-30), 1696-1700
- Yao, Y., Liu, L., Liao, L., Wei, M., Guo, J., & Li, Y. (2012, October). Sigmoid gradient vector flow for medical image segmentation. In *2012 IEEE 11th International Conference on Signal Processing* (Vol. 2, pp. 881-884). IEEE.
- Ye, P., & Doermann, D. (2012). No-reference image quality assessment using visual codebooks. *IEEE Transactions on Image Processing*, 21(7), 3129-3138.
- Yu, C. Y., & Li, Y. (2012, May). A watershed method for mr renography segmentation. In *2012 International Conference on Biomedical Engineering and Biotechnology* (pp. 700-703). IEEE.
- Zhang, M., Li, Q., Li, L., & Bai, P. (2013). An improved algorithm based on the gvf-snake for effective concavity edge detection. *Journal of Software Engineering and Applications*, 6(04), 174
- Zhang, M., Wu, T., Beeman, S. C., Cullen-McEwen, L., Bertram, J. F., Charlton, J. R., ... & Bennett, K. M. (2015). Efficient small blob detection based on local convexity, intensity and shape information. *IEEE transactions on medical imaging*, 35(4), 1127-1137.
- Zhu, G., Zhang, S., Zeng, Q., & Wang, C. (2010). Gradient vector flow active contours with prior directional information. *Pattern Recognition Letters*, 31(9), 845-856